USGS
science for a changing world

Toxic Substances Hydrology Program
Coastal and Marine Geology Program

Prepared in cooperation with the U.S. Environmental Protection Agency,
Office of Research and Development and Region 1 (New England)

Geochemical Conditions and Nitrogen Transport in Nearshore Groundwater and the Subterranean Estuary at a Cape Cod Embayment, East Falmouth, Massachusetts, 2013–14

Scientific Investigations Report 2018–5095

U.S. Department of the Interior
U.S. Geological Survey

Cover. Direct-push drilling rig on the shore of the Eel River, Seacoast Shores Peninsula, East Falmouth, Massachusetts, July 16, 2013. Photograph by Denis LeBlanc, U.S. Geological Survey.

Geochemical Conditions and Nitrogen Transport in Nearshore Groundwater and the Subterranean Estuary at a Cape Cod Embayment, East Falmouth, Massachusetts, 2013–14

By John A. Colman, Denis R. LeBlanc, J.K. Böhlke, Timothy D. McCobb, Kevin D. Kroeger, Marcel Belaval, Thomas C. Cambareri, Gillian F. Pirolli, T. Wallace Brooks, Mary E. Garren, Tobias B. Stover, and Ann Keeley

Toxic Substances Hydrology Program
Coastal and Marine Geology Program

Prepared in cooperation with the U.S. Environmental Protection Agency, Office of Research and Development and Region 1 (New England)

Scientific Investigations Report 2018–5095

U.S. Department of the Interior
U.S. Geological Survey

U.S. Department of the Interior
RYAN K. ZINKE, Secretary

U.S. Geological Survey
James F. Reilly II, Director

U.S. Geological Survey, Reston, Virginia: 2018

Suggested citation:
Colman, J.A., LeBlanc, D.R., Böhlke, J.K., McCobb, T.D., Kroeger, K.D., Belaval, M., Cambareri, T.C., Pirolli, G.F., Brooks, T.W., Garren, M.E., Stover, T.B., and Keeley, A., 2018, Geochemical conditions and nitrogen transport in near-shore groundwater and the subterranean estuary at a Cape Cod embayment, East Falmouth, Massachusetts, 2013–14: U.S. Geological Survey Scientific Investigations Report 2018–5095, 69 p., https://doi.org/10.3133/sir20185095.

ISSN 2328-0328 (online)

Acknowledgments

The support and cooperation of the Seacoast Shores Association and the residents near the study site are deeply appreciated. Many local citizens and officials provided assistance during the study, including Raymond Jack, Virginia Valiela, Mark Kaspryck, and Eric Turkington of the Town of Falmouth. The laboratory and field support of Mark White, Warren Boothman, Jim Latimer, Jerry Keefe, and Daniel Granz of the U.S. Environmental Protection Agency, and Douglas Kent, Richard Smith, Deborah Repert, Jason Sorenson, Jeffrey Grey, Adrian Green, Janet Hannon, and Stanley Mroczkowski of the U.S. Geological Survey are gratefully acknowledged.

Contents

Figures

Conversion Factors

International System of Units to U.S. customary units

Multiply	By	To obtain
	Length	
centimeter (cm)	0.3937	inch (in.)
millimeter (mm)	0.03937	inch (in.)
meter (m)	3.281	foot (ft)
kilometer (km)	0.6214	mile (mi)
	Area	
square kilometer (km^2)	247.1	acre
hectare (ha)	0.003861	square mile (mi^2)
	Volume	
liter (L)	0.2642	gallon (gal)
milliliter (mL)	0.03381	ounce, fluid (fl. oz)
	Flow rate	
cubic meter per day (m^3/d)	264.2	gallon per day (gal/d)
centimeter per year (cm/yr)	0.3937	inch per year (in/yr)
	Mass	
microgram (μg)	3.527×10^{-8}	ounce, avoirdupois (oz)
	Hydraulic conductivity	
meter per day (m/d)	3.281	foot per day (ft/d)

Temperature in degrees Celsius (°C) may be converted to degrees Fahrenheit (°F) as follows:

$$°F = (1.8 \times °C) + 32.$$

Temperature in degrees Fahrenheit (°F) may be converted to degrees Celsius (°C) as follows:

$$°C = (°F - 32) / 1.8.$$

Datum

Vertical coordinate information is referenced to the National Geodetic Vertical Datum of 1929 (NGVD 29).

Horizontal coordinate information is referenced to the North American Datum of 1983 (NAD 83).

Altitude, as used in this report, refers to distance above the vertical datum.

Supplemental Information

Specific conductance is given in millisiemens per centimeter at 25 degrees Celsius (mS/cm at 25 °C) or microsiemens per centimeter at 25 degrees Celsius (µS/cm at 25 °C).

Concentrations of chemical constituents in water are given either in micromoles per liter (µmol/L), microequivalents per liter (µeq/L), practical salinity units (psu), milligrams per liter (mg/L), or micrograms per liter (µg/L).

Concentrations of dissolved oxygen and dissolved nitrogen gas are reported in micromoles per liter (µmol/L) as O_2 and N_2, respectively, unless noted otherwise.

Concentration of nitrate plus nitrite ($NO_3 + NO_2$) is reported as micromoles per liter (µmol/L) nitrate-nitrogen (NO_3-N) unless noted otherwise because nitrite concentration was usually small.

Excess air concentrations are reported in units of cubic centimeters at standard temperature and pressure per liter of water (ccSTP/L).

Site identifiers use shorthand “F” for “MA-FSW” unless noted otherwise.

Abbreviations

DIC	dissolved inorganic carbon
EPA	U.S. Environmental Protection Agency
MEP	Massachusetts Estuaries Project
MLS	multilevel sampler
PVC	polyvinyl chloride
TMDL	total maximum daily load
USGS	U.S. Geological Survey

Geochemical Conditions and Nitrogen Transport in Nearshore Groundwater and the Subterranean Estuary at a Cape Cod Embayment, East Falmouth, Massachusetts, 2013–14

By John A. Colman,[1] Denis R. LeBlanc,[1] J.K. Böhlke,[1] Timothy D. McCobb,[1] Kevin D. Kroeger,[1] Marcel Belaval,[2] Thomas C. Cambareri,[3] Gillian F. Pirolli,[1] T. Wallace Brooks,[1] Mary E. Garren,[2] Tobias B. Stover,[2] and Ann Keeley[2]

Abstract

Nitrogen transport and transformation were studied during 2013 to 2014 by the U.S. Geological Survey, in cooperation with the U.S. Environmental Protection Agency, in a subterranean estuary beneath onshore locations on the Seacoast Shores peninsula, a residential area in Falmouth, Massachusetts, served by septic systems and cesspools, and adjacent offshore locations in the Eel River, a saltwater embayment connected to the ocean. The field investigation included installation and sampling of clusters of wells and temporary sampling points near a transect extending from about 35 meters (m) onshore to 18 m offshore.

The fresh groundwater at the study site formed a lens about 11 m thick at the shoreline that was underlain by saline groundwater. Groundwater flow in the water-table aquifer was oriented northwestward toward the embayment. Nitrate concentrations in the fresh groundwater at a site about 35 m onshore increased in the downward direction from less than 500 micromoles per liter near the water table to about 1,700 micromoles per liter just above the freshwater/saltwater transition zone. Dissolved oxygen was largely absent in the onshore fresh groundwater. Distributions of salinity, dissolved oxygen, and nitrate at the shoreline and offshore generally were similar to those onshore; at some locations, however, shallow saline water was present above the freshwater, and there were scattered occurrences of elevated dissolved oxygen concentrations.

Geochemical indicators of nitrate reduction, including concentrations of the reaction product nitrogen gas, stable isotope ratios of nitrate and nitrogen gas, and changes in alkalinity, provided evidence for nitrate reduction in two zones separated vertically by a zone 7–8 m thick with no evidence of nitrate reduction. The shallow nitrate-reduction zone was near the water table in fresh groundwater onshore, where nitrate reduction may be related to particular recharge conditions at nearby sources. The shallow nitrate-reduction zone also may be related to an interval of fine-grained sediments at about the same altitude (−1 to −6 m relative to the National Geodetic Vertical Datum of 1929), where flow is slower and reactive electron donors such as solid organic carbon, iron, or sulfide phases may be present to drive the reduction. The deep nitrate-reduction zone was near the freshwater/saltwater transition zone, where nitrate reduction may be related to mixing of freshwater containing nitrate and saltwater containing dissolved organic carbon and ammonium, or to fine-grained sediments near the transition zone. The maximum amount of nitrate converted to nitrogen gas was estimated to be less than or equal to 300 micromoles per liter in both nitrate-reduction zones.

The presence of nitrate and low dissolved oxygen concentrations in the 7–8-meter-thick zone between the shallow and deep nitrate-reduction zones are conditions that could permit nitrate reduction. The absence of evidence of nitrate reduction in the high-nitrate zone may have resulted from the lack of reactive electron donors in that depth interval. The high-nitrate zone dissipated somewhat in the offshore direction, but the current study did not extend far enough to encompass the fresh groundwater discharge area or determine how much of the nitrate was removed prior to discharge.

A shallow intertidal saltwater cell was formed during a spring tide by saltwater infiltration during tidal run-up on the beach. Nitrate reduction might have occurred if nitrate-containing fresh groundwater discharging to the estuary mixed with the saltwater containing dissolved organic carbon in this zone, but samples collected from the intertidal saltwater cell during this study were not analyzed for indicators of nitrate reduction.

Elevated dissolved oxygen concentrations in fresh groundwater 9 m offshore may indicate that groundwater flow was partly oblique to the sampling transect or that

[1]U.S. Geological Survey.

[2]U.S. Environmental Protection Agency.

[3]Cape Cod Commission.

groundwater from a regional flow system was converging under the river near the study area. Flow directions also may have been affected by aquifer heterogeneity such as the shallow fine-grained sediments onshore and at the bottom of the Eel River. Improved understanding of the fate of nitrate in this type of complex setting might be gained by including additional characterization of aquifer heterogeneity and groundwater flow and extending investigations of nitrate reduction to the shallow sediments in the intertidal saltwater cell and adjacent subtidal zone and to locations farther offshore beneath the estuary.

Introduction

Nutrient pollution is one of New England's most widespread, costly, and challenging environmental problems. On Cape Cod, nitrogen loading to embayments and the resulting eutrophication of estuaries are among the most pressing environmental challenges faced by coastal communities (Valiela and others, 1992; Nixon, 1995; Short and Burdick, 1996; Valiela and others, 2000; Howarth and others, 2002).

Nitrogen commonly is the limiting nutrient to phytoplankton and macroalgae in coastal marine systems. An increased supply of nitrogen can cause decreased water clarity from increased growth of plants and macroalgae that can obscure more desirable plant species (for example, eelgrass) and damage ecosystems that favor finfish and shellfish. Because tourism, retirement, and fishing are the mainstays of the Cape Cod economy, degradation of the coastal aquatic ecosystems is an important issue on Cape Cod.

In 2000, recognizing the importance of nitrogen in eutrophication of Cape Cod waters, the Massachusetts Department of Environmental Protection established the Massachusetts Estuaries Project (MEP) to evaluate nitrogen loading and assimilative capacity in 70 Cape Cod embayments (Massachusetts Department of Environmental Protection, 2018). In about 40 percent of the embayments studied to date (2018), these evaluations have resulted in total maximum daily loads (TMDLs), which establish regulatory, numeric limits on nitrogen loading. Currently (2018), Massachusetts towns covered by the MEP are weighing alternative nitrogen remediation actions that would meet the TMDL requirements.

On Cape Cod, principal sources of nitrogen are onsite disposal of domestic sewage (through cesspools and septic systems) and lawn fertilizer (Valiela and others, 2000). Nitrogen transport from these sources to coastal waters in most areas of Cape Cod is largely through groundwater because the more densely developed areas are near the coast, and streams obtain most of their flow from recharge onto less developed inland areas (Walter and others, 2004). In much of the Cape Cod aquifer, where subsurface conditions are aerobic and the predominant nitrogen form is nitrate, transport beyond the near field of septic systems, where approximately 20 percent nitrogen loss occurs (Costa and others, 2002), is likely to occur with relatively little natural attenuation. Where subsurface conditions are anaerobic, however, nitrogen transport can be attenuated. Nitrate can be converted to gaseous forms (N_2 or N_2O), and ammonium can be oxidized anaerobically or its transport can be retarded by sorption onto solid phases in the aquifer. Such conditions and losses have been documented in landfill plumes and in large plumes caused by municipal sewage disposal (LeBlanc, 1984; Christensen and others, 1994; DeSimone and others, 1996; Smith and others, 2004; Repert and others, 2006; Cozzarelli and others, 2011; Barbaro and others, 2013; Smith and others, 2013). The nitrogen attenuation reactions are facilitated by microbial processes and include denitrification—the transformation of nitrate (NO_3) and nitrite (NO_2) under anaerobic (no dissolved oxygen) conditions to molecular nitrogen gas (N_2)—and anammox—anaerobic oxidation of ammonium (NH_4) that transforms ammonium and nitrite to nitrogen gas.

The subterranean estuary (the area near the coastline and below the sediment/water interface, where freshwater and saltwater mix) through which groundwater must pass to move from land to offshore surface water represents an additional location of potential nitrogen attenuation. Biodegradation of organic carbon, which is likely present in offshore sediments and in infiltrating seawater, can consume oxygen and eventually nitrate as freshwater moves offshore before discharging to the coastal waters. Other electron donors such as sulfide and reduced iron also can contribute to oxygen and nitrate reduction. The distribution of such reactions and their relation to flow, which are less well documented in the subterranean estuary than in wastewater disposal plumes and landfills, are the subject of this investigation.

Although not widely investigated, nitrogen attenuation in the subterranean estuary has been studied at Waquoit Bay in Falmouth, Massachusetts (Kroeger and Charette, 2008; Spiteri and others, 2008). One limitation of the studies at Waquoit Bay was their location in an estuarine preserve where housing (and thus septic system sources of nitrogen) was restricted. A principal goal of our research was to extend investigation to a coastal site with dense housing and larger nitrogen sources.

The site chosen was the Eel River study site on the Seacoast Shores peninsula in East Falmouth, Mass. Nitrogen transport and transformation were studied at the site during 2013 to 2014 by the U.S. Geological Survey, in cooperation with the U.S. Environmental Protection Agency (EPA). Seacoast Shores is a typical coastal residential area with dense housing (9.14 houses per hectare) (figs. 1 and 2) that uses onsite cesspools and septic systems for wastewater disposal. Because of the dense housing, a high nitrogen concentration is likely in the underlying aquifer. This high concentration could facilitate assessment of the subterranean estuary's capacity to reduce nitrate concentrations by natural biogeochemical processes. Other selection criteria were length of settlement time (buildout was complete by 1970) and proximity to a coastal receptor, the Eel River estuary. Additionally, a previous study reported elevated nitrate concentrations in several monitoring wells on the peninsula (Thomas Cambareri, Cape Cod Commission, oral presentation for Waquoit Bay National Estuarine Research Reserve Research Exchange Day, 1994).

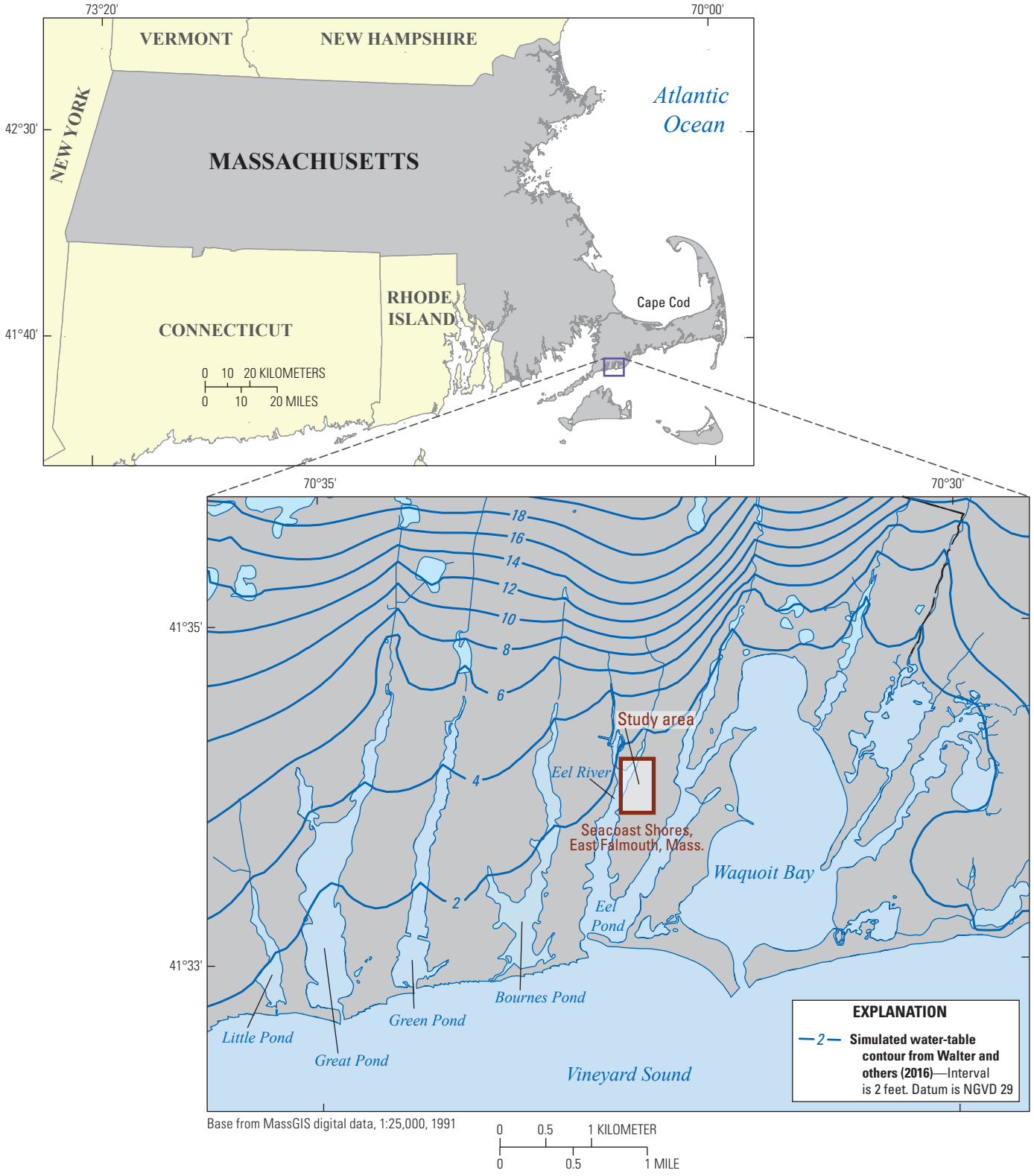

Figure 1. The coastal embayments in southern Falmouth, the regional water-table contours, and the location of the study area at the Eel River and Seacoast Shores peninsula in East Falmouth, Massachusetts.

Figure 2. Aerial photograph from 2009 showing the study area at the Eel River and Seacoast Shores peninsula, East Falmouth, Massachusetts.

This report describes the project development and the methods of collecting data and evaluating nitrogen attenuation; the report includes hydrogeologic and geochemical observations, discusses nitrogen fate and transport, and presents a resulting conceptual model of nitrogen attenuation at the Eel River subterranean estuary. Several methodological sections are included in an appendix. The report can be used in the design of future nitrogen remediation investigations because of its geochemical characterization of a peninsular, coastal area that has a high density of housing and that could be targeted for installation of sewers to prevent coastal eutrophication.

Geographic, Geologic, and Hydrologic Setting

The Seacoast Shores residential area occupies a peninsula that extends southward from the main land area of Cape Cod into the Waquoit Bay system (fig. 1). Bordered by saline, tidal surface-water bodies that include the Eel River on the west and Eel Pond and the Childs and Seapit Rivers on the south and east, the peninsula is about 2.6 kilometers long and as much as 615 meters (m) wide (fig. 2). Land-surface altitudes generally decrease from about 10 m (altitudes are given relative to the National Geodetic Vertical Datum of 1929 [NGVD 29]) in the north to less than 1 m in the south. The topography is generally flat, with steep bluffs along the sides of the peninsula and a few low-lying areas in the interior.

The peninsula and its adjacent, narrow saltwater bays are similar to other peninsulas and bays along the southern shore of Cape Cod in the town of Falmouth. The bays occupy valleys that were cut into the glacial outwash plain at the end of the Pleistocene Epoch. The valleys were subsequently drowned when sea level rose, leaving the intervening areas of the outwash plain as long, narrow peninsulas and coastal necks. The aquifer materials are glacial outwash sand and gravel that generally grade downward into fine-grained glaciolacustrine sand, silt, and clay (Oldale, 1992; Masterson and others, 1997). The unconsolidated sediments are about 90 m thick and lie on crystalline, granitic bedrock (Fairchild and others, 2012).

The Seacoast Shores peninsula is a part of the Sagamore flow lens, a part of the Cape Cod aquifer consisting of several hydrogeologic units (outwash plains, terminal and ground moraines, ice contact deposits) mainly composed of sand and gravel, with some silt and clay. The units were deposited during the last glaciation of New England. The regional aquifer is a shallow, unconfined hydrologic system in which groundwater flows radially outward from the top of a water-table mound that underlies western Cape Cod (LeBlanc and others, 1986; Masterson and others, 1997; Walter and Whealan, 2005). The study area is along the southern coastline, where the regional groundwater system discharges to Vineyard Sound. The peninsular freshwater aquifer is bounded at the top by the water table, at the bottom by the freshwater/saltwater interface, and at the lateral boundaries by the tidal saltwater bodies. The freshwater aquifers beneath the peninsulas are seaward extensions of the much larger regional groundwater-flow system that also discharges to the tidal saltwater bodies. The effects of the discharge from the regional system on local freshwater flow on the peninsulas are not well understood.

The Seacoast Shores peninsula receives an estimated 114 centimeters per year (cm/yr) of precipitation. About 60 percent of the precipitation (69 cm/yr) recharges the aquifer at the water table (Walter and Whealan, 2005); the remainder largely is lost to evapotranspiration. Surface runoff is negligible owing to the sandy soils and low topographic relief of the area. The horizontal hydraulic conductivity of the sand and gravel is estimated to be about 60 to 110 meters per day (m/d), and that of the interbedded fine sands and silts in the aquifer is estimated to be less than 15 m/d (Walter and Whealan, 2005).

Seacoast Shores is one of the most densely developed neighborhoods on Cape Cod. Water supply is public water obtained from wells and a lake inland from the peninsula. Wastewater disposal is by private onsite systems. The peninsula was undeveloped and forested until the late 1930s. During World War II, it was used by the U.S. Army to access an adjacent island in Waquoit Bay for amphibious training (Keay, 2001). The peninsula was subdivided in 1947 into the street layout seen today. Building began slowly in the late 1940s and early 1950s along the eastern shore near Bayside Drive (fig. 2), but the pace of building increased during the 1960s. By about 1970, buildout was essentially complete.

The earliest homes were supplied by onsite domestic wells. Installation of town water was done in phases and largely completed by 1970. Water-use records indicate a mixture of year-round and seasonal homes, although year-round homes currently (2018) predominate. Data from the Cape Cod Commission indicate about 1,000 dwellings are on the peninsula, with total water use (2010) averaging over 92,000 gallons per day (Cape Cod Commission, 2015), most of which is recharged to the local groundwater-flow system through onsite domestic wastewater disposal. This amount of water use, if spread over the total area of the peninsula (1.2 square kilometers), would be equivalent to approximately 10.5 cm/yr, or about 15 percent of the annual recharge from precipitation over the same area.

Previous Investigations at Seacoast Shores and Waquoit Bay

Previous studies examined the Seacoast Shores groundwater system and the subterranean estuary and tidal mixing at Waquoit Bay. The Waquoit Bay investigations provided insights into groundwater-flow patterns and nitrogen transport in the subterranean estuary.

Seacoast Shores Groundwater System

In 1993, the Cape Cod Commission collected sediment cores, installed monitoring wells, and collected groundwater samples at three sites (SCS–2, SCS–3, and SCS–4) along an east-west line (fig. 2, section *A–A′*) across the Seacoast Shores peninsula to examine nitrogen concentrations in shallow groundwater in an area served by onsite wastewater disposal (Thomas Cambareri, Cape Cod Commission, oral presentation for Waquoit Bay National Estuarine Research Reserve Research Exchange Day, 1994). At each location, sediment samples were collected during drilling by using the split spoon method. A cluster of 4 to 5 monitoring wells was installed to a maximum depth of 18 m in each auger boring (fig. 3). Specific conductance was measured for water samples collected from a screened hollow-stem auger and the wells to determine the distribution of fresh and saline groundwater (fig. 3*B*), and the installed wells were sampled for laboratory analysis of nitrate and ammonium concentrations (fig. 3*C*).

The borings encountered mostly medium to coarse sand. At the western site (SCS–2), however, medium sand and silt were present from about 1 to 6 m below NGVD 29, and fine sand and silt were present below the freshwater/saltwater interface near the bottoms of the eastern and western borings (SCS–2 and SCS–3, fig. 3*A*). The altitude of the water table at the three sites was approximately 0.4 m above NGVD 29. The freshwater/saltwater interface was encountered at each site. The freshwater lens was about 14 m thick near the western side and middle of the peninsula and about 8 m thick at the eastern site (fig. 3*B*).

Elevated nitrate concentrations as high as 1,200 micromoles per liter (µmol/L) were measured in the deepest freshwater immediately above the freshwater/saltwater interface at the nearshore clusters (fig. 3*C*). Elevated nitrate concentrations were not measured at the midpeninsula site, although sampling for nitrate at this site did not extend to the freshwater/saltwater interface. Ammonium concentrations in freshwater were less than 20 µmol/L.

Nitrogen Transport and Groundwater Flow in the Cape Cod Subterranean Estuary

Past investigations of the subterranean estuary on Cape Cod focused on the upper end of Waquoit Bay in Falmouth (Belaval and others, 2003; Michael and others, 2003, 2005, 2011; Kroeger and Charette, 2008; Spiteri and others, 2008; Abarca and others, 2013), Red Brook Harbor in Falmouth (McCobb and LeBlanc, 2002), and Salt Pond on the outer Cape (Crusius and others, 2005; Cross and others, 2008). Of these investigations, only the work at Waquoit Bay included estimation of nitrogen loss in the subterranean estuary, and results there varied. For example, Spiteri and others (2008) concluded that a shallow anaerobic ammonium plume moved conservatively toward the beach until ammonium was nitrified where aerobic conditions were encountered. Removal of nitrate, carried in a deeper aerobic plume, was not observed and was thought to be limited by a lack of reactive dissolved organic carbon. In contrast, Kroeger and Charette (2008) indicated that approximately 65 percent of dissolved inorganic nitrogen was lost during transit toward the discharge zone, within both the freshwater zone and the subterranean estuary, based on observed decreasing concentrations of both nitrate and ammonium co-occurring with ^{15}N enrichment of the residual pools. The apparent loss occurred in regions of mixing between nitrate-bearing, suboxic, fresh groundwater and ammonium-bearing near-anoxic fresh or saline groundwater. The different interpretations from Kroeger and Charette (2008) and Spiteri and others (2008) may be due in part to seasonal or interannual variations in chemical and hydrological conditions. Modeling investigations based on hydrologic and geochemical conditions at Waquoit Bay (Anwar and others, 2014) and the coastal peninsulas in Falmouth (Colman and others, 2015) indicated nitrate removal rates in the subterranean estuary that ranged from 20 percent in a simulation using aquifer chemistry conditions of no dissolved oxygen, 500 µmol/L nitrate, slow organic matter degradation kinetics, and a small tidal amplitude (0.2 m) (Colman and others, 2015), to 90 percent in a simulation with more labile marine organic matter entrained with infiltrating seawater and tides of 0.5-m amplitude (Anwar and others, 2014).

The investigations at the Waquoit Bay site in Falmouth (Belaval and others, 2003; Michael and others, 2003, 2005, 2011; Kroeger and Charette, 2008; Spiteri and others, 2008; Abarca and others, 2013) also examined groundwater flow in the subterranean estuary. The physics of tidal mixing were investigated at Waquoit Bay by using two-dimensional computer models calibrated by seepage-meter, subsurface-salinity, and hydraulic-head measurements (Michael and others, 2003, 2005; Abarca and others, 2013). The modeling efforts from these investigations led to a description of flow in the subterranean estuary (fig. 4). In general, fresh groundwater discharge occurs just below the level of low tide. Saltwater discharge from an intertidal saltwater cell formed by intertidal saltwater infiltration occurs just landward of the fresh groundwater discharge. Deep saltwater discharge from a deep saltwater wedge occurs seaward of the fresh groundwater discharge. Farthest offshore, deep saltwater infiltration occurs seaward of the deep saltwater discharge.

Methods

Methods for sampling design, well installation, water-level determination, and water sampling and analysis are described in the following sections, appendix 1, and Huntington and others (2018).

A. Lithology

B. Specific conductance

C. Ammonium and nitrate

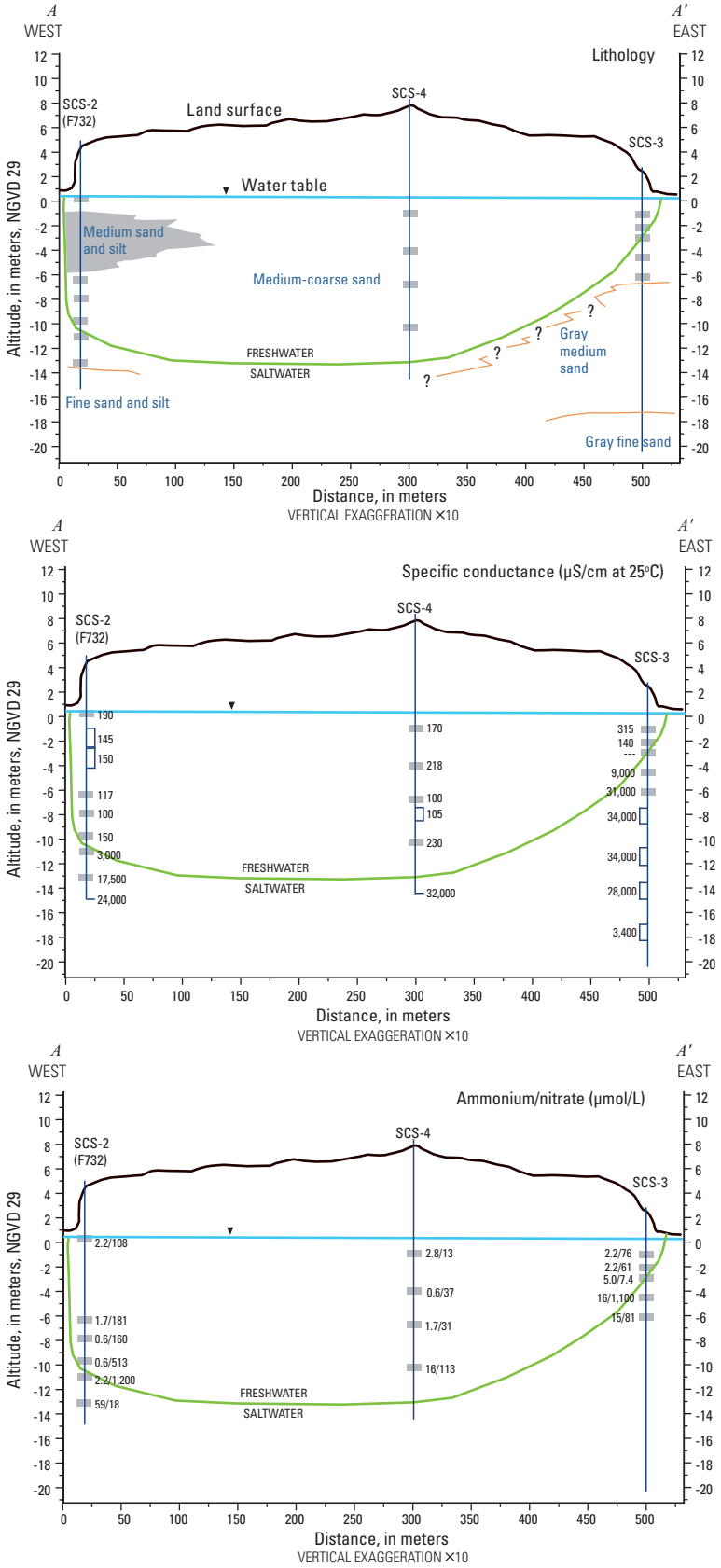

Figure 3. Section *A*–*A*′ showing the approximate locations of geologic borings and monitoring wells installed and sampled in 1993, and *A*, lithology, *B*, specific conductance, and *C*, ammonium and nitrate concentrations, Seacoast Shores peninsula, East Falmouth, Massachusetts. Gray rectangles indicate positions of well screens. Open boxes indicate intervals sampled by using a screened hollow-stem auger. The gray area indicating medium sand and silt is approximate. Figure is adapted from a presentation by Thomas Cambareri for Waquoit Bay National Estuarine Research Reserve Research Exchange Day, March 21, 1994, filed at the Cape Cod Commission, Barnstable, Mass. Location of the section is shown on figure 2. µS/cm at 25 °C, microsiemens per centimeter at 25 degrees Celsius; µmol/L, micromole per liter.

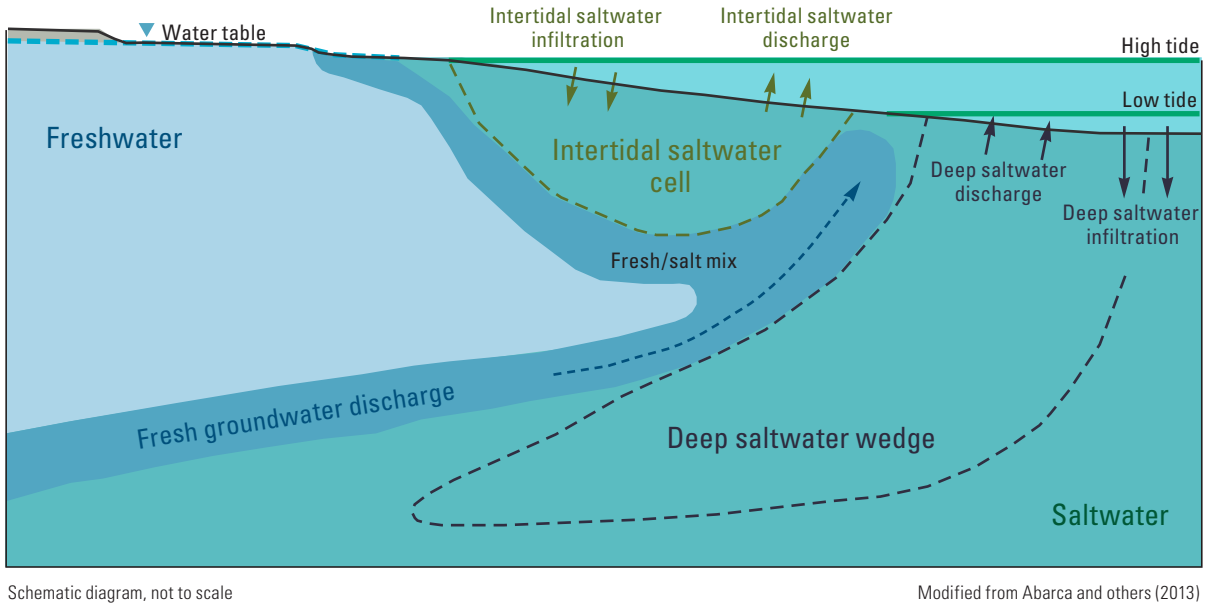

Figure 4. Schematic diagram showing groundwater-flow patterns in the subterranean estuary at Waquoit Bay, East Falmouth, Massachusetts.

Sampling Design and Data-Collection Network

Several sites near saltwater ponds in southern Falmouth, including Great Pond, Green Pond, and the Eel River, were considered for the study (fig. 1). Details on site selection are given in appendix 1.

Limitations on access to the shore narrowed the potential sites to two locations near the Eel River on the western side of the Seacoast Shores peninsula (near the intersections of Bayside Drive and Woodside Drive with Edgewater Drive West). A multilevel sampler (MLS) was installed at each location (F723–M01 and F724–M01, fig. 5). On the basis of preliminary lithologic and chemical data collected from the MLSs, the Bayside Drive site was selected for further study. Five water-table wells were installed upgradient of the site, and more than 35 additional sampling locations were established on land near the shore and offshore in the Eel River (fig. 6). Well-installation methods are described in appendix 1.

A pressure-transducer tide gage was installed to monitor the water level in the Eel River near the study area. The gage consisted of an open-bottom polyvinyl chloride (PVC) standpipe that was secured to a permanent dock piling at a nearby private residence (figs. 5 and 6). The tide gage installation is described in appendix 1.

Instrumentation for collecting samples at depth was deployed primarily along section *B–B′*, extending from site F724, which is 35 m landward of the shore, to site F743, which is 18 m offshore (fig. 7).

Groundwater levels in the water-table wells were measured manually on four occasions during the study by using an electric tape. Manual measurements of water levels were also made in pairs of shallow and deep monitoring wells at two nearshore well clusters (sites F726 and F732) during a full tidal cycle in August 2014 to examine the effects of tide on hydraulic heads in the fresh groundwater system.

For the period from August 7, 2013, to October 23, 2013, water levels were recorded continuously in the five water-table wells and in the shallowest and deepest wells set in fresh groundwater at the shoreline cluster (F726) by using pressure transducers (Onset Computer Corp., HOBO logger U20–001–04, Bourne, Mass.). Water-level measurements made at 15-minute intervals were used to determine hydraulic gradients; for the set of measurements made at each interval, planes were fit to the water-level altitudes for triangular arrangements of the wells (McCobb and others, 1999).

The thickness of the soft bottom sediment beneath the Eel River was measured at seven points in the study area by pushing a 1-centimeter-diameter steel tile probe by hand into the soft sediment until a firm layer was encountered. The depths of penetration were recorded in an area that extends to 66 m from shore.

Water-Quality Sampling and Quality Assurance

Samples for water-quality determination were collected by peristaltic pumping from tubing attached to the tops of sampling ports for the MLSs, well points, and pushpoints, and from tubing extended below the water level in monitoring wells. Field measurements of temperature and pH were made by using an Orion pH meter; dissolved oxygen was measured in the field by using a portable colorimeter and a Yellow

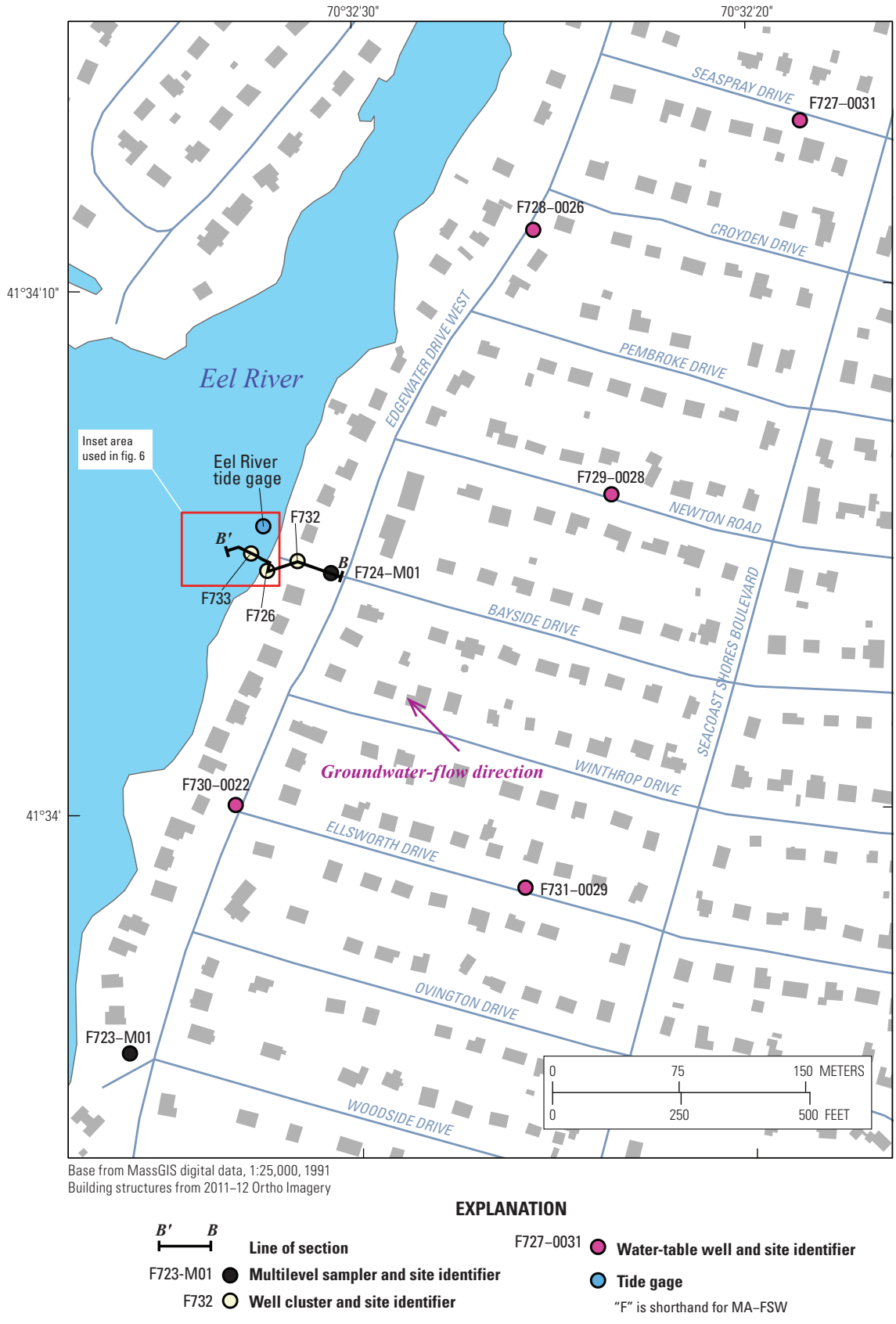

Figure 5. Locations of monitoring sites near the eastern shore of the Eel River, Seacoast Shores peninsula, East Falmouth, Massachusetts.

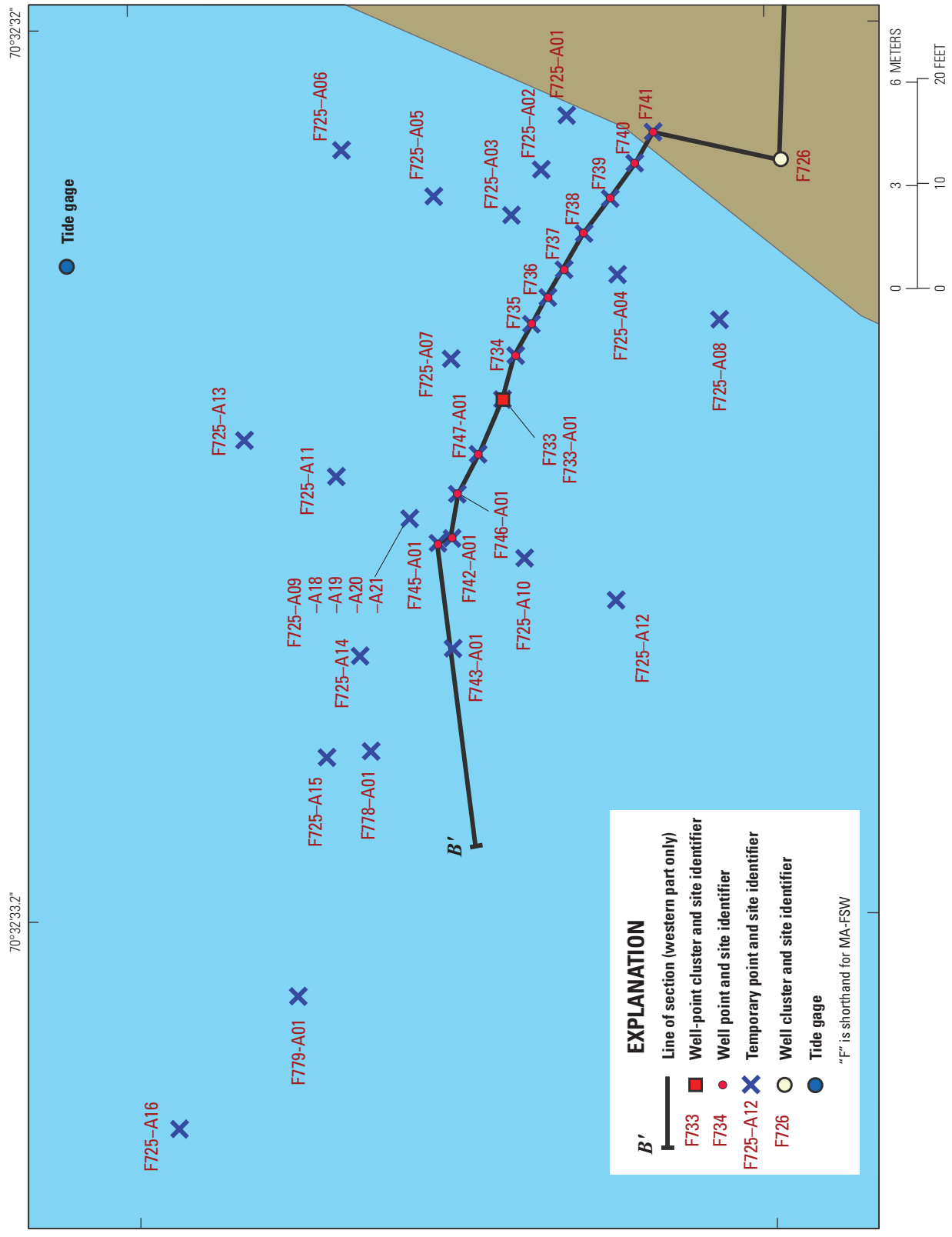

Figure 6. Locations and types of monitoring sites near the western part of section *B–B′*, eastern shore of the Eel River, Seacoast Shores peninsula, East Falmouth, Massachusetts.

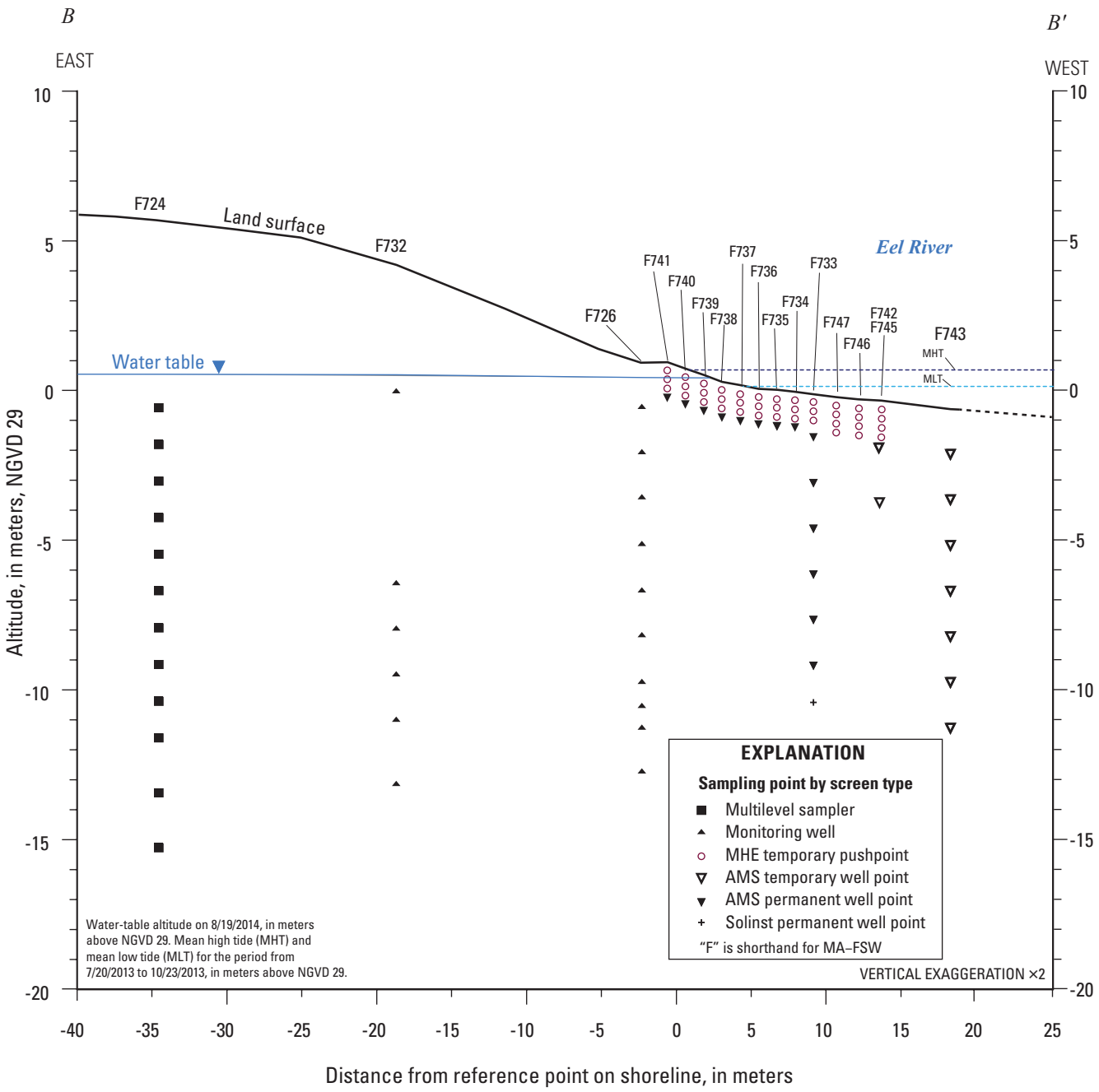

Figure 7. Section *B–B′* showing vertical locations of monitoring sites, land surface, and the water table near the shore of the Eel River, Seacoast Shores peninsula, East Falmouth, Massachusetts. Location of the section is shown on figures 5 and 6.

Springs Instruments dissolved oxygen probe and meter. Salinity was estimated from specific conductance (American Water Works Association, 2017), except where noted. Details about the water-quality sampling and chemical analysis are given in appendix 1 and the data dictionary in Huntington and others (2018), respectively. Bottles used, volumes collected, preservation and shipping methods, and analytical techniques were consistent with the EPA quality-assurance project plan when applicable, or with those of other laboratories for specialized analyses (table 1.2, appendix 1).

Quality assurance was addressed by field duplicates, interlaboratory split samples, and standard reference samples. The quality-assurance samples were collected at the minimum rate of 5 percent of the total sample load for each constituent. Blind standard reference samples were analyzed to confirm the high concentrations of nitrate that were measured. Quality-assurance data are described in appendix 1. An analytical-method comparison dataset was generated for measurements of dissolved gas concentrations (N_2 and Ar) by membrane-inlet mass spectrometry and by gas chromatography (fig. 1.3, appendix 1).

Determination of Nitrogen Attenuation

Flow-path analysis and direct measurements were used for evaluating nitrogen attenuation. Flow-path analysis was based on the assumption of a constant source of nitrogen at the recharge location and steady-state recharge conditions so that changes in nitrogen concentration downgradient along a flow path could be attributed to reactions such as denitrification. Application of the method also required a monitoring network with sampling points distributed along a groundwater flow path. The ratio of nitrogen concentration in recharge at the beginning of the flow path to concentration at the downgradient site indicated the loss factor. Even in cases where a constant source and steady-state flow may not pertain, the approach may be useful for setting limits or ranges of nitrogen change.

The direct-measurement approach included three different techniques for assessing nitrate losses: (1) use of concentrations of the dissolved gases nitrogen and argon to estimate amounts of excess N_2 produced by nitrate reduction; (2) evaluation of stable isotope ratios in nitrate and nitrogen gas for evidence of isotopic fractionation caused by nitrate reduction; and (3) determination whether alkalinity gradients were consistent with organic carbon oxidation coupled with apparent nitrate reduction. These techniques are described in appendix 1.

Hydrogeologic and Geochemical Observations

Observations reported in this section include water levels measured at wells, field water-quality characteristics measured during sampling, and chemical analytical results from laboratory analyses. All well-location and water-level data collected in this investigation are stored in the National Water Information System database (U.S. Geological Survey, 2018), available at https://doi.org/10.5066/F7P55KJN. All water-quality data are listed in the data release associated with this publication (Huntington and others, 2018), available at https://doi.org/10.5066/F7RR1WF0.

Thickness of Soft River-Bottom Sediments

Measurements of the thickness of the soft fine-grained sediments on the bottom of the Eel River indicated an increasing thickness in the offshore direction (fig. 8). Thickness ranged from 0 m at a distance of 11 m offshore to 1.74 m at a distance of 60 m offshore.

Water Levels and Hydraulic Gradients

The water table generally sloped downward toward the Eel River from the interior of the peninsula (fig. 9). The largest water-table gradients were near the shore. East of Edgewater Drive West, the water table was nearly flat north of Bayside Drive (one-tenth of the gradient at the shore) and formed a mound south of Bayside Drive. The mound may be related to the increasing width of the peninsula south of Bayside Drive (fig. 2). The mound also could be the result of localized fine-grained sediments, but borings have not been drilled in this area to characterize the aquifer sediments.

Time series of horizontal hydraulic gradients were derived from five water-table wells with continuous records of water levels for an 11-week period from August 7, 2013, to October 23, 2013. The mean magnitude of the hydraulic gradient during the period was 0.00067. The estimated groundwater velocity from Darcy's Law for this gradient, given a hydraulic conductivity of about 30–80 m/d and effective porosity of 0.35 for the glacial sediments near the study site (Walter and Whealan, 2005), is about 0.06–0.15 m/d.

The mean direction of the horizontal hydraulic gradient at the water table during the period was to the northwest (46 degrees west of true north and approximately 20 degrees north of perpendicular to the shoreline [fig. 10*A*]). The standard deviations of the gradient directions for gradient triangles 1, 2, and 3 were 7.9, 27.0, and 4.5 degrees, respectively (fig. 10*B*). The variation in direction for triangle 2 was larger than for the other triangles because the water-table surface between the wells that form that triangle was nearly flat and small differences in water levels substantially affect the computed gradient.

The triangles used to compute the gradient are all east of Edgewater Drive West, which is about 45 m from and parallel to the shore of the Eel River (fig. 10*A*). The water-table contours west of the road become approximately parallel to the shore as the water table slopes downward to the hydrologic boundary formed by the embayment (fig. 9).

The mean tide stage of the Eel River for the period from August 7, 2013, to October 23, 2013, was 0.411 m above NGVD 29. The mean tidal range during this period was 0.52 m (fig. 11*A*). The tidal surface-water body is a discharge boundary for the fresh groundwater system, so groundwater discharge flux is expected to be higher during low tides and lower during high tides.

Water levels at the water-table wells (not including well F726–0005 at the shoreline) were less than 0.38 m above the mean stage of the Eel River during August to October 2013 (fig. 9). Water levels were recorded continuously in 5 of the 7 water-table wells during this period. The water levels varied by less than 0.15 m in all five wells (mean range of variation of 0.11 m). The groundwater level in the shallowest monitoring well at the shore (F726–0005) responded to tidal variations in the Eel River (figs. 11*A* and *C*), but that of well F729–0028, for example, showed only small variations over time and no apparent response to tides in the nearby Eel River (fig. 11*B*).

Groundwater levels were measured during an 8-hour period in pairs of shallow (water table) and deep (near the bottom of the freshwater zone) wells at the shoreline (F726, fig. 5) and 19 m landward of shore (F732, fig. 5) on

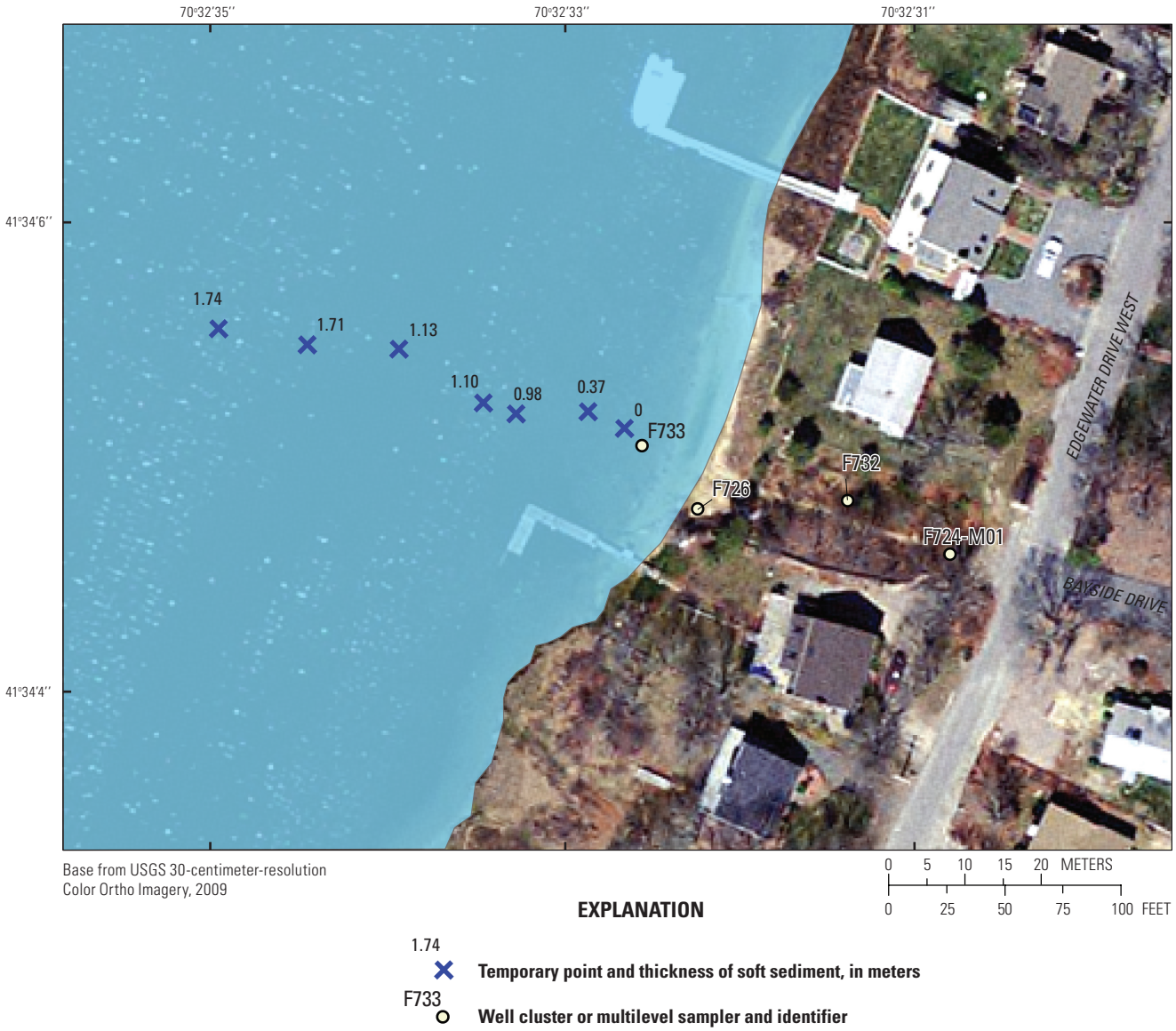

Figure 8. The thickness of soft, fine-grained sediments on the bottom of the Eel River, Seacoast Shores peninsula, East Falmouth, Massachusetts.

August 19, 2014, to examine the effects of tides on hydraulic head at different depths in the aquifer. The tidal response at the water table diminished rapidly with distance from the estuary and was not observed in F732–0015 (fig. 12), which was only 19 m from shore.

The hydrographs for the two shallow wells (solid lines in fig. 12) indicate that the horizontal component of the water-table gradient along the line connecting the wells was consistently toward the Eel River, although the magnitude of the gradient was smaller at high tide. The hydrographs for the two deep wells (dashed lines in fig. 12) indicate that the horizontal component of the hydraulic gradient near the bottom of the freshwater zone along the line connecting the wells also was consistently toward the Eel River. The water level in the deep well at the landward site (F732–0046) responded to the tidal variations, whereas the level in the shallow well (F732–0015) did not, possibly because partial confinement of aquifer flow permitted landward transmittal of tidal effects in the deep parts of the freshwater zone but not in the shallow parts. Confining conditions may have been caused by the zone of fine-grained sediments at an altitude of about 1 to 6 m below NGVD 29 (or about 1.5 to 6.4 m below the water table at well F732–0015) (fig. 3*A*). Comparison of water levels in the shallow and deep wells indicates a consistent upward component of the hydraulic gradient at each site, except for a 1-hour period at low tide when there was a downgradient component at the landward site (F732, fig. 12).

The horizontal and vertical components of the hydraulic gradient are consistent with a conceptual model of fresh groundwater flow from the peninsula toward the Eel River.

Figure 9. Water-level altitudes in seven shallow monitoring wells, the estimated mean stage of the Eel River, and water-table contours on August 19, 2014, Seacoast Shores peninsula, East Falmouth, Massachusetts.

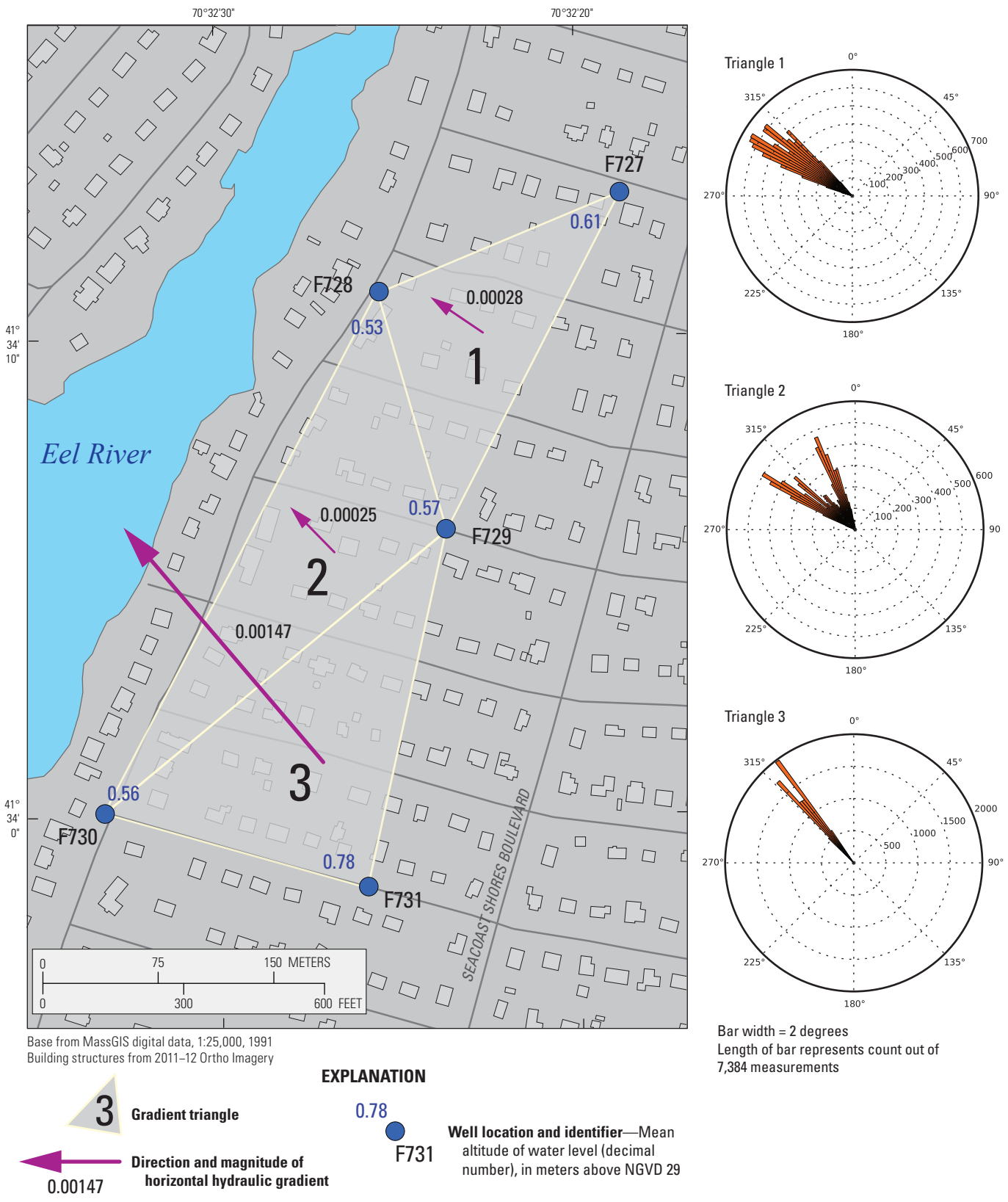

Figure 10. *A*, Mean water levels in five water-table monitoring wells and the estimated mean direction and magnitude of the horizontal hydraulic gradient, and *B*, rose diagrams showing frequency of gradient direction from 15-minute data for the period from August 7, 2013, to October 23, 2013.

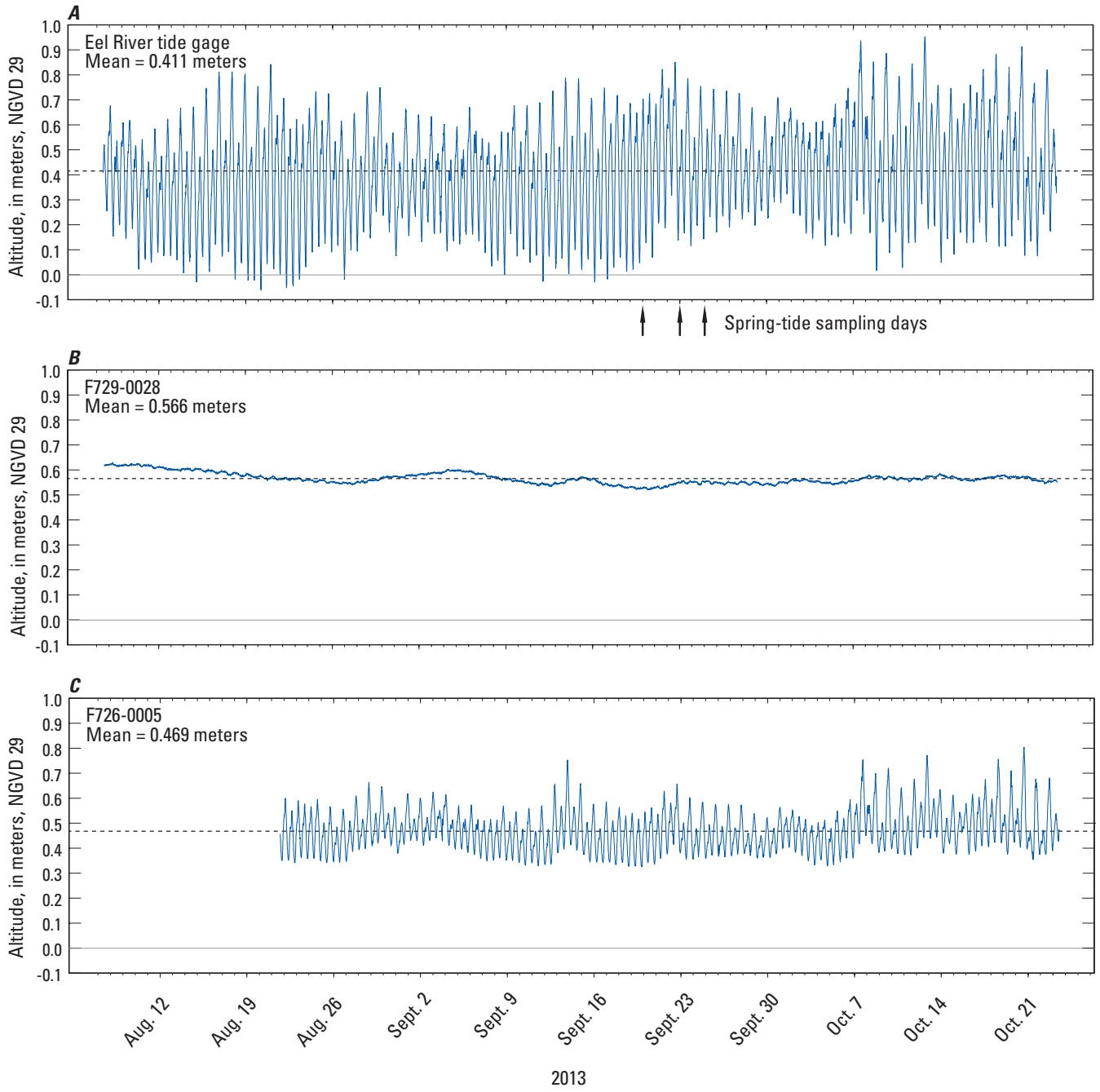

Figure 11. *A*, The tidal stage and sampling days during a spring tide for repeat sampling of surface-water salinity and the shallow nearshore groundwater, and *B*, *C*, water levels in selected monitoring wells near the Eel River, Seacoast Shores peninsula, for the period from August 7, 2013, to October 23, 2013, East Falmouth, Massachusetts. Locations of the wells are shown on figures 5 and 9.

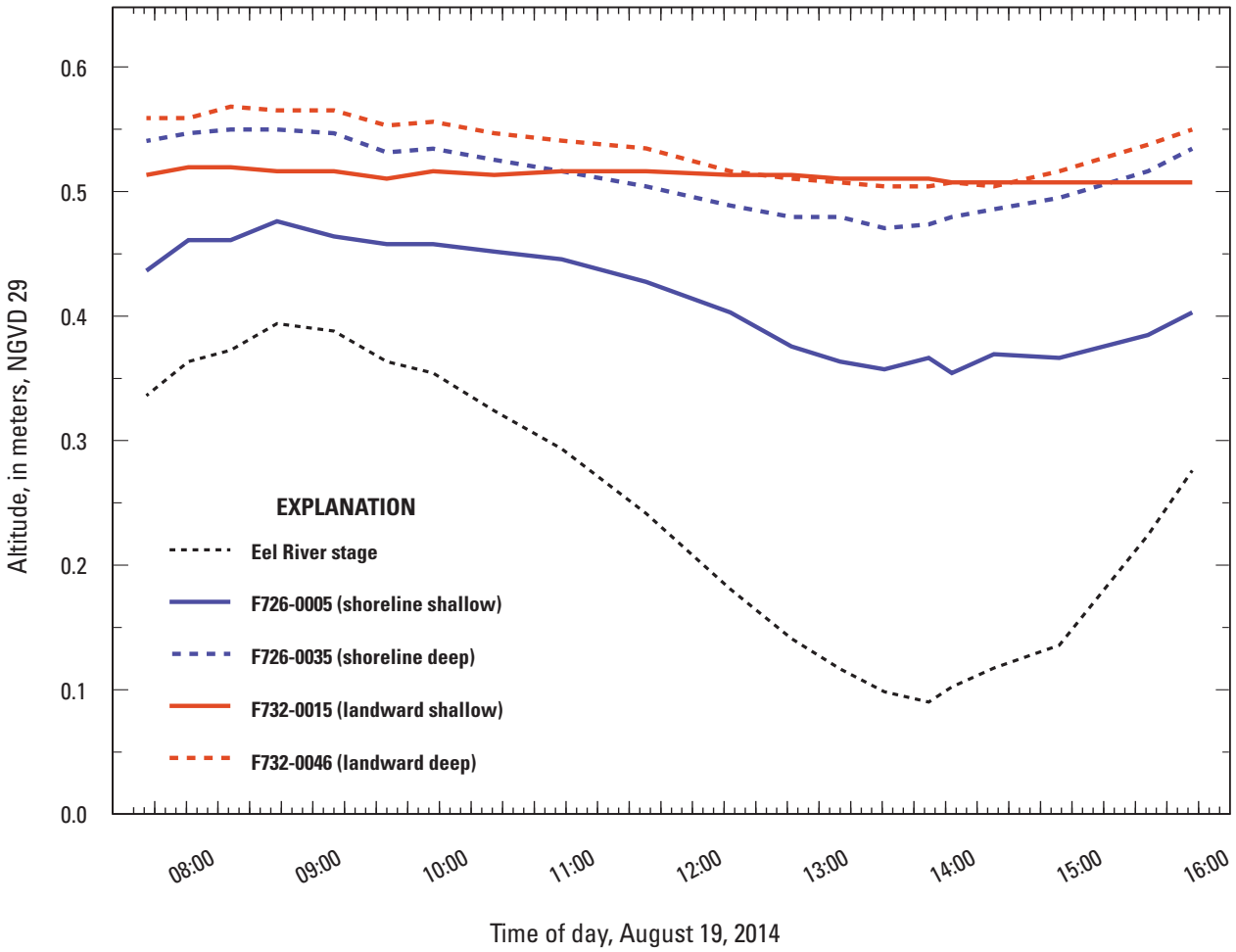

Figure 12. Water-level altitudes during an 8-hour period in shallow and deep monitoring wells and the Eel River, August 19, 2014, Seacoast Shores peninsula, East Falmouth, Massachusetts. Locations of wells are shown on figures 5 and 9.

The horizontal gradient at the water table was consistently northwestward toward the river. The consistently upward gradients in the well pairs also indicate that fresh groundwater in the study area on the western side of the peninsula was flowing upward and discharging to the Eel River.

Freshwater/Saltwater Boundary

The freshwater/saltwater boundary was detected in vertical profiles at four locations between site F724, 35 m onshore, and site F733, about 9 m offshore, along section *B*–*B*′ (fig. 13). The freshwater zone was about 13 m thick at 35 m onshore and about 11 m thick at the shoreline. The transition between fresh and saline groundwater was about 2 m thick. The altitude of the freshwater/saltwater boundary beneath the Eel River decreased slightly with distance offshore, but the boundary did not curve strongly upward to intersect the estuary bottom as in the conceptual model of a typical subterranean estuary flow system (fig. 4). The location of discharge of the deeper fresh groundwater to the estuary was not identified in this investigation. Sampling of freshwater at the study site from shallow points pushed about 0.8 to 2.1 m into the river bottom as far as 27 m from shore (F778–A01, F779–A01, and F725–A14 to F725–A16, fig. 6, and Huntington and others, 2018) and geophysical streaming resistivity surveys along the entire length of the Eel River (Eric White and Carole Johnson, U.S. Geological Survey, written commun., 2015) suggest that the discharge location of the deep fresh groundwater may be farther offshore and possibly farther to the south in the estuary than the extent of this investigation.

Geochemical Characteristics

The geochemical environment of the subsurface and the distributions of selected nitrogen species were ascertained from chemical results for samples from four vertical profiles (F724, F726, F733, F743) on an approximately east-west transect extending from 35 m onshore to 18 m offshore (figs. 5 and 6 for sampling locations, fig. 14 for concentrations). The orientation of the transect (N 65° W) was about 20 degrees

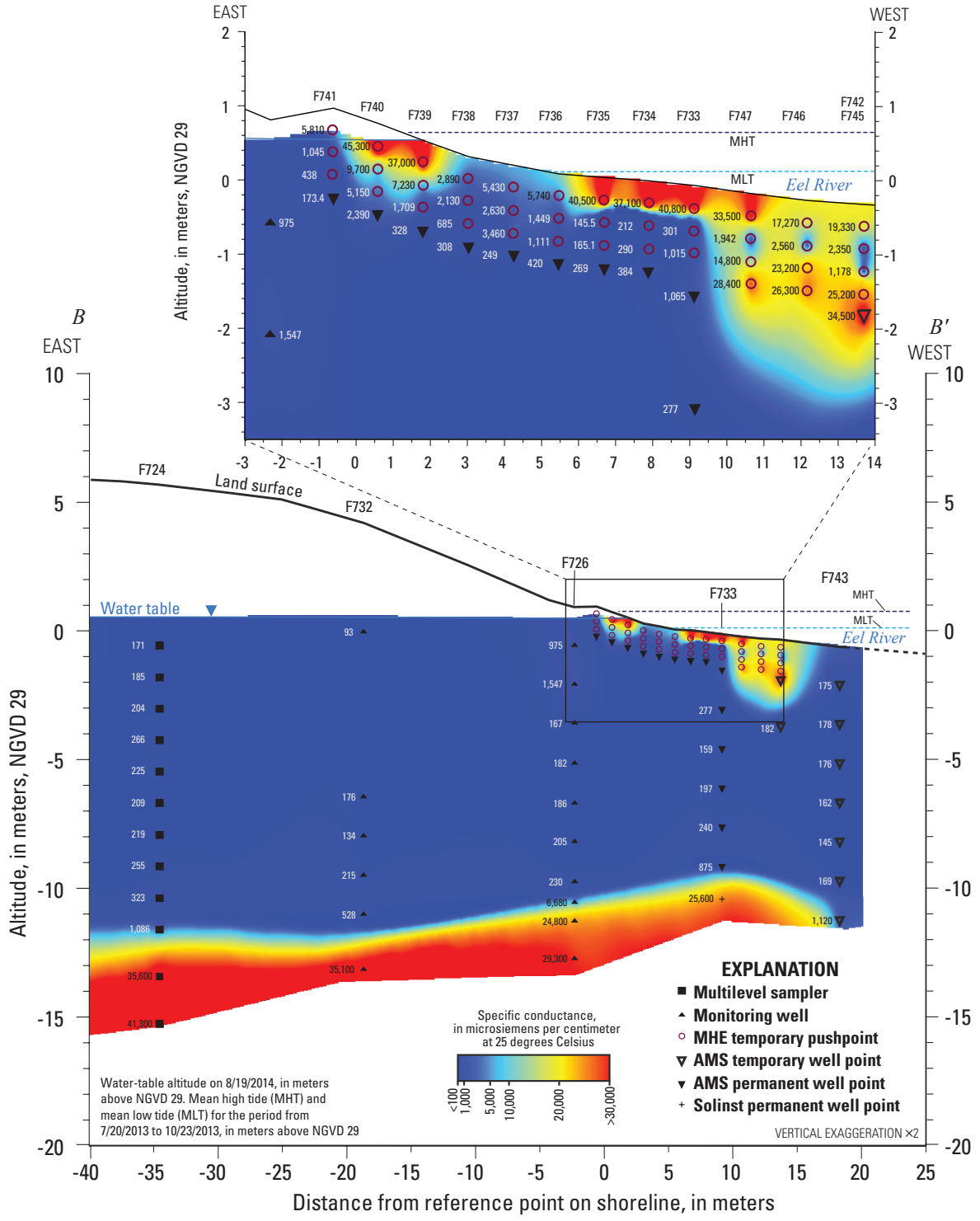

Figure 13. Distribution of specific conductance in groundwater along section *B*–*B*′ in September 2013 near the Eel River, Seacoast Shores peninsula, East Falmouth, Massachusetts, sampled September 22 to 25, 2013, except F742 and F743 sampled September 5, 2013. Location of the section is shown on figure 5.

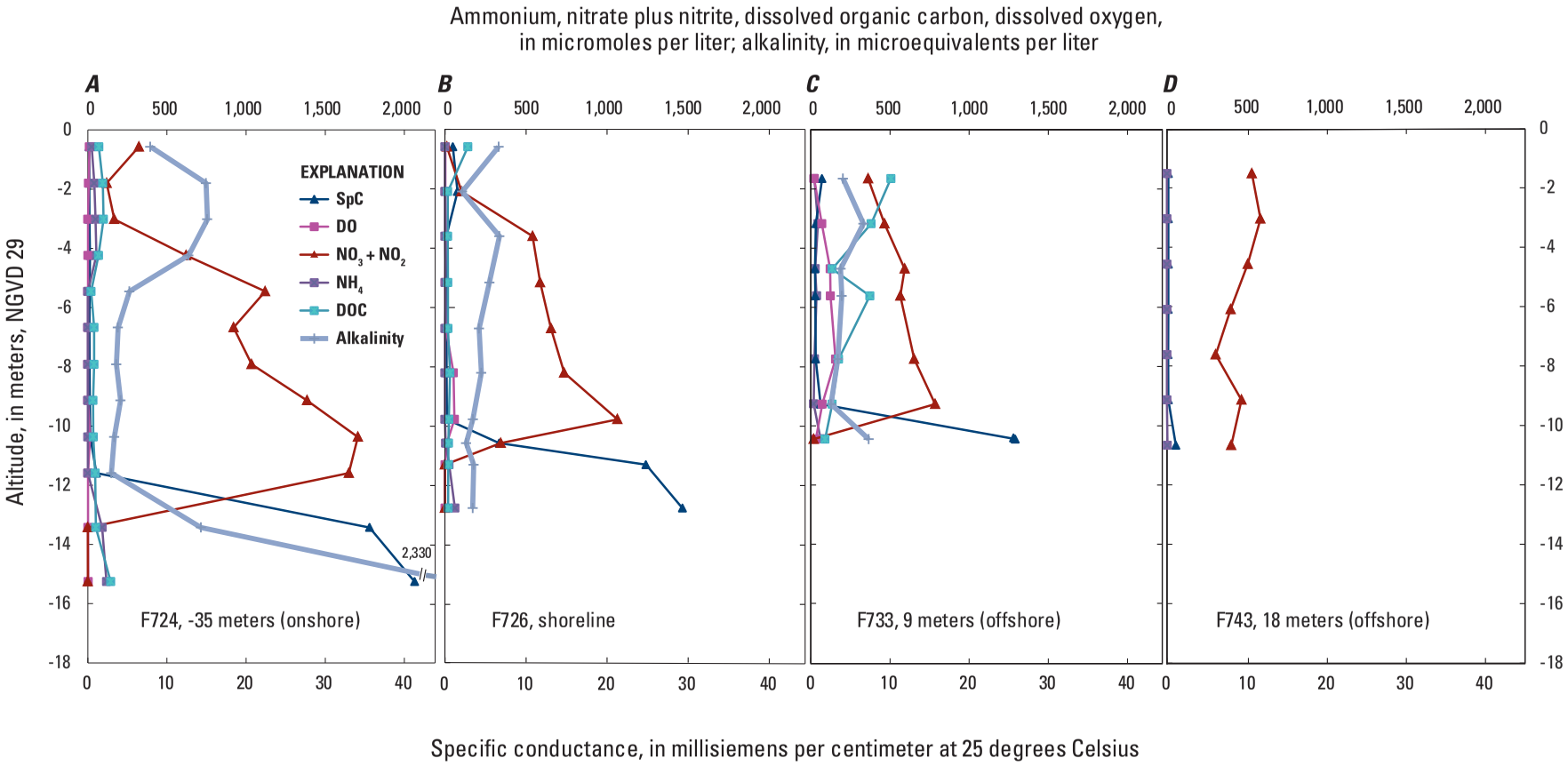

Figure 14. Vertical profiles of solutes at *A*, multilevel sampler F724, *B*, well cluster F726, *C*, well cluster F733, and *D*, temporary well points F743, along section *B*–*B′*, extending 35 meters (m) onshore to 18 m offshore at the Eel River, Seacoast Shores peninsula, East Falmouth, Massachusetts, sampled September 23 to 25, 2013, except F743 sampled September 5, 2013. Location of the section is shown on figure 5. SpC, specific conductance; DO, dissolved oxygen as O_2; NO_3+NO_2, nitrate plus nitrite; NH_4, ammonium; DOC, dissolved organic carbon.

to the south relative to the direction of groundwater flow (N 46° W) indicated by the estimated mean direction of the horizontal hydraulic gradient (fig. 10) east of Edgewater Drive West. The water-table contours west of the road, however, indicate that the transect is approximately parallel to the direction of groundwater flow close to the shoreline (fig. 9).

Nitrogen and Redox Conditions

All groundwater profiles included intervals with high dissolved inorganic nitrogen concentrations, mostly in the form of nitrate (fig. 14). The highest nitrate concentrations were deep in the freshwater sections of the onshore, shoreline, and offshore profiles, just above the freshwater/saltwater interface. This distribution is consistent with the previous data reported in figure 3 for wells SCS–2 (F732) and SCS–3. Ammonium was below the detection level (less than [<] 1.4 µmol/L) in the freshwater at the shoreline cluster (F726) and in the deeper parts of freshwater at the F724 profile. Ammonium concentrations above the detection level (as high as 55 µmol/L) occurred in freshwater only at F724 in the shallow depths between altitudes of 0 and −4 m (fig. 15). Saline groundwater below the freshwater had ammonium concentrations ranging from 89 to 119 µmol/L at F724 and from 4 to 62 µmol/L at F726 and F733.

Dissolved oxygen concentrations (reported as O_2 in this report unless noted otherwise) were low (1.5 to 3 µmol/L) through most of the onshore profile at F724 but were slightly higher (up to 10 µmol/L) near the water table (altitude range of 0 to −4 m). One higher value (15 µmol/L) was measured at an altitude of −11 m. Dissolved oxygen concentrations were uniformly low (<7 µmol/L) at the shoreline cluster F726, except for values of 52, 58, and 12 µmol/L at altitudes of −8.2, −9.8, and −10.6 m, respectively (fig. 14). Higher dissolved oxygen concentrations (50 to 140 µmol/L) were measured in the F733 cluster 9 m offshore between altitudes of −3 to −9 m. Dissolved oxygen measurements were not made in the F743 temporary well points 18 m offshore.

Low dissolved oxygen concentrations—less than 30 µmol/L—are favorable to denitrification (Spiteri and others, 2008), yet the lowest dissolved oxygen values at F724, which were below an altitude of −4 m, were associated with high nitrate concentrations. Dissolved oxygen concentrations were low in deep saline groundwater, which is consistent with the occurrence of detectable ammonium.

Alkalinity in freshwater in the F724 profile (fig. 15) was higher above than below an altitude of −4 m; it also was high in saltwater. Elevated alkalinity can be an indicator of biochemical reactions, such as oxygen reduction and denitrification, which can generate alkalinity in groundwater (Abrams and others, 1999), especially given that little alkalinity is generated from dissolution of quartz and feldspar minerals that compose the bulk of the Cape Cod aquifer (Bau and others, 2004). Because alkalinity is high in seawater, it is relatively difficult to detect minor changes in alkalinity that might be related to subsurface reactions in saline and mixed saline and fresh groundwater.

Relatively high concentrations of dissolved organic carbon were present in the offshore surface water (158 to 248 µmol/L) and in deep, saline zones of the onshore and offshore profiles (100 to 490 µmol/L) (figs. 14 and 15). Dissolved organic carbon concentrations generally were lower in freshwater (20 to 99 µmol/L) than in saltwater. In the onshore profile at F724, dissolved organic carbon concentrations were relatively high in shallow freshwater samples (67 to 99 µmol/L between 0 and −4 m altitude) in comparison to the deeper freshwater samples (20 to 34 µmol/L below −4 m altitude) (fig. 15). Dissolved organic nitrogen concentrations (determined from the difference between total Kjeldahl nitrogen and ammonium nitrogen) generally were low (less than 10 µmol/L) in freshwater and higher (up to 37 µmol/L) in saltwater (fig. 15).

The high concentrations of dissolved organic carbon that were associated with the saltwater zone were more likely from offshore saltwater infiltration into the bottom sediments than from the onshore infiltration of wastewater through the unsaturated zone. The high concentrations of organic carbon in offshore profiles may be expected from saltwater infiltration; however, organic carbon concentrations were not well correlated with salinity (as indicated by specific conductance in fig. 14) and may have been altered by mineralization of sediment organic matter.

Strong reducing conditions in the saline zone in the bottom of the profiles were indicated by the absence of nitrate and by elevated concentrations of ammonium and dissolved iron and manganese (figs. 15 and 16). Above the saline zone, the dissolved iron concentration was generally less than 7 µmol/L, whereas in the saline zone, iron concentrations ranged from 346 to 1,218 µmol/L. Iron apparently was not reduced in the freshwater zone because of the presence of nitrate, which is energetically the preferred electron acceptor. Manganese reduction occurs at a similar reduction potential to nitrate reduction, and elevated dissolved manganese concentrations were measured in the upper zone at F724, in contrast to low concentrations deeper in the profile. In comparison to values at F724, manganese was essentially absent in the shoreline (F726) and offshore (F733) well clusters.

Major Ion Distributions

As illustrated for the redox-sensitive elements, major-ion distributions also can be compared by using vertical profiles along the east-west section (figs. 17 and 18). At the F724 MLS site, silicate and phosphorus had similar distributions, with slightly higher concentrations in the shallow freshwater than in the deep freshwater. In contrast, sulfate concentrations were slightly lower in the shallow freshwater than in the deep freshwater. Boron and chloride concentrations varied substantially in the freshwater profile, but not as systematically as did nitrate concentrations.

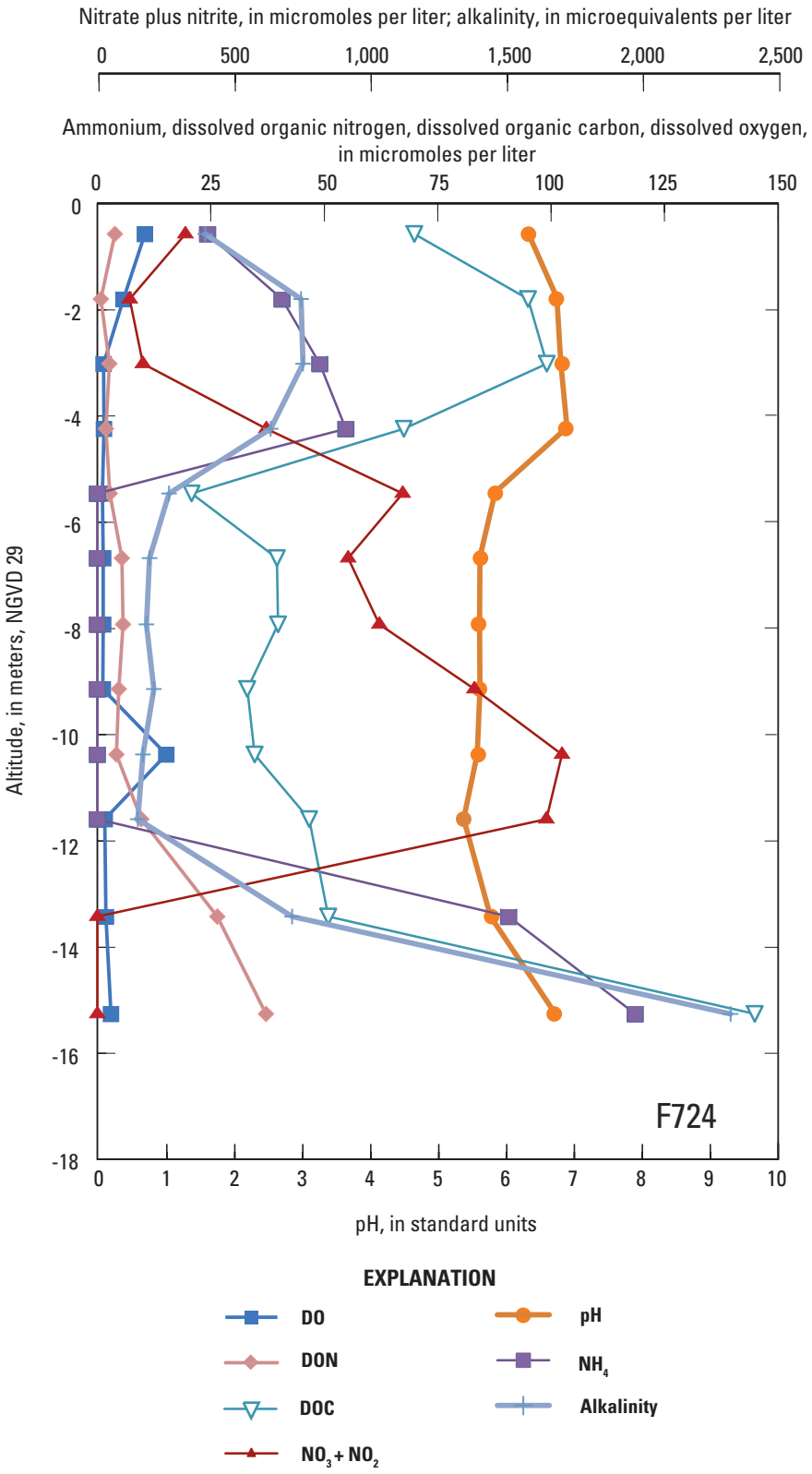

Figure 15. Vertical profiles of solutes for multilevel-sampler site F724 near the Eel River, Seacoast Shores peninsula, East Falmouth, Massachusetts, sampled September 23, 2013. Location of the site is shown on figure 5. DO, dissolved oxygen as O_2; DON, dissolved organic nitrogen; DOC, dissolved organic carbon; NO_3+NO_2, nitrate plus nitrite; NH_4, ammonium.

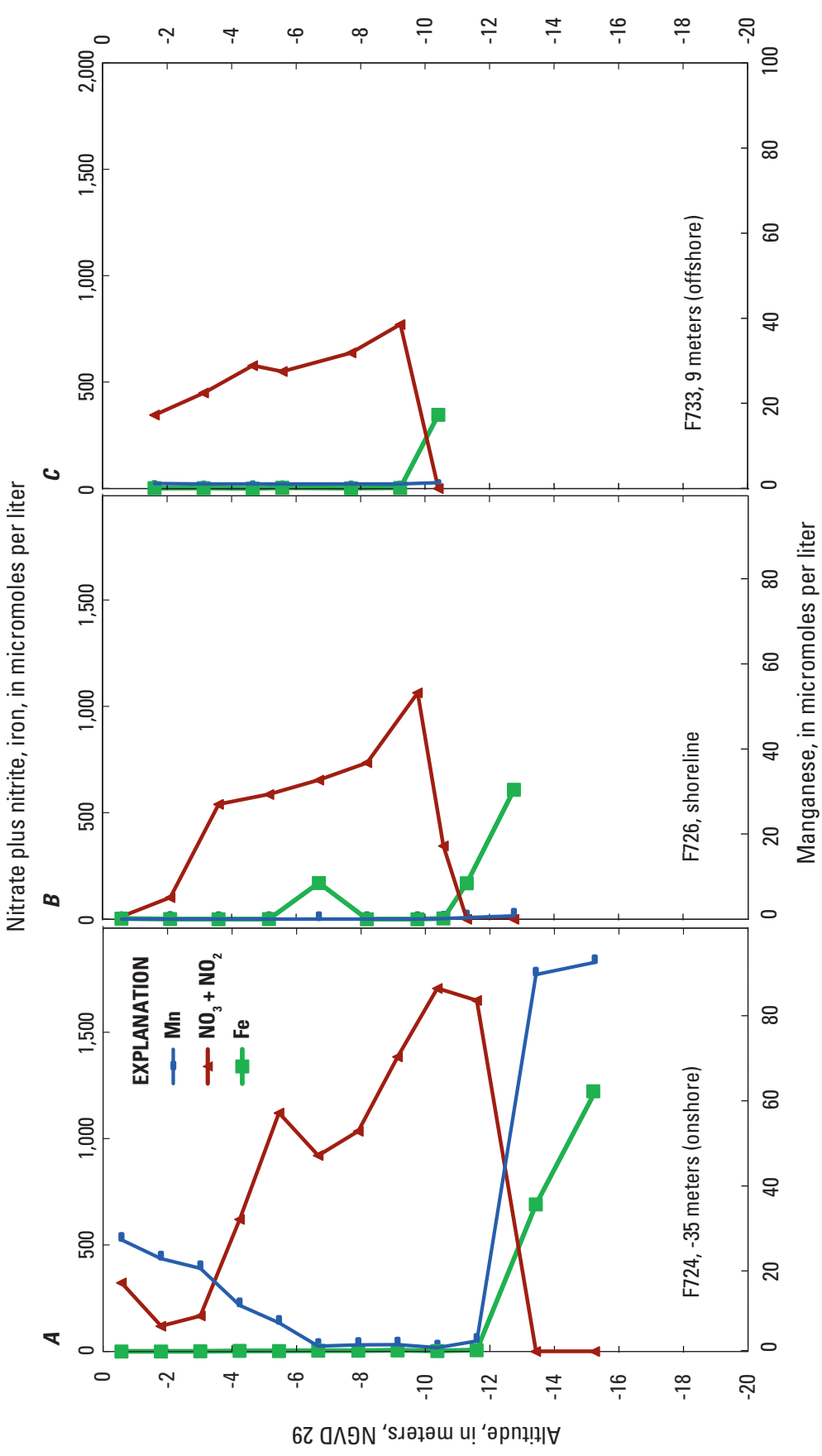

Figure 16. Vertical profiles of nitrate plus nitrite (NO_3+NO_2) and dissolved iron (Fe) and manganese (Mn) at *A*, multilevel sampler F724, *B*, well cluster F726, and *C*, well cluster F733 along section *B–B′* near the Eel River, Seacoast Shores peninsula, East Falmouth, Massachusetts, sampled September 23 to 25, 2013. Location of the section is shown on figure 5.

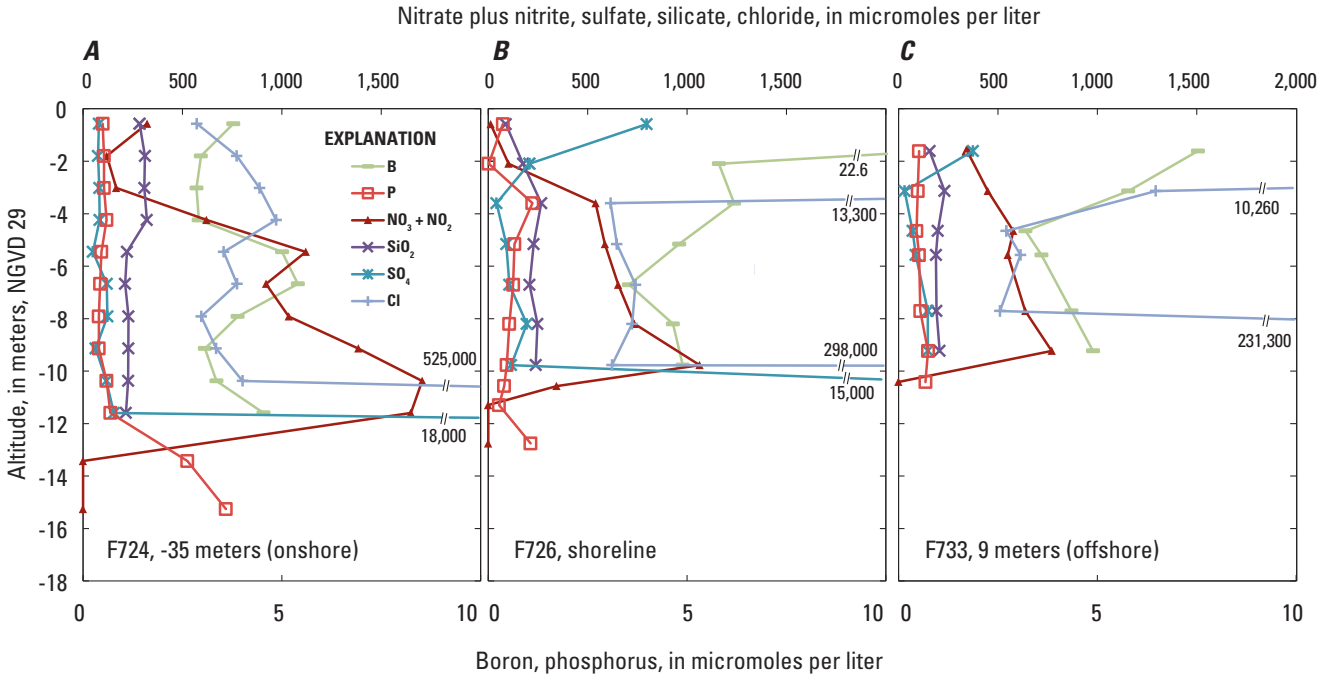

Figure 17. Vertical profiles of nitrate plus nitrite and major anions in groundwater at *A*, multilevel sampler F724, *B*, well cluster F726, and *C*, well cluster F733, along section *B*–*B′* near the Eel River, Seacoast Shores peninsula, East Falmouth, Massachusetts, sampled September 23 to 25, 2013. Location of the section is shown on figure 5. B, boron; P, phosphorus; NO_3+NO_2, nitrate plus nitrite; SiO_2, silicate; SO_4, sulfate; Cl, chloride.

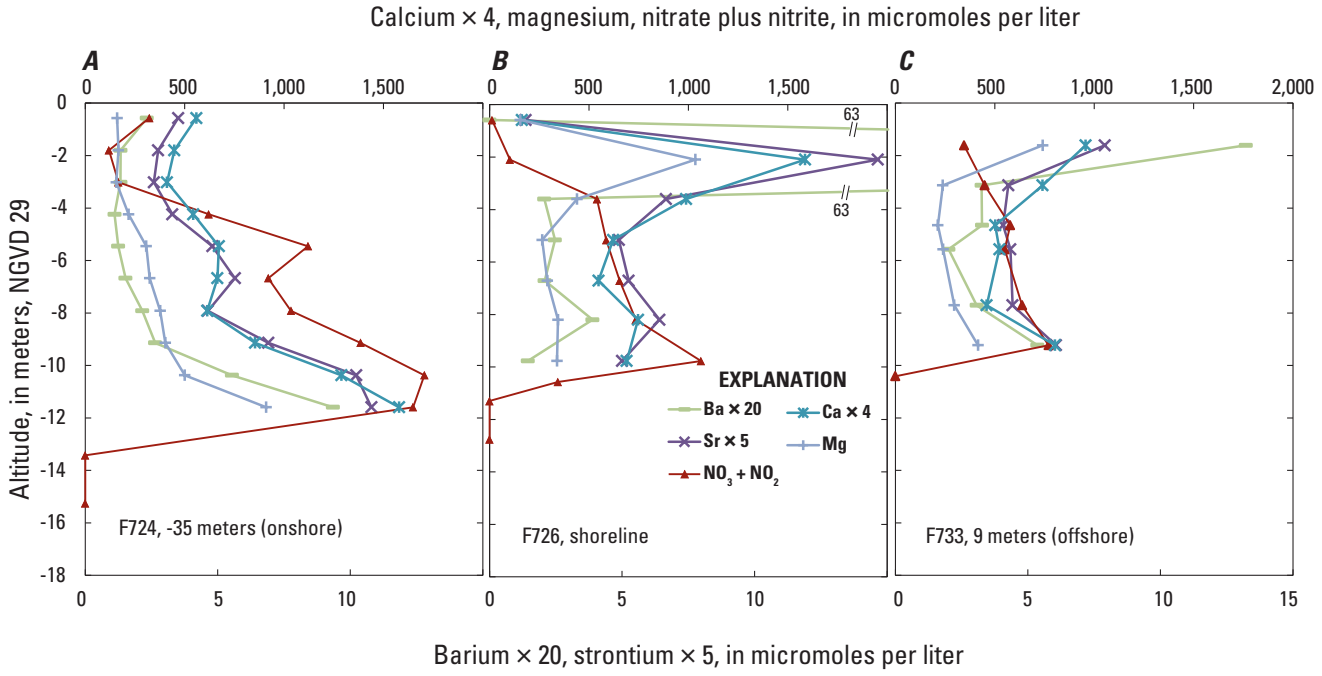

Figure 18. Vertical profiles of nitrate plus nitrite and divalent cations in groundwater at *A*, multilevel sampler F724, *B*, well cluster F726, and *C*, well cluster F733, along section *B*–*B′* near the Eel River, Seacoast Shores peninsula, East Falmouth, Massachusetts, September 23 to 25, 2013. Location of the section is shown on figure 5. To adjust scales, concentrations of some constituents are increased by the factors shown in the axis labels. Ba, barium; Sr, strontium; NO_3+NO_2, nitrate plus nitrite; Ca, calcium; Mg, magnesium.

At site F724 onshore, the divalent cations were correlated among themselves and with nitrate more strongly than were the anions (fig. 18). Cation concentrations, like nitrate concentrations, generally increased with depth in the freshwater. Calcium was the cation most closely correlated with nitrate (R^2=0.74). Some of these constituents may be correlated in part because they are present in the same sources (for example, septic leachate and fertilizer) and have similar chemical properties. In contrast, the univalent cations sodium and potassium had patterns more similar to those of chloride and sulfate, respectively (fig. 19).

Offshore Surface Water

In the Eel River surface water, salinity was essentially constant in samples collected during the 4-day period of August 21–24, 2013 (27.0 to 27.3 practical salinity units [psu] measured in the laboratory) but was higher in a single sample collected on September 25, 2013 (31.3 psu estimated from specific conductance). Nitrate and ammonium were below detection limits, whereas concentrations of dissolved organic carbon (160 to 250 µmol/L) and dissolved organic nitrogen (22 µmol/L) were high compared to those of fresh groundwater samples (<150 and <15 µmol/L, respectively). The offshore water is the supply for seawater infiltration as shown in the conceptual model (fig. 4). As the infiltrating seawater is modified during passage through biologically active sediments, it can provide organic carbon reactants at the deep freshwater/saltwater interface and to the intertidal saltwater cell.

Time Series of Concentrations

Several well clusters and shallow offshore transects were sampled multiple times to examine temporal variability of aquifer conditions. Two rounds of sampling examined variations through the full fresh groundwater section, and three rounds of sampling examined variations in shallow groundwater in the nearshore intertidal saltwater cell (fig. 4).

Full-Depth Profiles

The depth profiles along section *B–B′* were sampled twice over periods of 1 month for F726 and F733 and 3 months for F724 (fig. 20). Concentration profiles were similar over time for specific conductance, dissolved oxygen, and nitrate at the three profile locations 35 m onshore, at the shoreline, and 9 m offshore. The similarity over time indicates that geochemical conditions at the scale of the full-depth profiles did not vary on the time scale of tidal variations and short-term changes in groundwater-flow direction (figs. 10 and 11).

Additional profiles from a previous investigation (Thomas Cambareri, Cape Cod Commission, oral presentation for Waquoit Bay National Estuarine Research Reserve Research Exchange Day, 1994) were used to extend

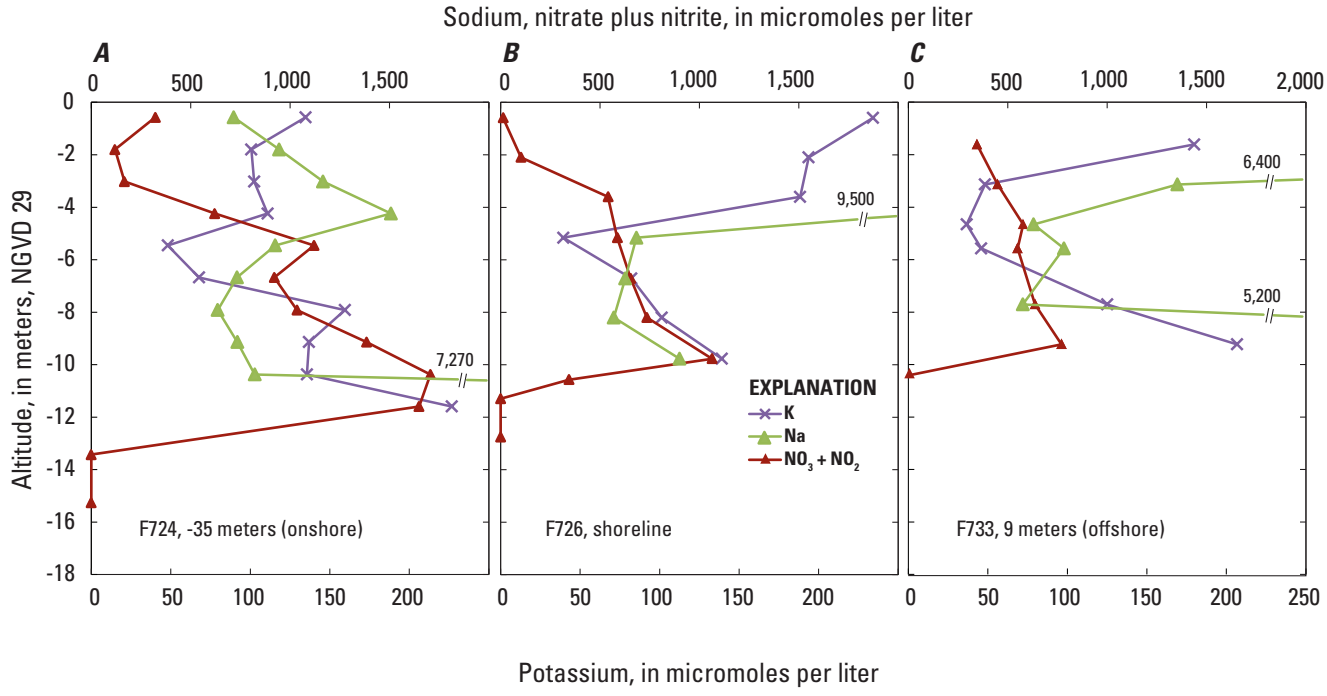

Figure 19. Vertical profiles of nitrate plus nitrite and monovalent cations in groundwater at *A*, multilevel sampler F724, *B*, well cluster F726, and *C*, well cluster F733, along section *B–B′* near the Eel River, Seacoast Shores peninsula, East Falmouth, Massachusetts, sampled September 23 to 25, 2013. Location of the section is shown on figure 5. K, potassium; Na, sodium; NO_3+NO_2, nitrate plus nitrite.

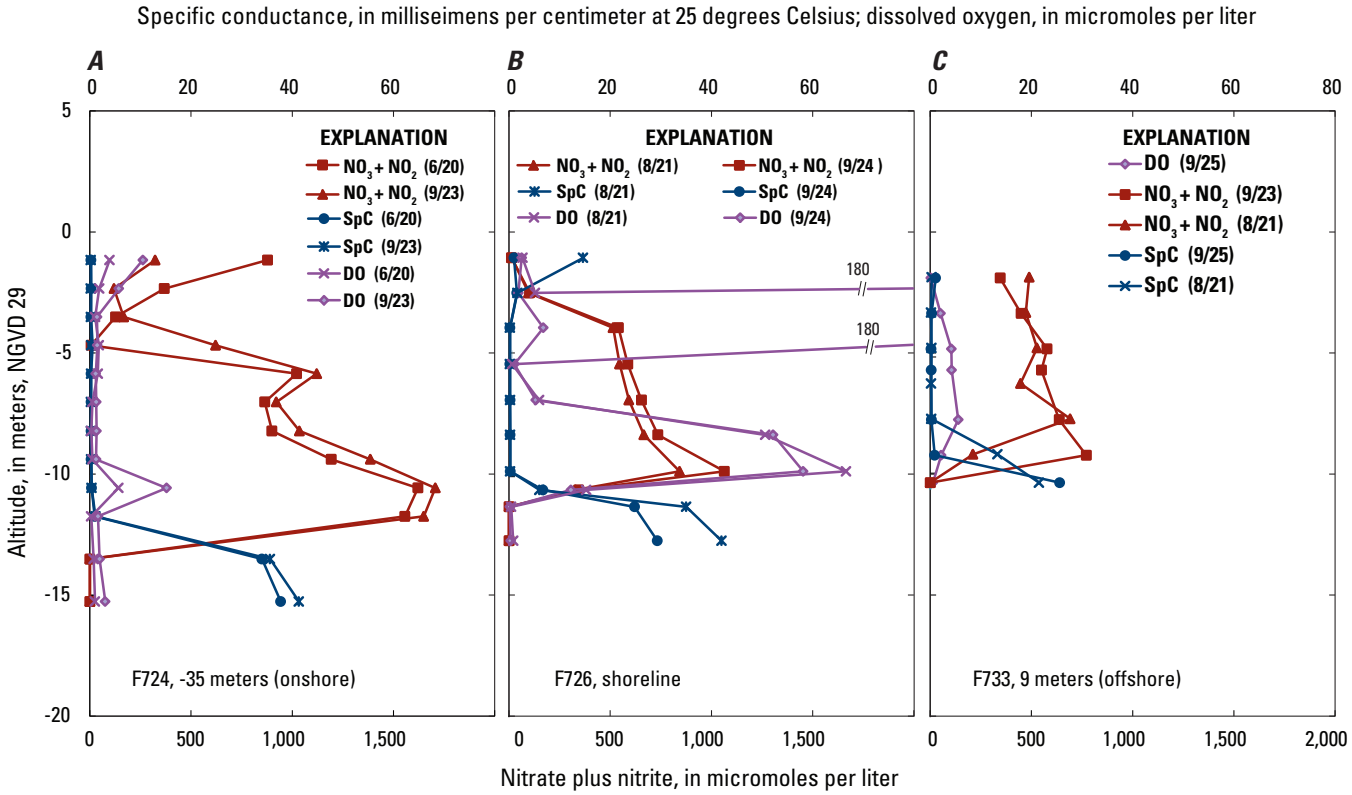

Figure 20. Vertical profiles of specific conductance (SpC), nitrate plus nitrite (NO_3+NO_2), and dissolved oxygen (DO) as O_2 at *A*, multilevel sampler F724, *B*, well cluster F726, and *C*, well cluster F733, along section *B*–*B′* near the Eel River, Seacoast Shores peninsula, East Falmouth, Massachusetts. Each site was sampled twice between June 20 and September 25, 2013. Location of the section is shown on figure 5.

knowledge of nitrate over time and areal extent (fig. 21 for concentrations, fig. 2 for location). The profiles indicate that high nitrate concentrations extended to both sides of the peninsula (compare SCS–2 with SCS–3), and high nitrate concentrations have existed at altitudes between −7 and −13 m for at least 20 years (compare SCS–2 with SCS–3 in 1993 and SCS–2 with F724 in 2013).

Shallow Subsurface Offshore Profiles

The nearshore, shallow subsurface was sampled three times during a 5-day period by using pushpoint samplers to investigate the effects of spring tides on the shallow groundwater. The sampling was repeated on September 20, 23, and 25, 2013. The altitude of the mean stage of the Eel River during this period was 0.47 m relative to NGVD 29. The differences in high tide altitude between the sampling events were small, but the antecedent condition was a slightly increasing high tide altitude from September 15 (0.71 m) to September 20 (0.73 m). During the sampling, high tide altitude increased from 0.73 m on September 20 to 0.85 m on September 22 and then decreased to 0.74 m on September 25, the last day of sampling (fig. 11*A*). The result expected for the 5-day period would be a replenishment of saltwater in the near-surface sediments nearest the shore as saltwater moved inland during high tide periods.

Even with the small range in high tide altitudes during the sampling period, increased salinity (estimated from specific conductance) was measured in the nearshore area of tide run-up during the sampling period (fig. 22). Salinity in the three shallowest pushpoints closest to land increased between sampling events by as much as 11.9 psu. Salinity at the farthest landward site (F741) increased from 1.5 to 11.7 psu and then decreased to 3.0 psu over the course of the three samplings. Changes were also observed in the dissolved oxygen distribution in the nearshore shallow subsurface (fig. 23). The nearshore oxygen concentrations were highest during the first sampling event and decreased during both subsequent samplings.

Whereas there was some salinity change near the shore, the time series show less change offshore (fig. 22). For example, in the middle of the low-salinity area (F738 to F736), salinity ranged from 1.4 to 5.3 psu over the course of the sampling. In the middle of the offshore high-salinity zone (F735 to F733), the salinity ranged from 15.7 to 28.0 psu. Changes in dissolved oxygen similarly showed less change offshore than near the shore (fig. 23). Dissolved oxygen concentrations increased where salinity also increased, indicating that the dissolved oxygen was entrained with the infiltrating seawater.

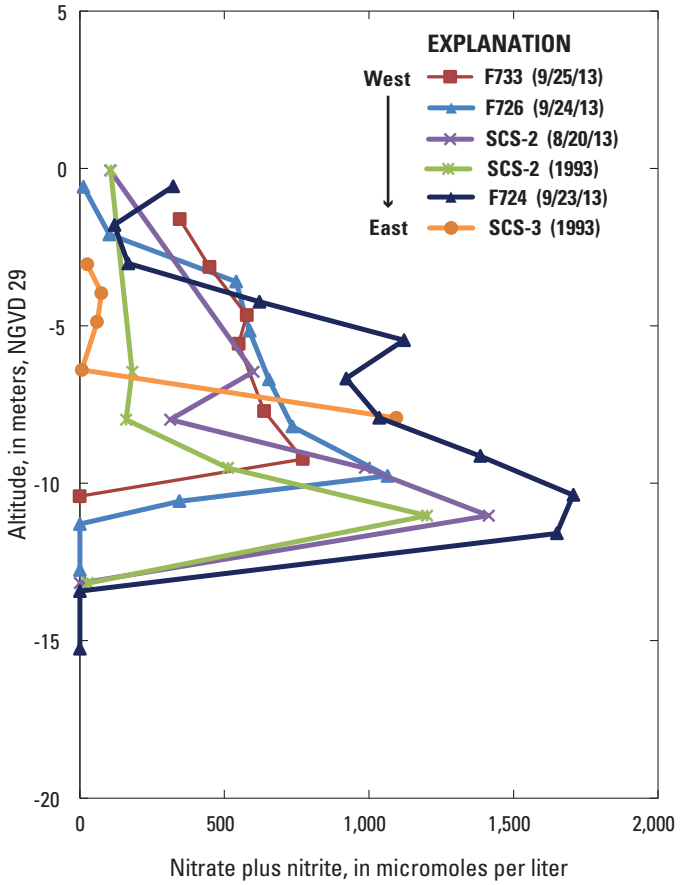

Figure 21. Vertical profiles of nitrate (plus nitrite for 2013 data) in groundwater at sites along an east-west line across the Seacoast Shores peninsula, East Falmouth, Massachusetts, 1993 to 2013. Sites are listed from west to east in the explanation. Sites near Eel River: F733, 9 meters (m) offshore; F726, at shoreline; F732, 19 m onshore; F724, 35 m onshore. Site near Seapit River: SCS–3, 30 m onshore. Data from 1993 at F732 (SCS–2) and SCS–3 are adapted from a presentation by Thomas Cambareri for Waquoit Bay National Estuarine Research Reserve Research Exchange Day, March 21, 1994, filed at the Cape Cod Commission, Barnstable, Mass. Locations of the sites are shown on figures 2 and 5.

Geochemical Indicators of Nitrogen Attenuation

Low dissolved oxygen concentrations, as observed in much of the aquifer where sampled, indicate conditions may have been compatible with nitrate reduction but are not sufficient to indicate that nitrate reduction was occurring. Therefore, additional evidence for nitrate reduction was evaluated, including concentrations of the reaction product nitrogen gas, stable isotope ratios of nitrate and nitrogen gas, changes in alkalinity, and differences between nitrate concentrations estimated from local sources and those measured in the aquifer (fig. 24).

The volume-averaged concentration of nitrogen that might be expected in groundwater in the Seacoast Shores peninsula is about 500 µmol/L based on water use, housing density, and dilution by recharge (Colman and others, 2015). Nitrogen concentrations less than this value (for example, between altitudes of 0 and −4 m at F724 and the shoreline cluster; fig. 24) could be an indicator of nitrate reduction, but other evidence is needed to test this hypothesis.

Excess Nitrogen Gas

Estimated concentrations of excess N_2 provide direct evidence that nitrate reduction by denitrification or anammox was at least partly responsible for low nitrate concentrations in some of the fresh groundwater and mixtures of freshwater and saltwater. In denitrification, excess N_2 is derived entirely from nitrate-N; in anammox, excess N_2 is derived subequally from nitrate-N and ammonium-N. Interpretation of N_2 data requires inferences about temperature of recharge and amount of excess air in samples, as determined by comparing N_2 against argon (Ar) concentrations (fig. 25). Most freshwater samples analyzed for N_2 and Ar plot in the region of the diagram that indicates recharge temperatures between about 10 and 15 degrees Celsius (°C), with excess air concentrations between about 0 and 2 cubic centimeters at standard temperature and pressure per liter of water (ccSTP/L). Five freshwater samples and two brackish samples plot to the right outside this region (for example, F724 −1.80), indicating additional N_2, which is interpreted as excess N_2 likely resulting from denitrification (or possibly anammox). Assuming a mean value of 1±1 ccSTP/L excess air for recharge, which corresponds to uncertainty of approximately ±20 µmol/L N_2 (equal to ±40 µmol/L as N_2-N), calculated excess N_2 concentrations were as high as 147±20 µmol/L, which would correspond to 294±40 µmol/L nitrate reduced to N_2-N by denitrification (fig. 25). Some samples that plot to the left of the freshwater or seawater air-saturation lines (fig. 25) had anomalously low Ar and N_2 concentrations (high calculated recharge temperature), and some of those samples also had negative calculated excess air. Some of these results could indicate real variation of recharge conditions, but some results could indicate degassing during sample collection. Also, it is possible that saline groundwater recharged beneath the estuary had less excess air than fresh groundwater recharged beneath land (Böhlke and Krantz, 2003), which would alter the assumptions used in the calculations. It is important to note that N_2 produced by nitrate reduction in the unsaturated zone is likely to be underrepresented in recharge, so that excess N_2 concentrations in groundwater are interpreted to represent nitrate reduction within the saturated zone.

Some of the highest calculated excess N_2 concentrations were in shallow, fresh groundwater at F724, where nitrate concentrations were relatively low (fig. 24). Elevated excess N_2 concentrations were also observed in shallow fresh groundwater in the offshore profile (F733 −1.61) and in deep mixed groundwater in the freshwater/saltwater transition zone in the shoreline and offshore profiles (fig. 25). Denitrification and anammox in these settings would be consistent with low dissolved oxygen concentrations and elevated concentrations of ammonium, reduced iron, and manganese.

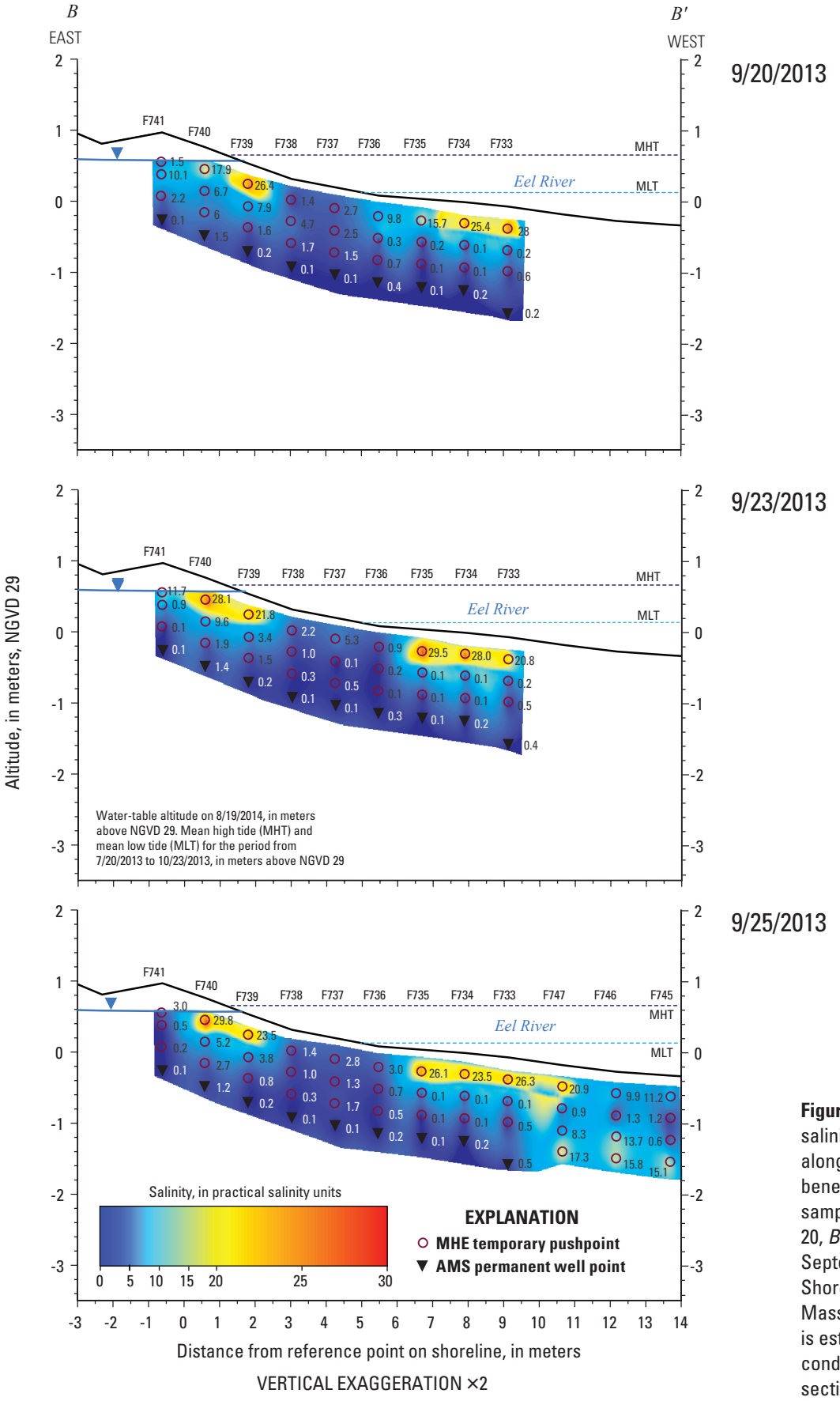

Figure 22. Distributions of salinity in shallow groundwater along a portion of section *B*–*B*′ beneath the Eel River during sampling events on *A*, September 20, *B*, September 23, and *C*, September 25, 2013, Seacoast Shores peninsula, East Falmouth, Massachusetts. Salinity is estimated from specific conductance. Location of the section is shown on figure 6.

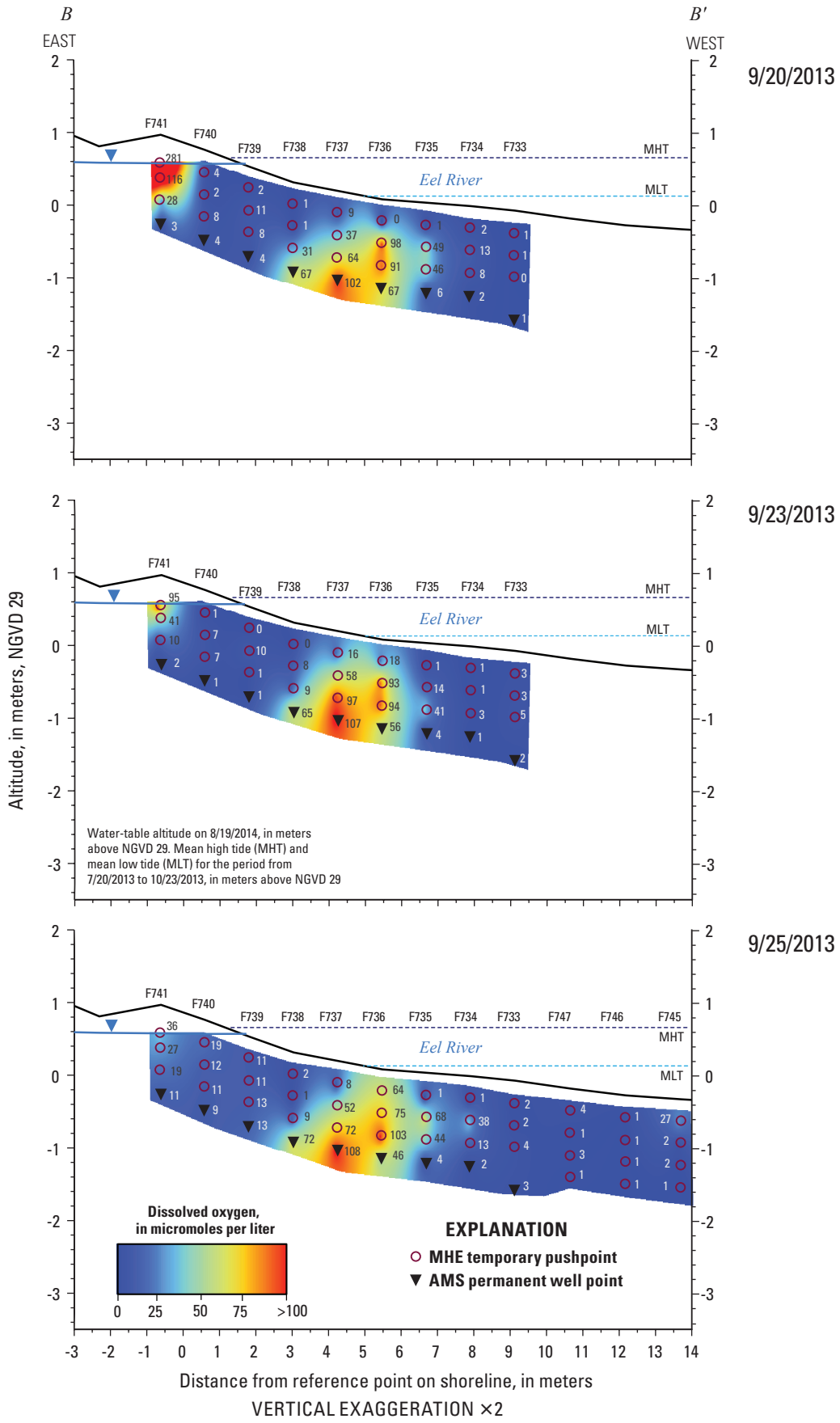

Figure 23. Distributions of dissolved oxygen in shallow groundwater along a portion of section *B*–*B*′ beneath the Eel River during sampling events on *A*, September 20, *B*, September 23, and *C*, September 25, 2013, Seacoast Shores peninsula, East Falmouth, Massachusetts. Dissolved oxygen concentrations are reported in micromoles per liter as O_2. Location of the section line is shown on figure 6.

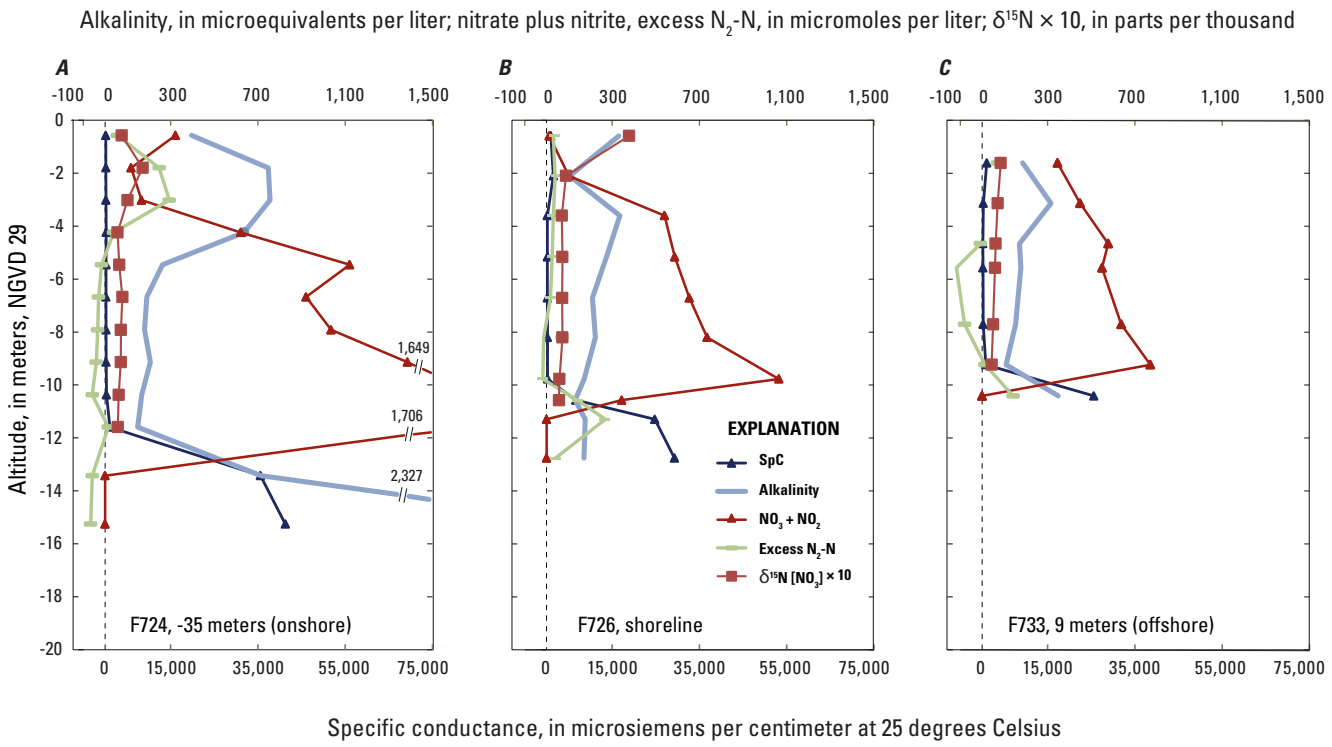

Figure 24. Vertical profiles of nitrate plus nitrite (NO_3+NO_2), specific conductance (SpC), and three potential indicators of nitrogen attenuation—alkalinity, excess nitrogen gas as N (N_2-N), and delta nitrogen-15 of nitrate ($\delta^{15}N[NO_3]$)—at *A*, multilevel sampler F724, *B*, well cluster F726, and *C*, well cluster F733, along section *B*–*B′* extending from 35 meters (m) onshore to 9 m offshore at the Eel River, Seacoast Shores peninsula, East Falmouth, Massachusetts, sampled September 23 to 25, 2013. Location of the section is shown on figure 5. Negative calculated excess N_2-N concentrations can indicate degassing (for example during sampling) or errors in assumed recharge gas components (for example, excess air).

Isotopic Composition of Nitrate and Nitrogen Gas

The isotopic composition of nitrate can provide useful information about the source of the nitrate and the likelihood that nitrate reduction has occurred. Most samples collected along the *B*–*B′* section and analyzed for nitrate isotopes had delta nitrogen-15 ($\delta^{15}N$) values between about +4 and +8 parts per thousand (‰) and delta oxygen-18 ($\delta^{18}O$) values between about +3 and +7‰ (fig. 26). Samples with significantly higher nitrate $\delta^{15}N$ values (greater than [>] 8‰) also had higher nitrate $\delta^{18}O$ values, which is consistent with isotopic fractionation effects of nitrate reduction. Samples with elevated (fractionated) $\delta^{15}N$ and $\delta^{18}O$ values were in or near areas where excess N_2 was present. Samples apparently not fractionated or not associated with substantial excess N_2 had mean nitrate $\delta^{15}N$ = +6.6±0.9‰ (*n*=14) and nitrate $\delta^{18}O$ = +5.2±1.2‰ (*n*=14). The mean $\delta^{18}O$ value of unfractionated samples is consistent with nitrate produced by nitrification of reduced nitrogen from organic matter or ammonium from various sources. The mean $\delta^{15}N$ value is relatively low for reported wastewater-derived nitrate in general but is within the range of values documented in recharge from septic systems (fig. 26). This $\delta^{15}N$ value is high compared to many reported values for nitrate in recharge beneath agricultural land receiving artificial fertilizers in the mid-Atlantic region (Böhlke, 2003; Hyer and others, 2016). Exceptions not included in the mean included 1 sample (well F727 −0.65) with anomalously low $\delta^{15}N$ (+1‰) and 5 samples with elevated $\delta^{15}N$ values (+9 to +38‰) that are attributable to isotopic fractionation caused by nitrate reduction. The sample with the highest $\delta^{15}N$ and $\delta^{18}O$ values, indicating substantial isotopic fractionation (F726 −0.59), had a relatively small concentration of excess N_2, presumably because it had relatively little nitrate when the sampled water originally recharged the aquifer.

Concentrations of nitrite in selected samples ranged from 0.1 to 4.9 µmol/L and averaged 1.0±1.4 µmol/L (*n*=23). Relatively high nitrite concentrations (>1 µmol/L) can indicate the presence of active denitrification (Repert and others, 2006), and such values commonly were associated with other indicators of nitrate reduction measured in this investigation. Relative abundances of nitrite were too low to affect isotopic analyses of nitrate substantially (Casciotti and others, 2007).

The $\delta^{15}N$ value of dissolved N_2 gas can be used as additional evidence for nitrate reduction, and in some cases it can be used to reconstruct the initial $\delta^{15}N$ value of the nitrate when the sampled water was recharged (Böhlke and others, 2002; Böhlke, 2002). For example, during denitrification, nitrate

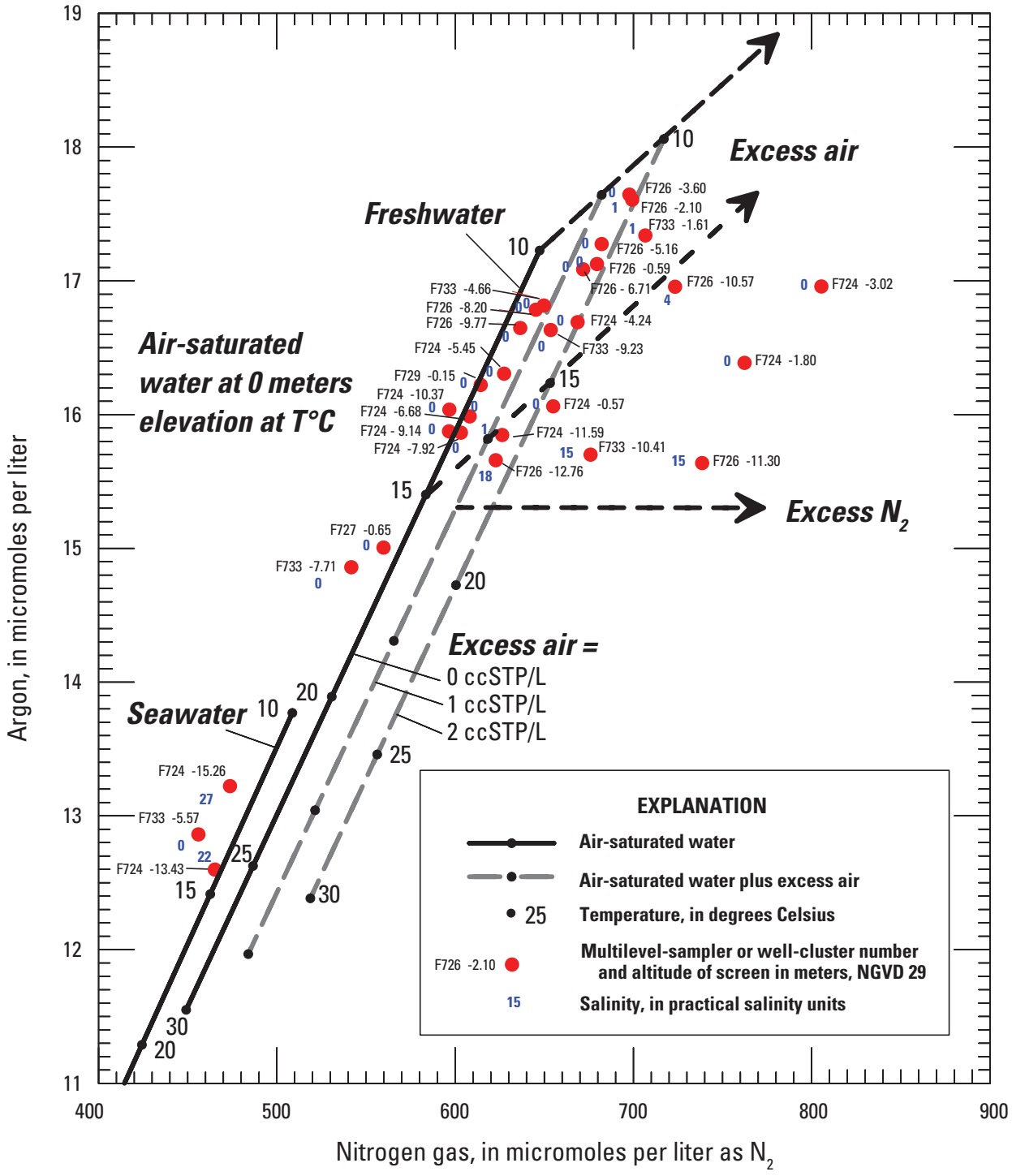

Figure 25. Relation between argon (Ar) and nitrogen gas (N_2) concentrations at multilevel-sampler F724 and well clusters F726, F727, F729, and F733 near the Eel River, Seacoast Shores peninsula, East Falmouth, Massachusetts, sampled September 23 to 25, 2013. Locations of sites are shown on figure 5. Solid lines on the left indicate concentrations in equilibrium with air for freshwater and seawater at various temperatures. Dotted lines parallel to the equilibrium lines indicate air-saturated freshwater with 1 or 2 cubic centimeters of excess air at standard temperature and pressure per liter of water (ccSTP/L). Most samples (indicated by well-cluster number and well-screen altitude in meters relative to NGVD 29) plot in a region of the diagram indicating recharge temperatures (T) between about 10 and 15 degrees Celsius (°C) with excess air concentrations between about 0 and 2 milliliters excess air STP/L. Samples most likely to have excess N_2 from denitrification plot to the right of the 2-ccSTP/L excess-air line.

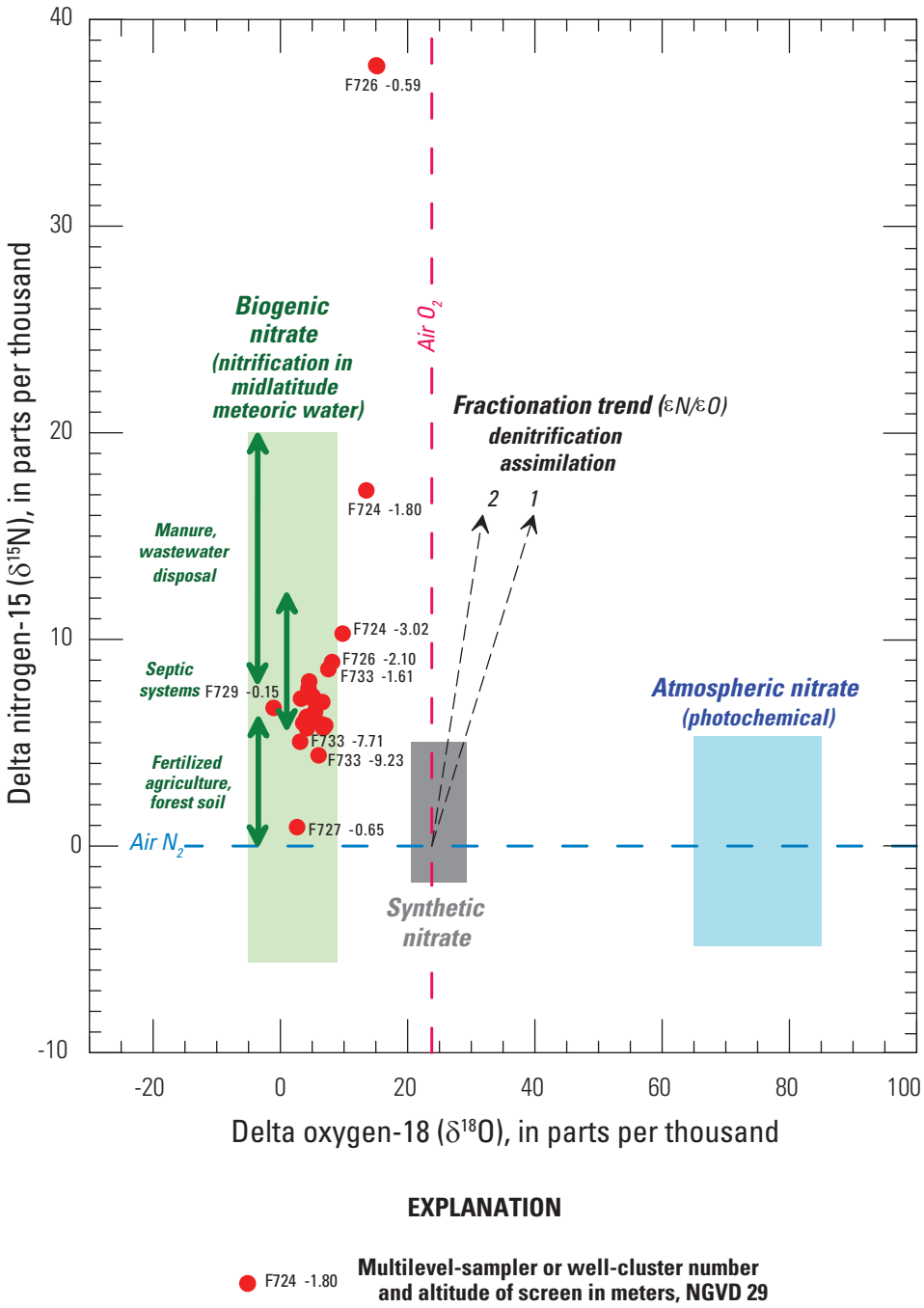

Figure 26. Delta nitrogen-15 ($\delta^{15}N$) and delta oxygen-18 ($\delta^{18}O$) values of groundwater nitrate from multilevel sampler F724 and well clusters F726, F727, F729, and F733 near the Eel River, Seacoast Shores peninsula, East Falmouth, Massachusetts, compared with common values for various nitrate sources (Böhlke, 2002, 2003; Jackson and others, 2010; Hyer and others, 2016). Samples were collected September 23 to 25, 2013. Locations of sites are shown on figure 5. N_2, nitrogen gas; O_2, oxygen gas; $\varepsilon N/\varepsilon O$, ratio of isotopic fractionation factors for nitrogen and oxygen commonly reported for nitrate-reducing processes.

$\delta^{15}N$ increases monotonically with reaction progress while the $\delta^{15}N$ of excess N_2 reaction product remains lower than that of the nitrate because the reaction rate is higher for nitrate with lower molecular weight. However, because excess N_2 mixes with preexisting atmospheric N_2 in groundwater, the $\delta^{15}N$ of total N_2 (atmospheric and denitrification product) commonly decreases at first and then increases as the reaction proceeds. Thus, denitrification reactions chart unique paths through a plot of $\delta^{15}N[N_2]$ in relation to Ar/N_2 that depend on the initial concentration and reaction progress (fig. 27).

The total range of reaction progress values estimated for groundwater samples was 0 to 100 percent. Some samples with no measurable nitrate had substantial nitrate concentrations when originally recharged, whereas some wholly or partially reacted samples had relatively low nitrate concentrations when recharged. For example, assuming denitrification was the predominant nitrate-reduction process, two samples from the onshore shallow freshwater zone (F724 −1.80 and F724 −3.02) were estimated to have had initial nitrate concentrations of approximately 367 and 461 µmol/L, respectively, and to have lost approximately 68 and 64 percent, respectively, of their nitrate by denitrification. Similarly, two samples from the deep freshwater/saltwater transition zone (F726 −11.3 and F733 −10.41) had initial nitrate concentrations of approximately 270 and 142 µmol/L, respectively, and both were completely denitrified.

Isotopic Composition of Ammonium

Because ammonium concentrations below the detection limit were widespread, $\delta^{15}N$ in ammonium was measured in only 10 samples. With two exceptions, $\delta^{15}N$ values of ammonium were essentially uniform, yielding a "baseline" mean value of +5.7±0.7‰ (*n*=8). This baseline group included samples from both freshwater and saltwater and with ammonium concentrations ranging from 6 to 116 µmol/L, indicating that most concentration variations were not associated with isotopic fractionation. The baseline mean $\delta^{15}N$ value is similar to values commonly reported for nitrogen in estuarine sediment and, therefore, the baseline value could be derived in part from degradation of organic matter beneath the Eel River, as most of the high ammonium concentrations were in saltwater samples. This $\delta^{15}N$ value is also similar to reported values of ammonium in septic-system leachate and to reported values of organic nitrogen in many soils and plants in temperate regions; these soils and plants could have been sources of ammonium in a few of the freshwater samples. The highest ammonium $\delta^{15}N$ values (+6.5 and +6.6‰) were near the deep freshwater/saltwater transition at the shoreline site (F726, fig. 5) in samples that had evidence of excess N_2, which could potentially indicate minor ammonium oxidation, conceivably related to anammox (Brunner and others, 2013), but the 1‰ difference between these values and the baseline mean value is small and may not be significant. Relatively low $\delta^{15}N$ values (+0.6 and +1.8‰) not included in the baseline mean value were in freshwater from two of the relatively shallow ports at site F724, where they were separated by two higher values (+4.5 and +5.3‰). The isotopic variation among these shallow-zone samples is not understood.

Alkalinity

Microbial reduction of nitrate commonly is coupled with oxidation of organic carbon, which can increase the alkalinity and the concentration of dissolved inorganic carbon (DIC) in groundwater. The stoichiometry of denitrification coupled with oxidation of organic carbon (eq. 1.1 in appendix 1) indicates that DIC production could be approximately 1.25 times the amount of nitrate reduced on a molar basis, and alkalinity production (as HCO_3^-) could be roughly equal to the amount of nitrate reduction if other pH buffers are not important.

In the profile at site F724, 35 m onshore, measured alkalinities in shallow freshwater were substantially higher than those in deep freshwater (fig. 24). The highest alkalinity values (about 750 microequivalents per liter [µeq/L]) were in two samples with isotopically fractionated nitrate and relatively large concentrations of excess N_2 (248 and 294 µmol/L as N_2-N), whereas the lower alkalinity values about 200 µeq/L were in samples with no evidence of denitrification. The relation between alkalinity and excess N_2-N in these representative samples would yield an apparent molar ratio of around 2, which could be qualitatively consistent with denitrification coupled with organic carbon oxidation in some of the shallow freshwater, given uncertainties in estimated excess N_2-N and other causes of variation in alkalinity.

Alkalinities generally were relatively low in freshwater samples from other profiles where excess N_2 concentrations were low; however, the sample at F724 −4.24 was an exception (high alkalinity with low excess N_2-N). Relations between alkalinities and nitrogen reactions are difficult to evaluate in the deep freshwater/saltwater transition zone because of the much higher alkalinity of infiltrated seawater.

Nitrogen Fate and Transport in the Subterranean Estuary

The fate and transport of nitrogen in the subterranean estuary is governed by groundwater flow and biogeochemical reactivity, which are discussed in this section.

Source of High Nitrate Concentrations in Deep Fresh Groundwater

Although 500 µmol/L is the estimated volume-averaged concentration for groundwater nitrogen at Seacoast Shores on the basis of precipitation recharge and septic inputs (Colman and others, 2015), few concentrations in the profiles were at or near 500 µmol/L. Above an altitude of −4 m, concentrations were lower than 500 µmol/L, in part because

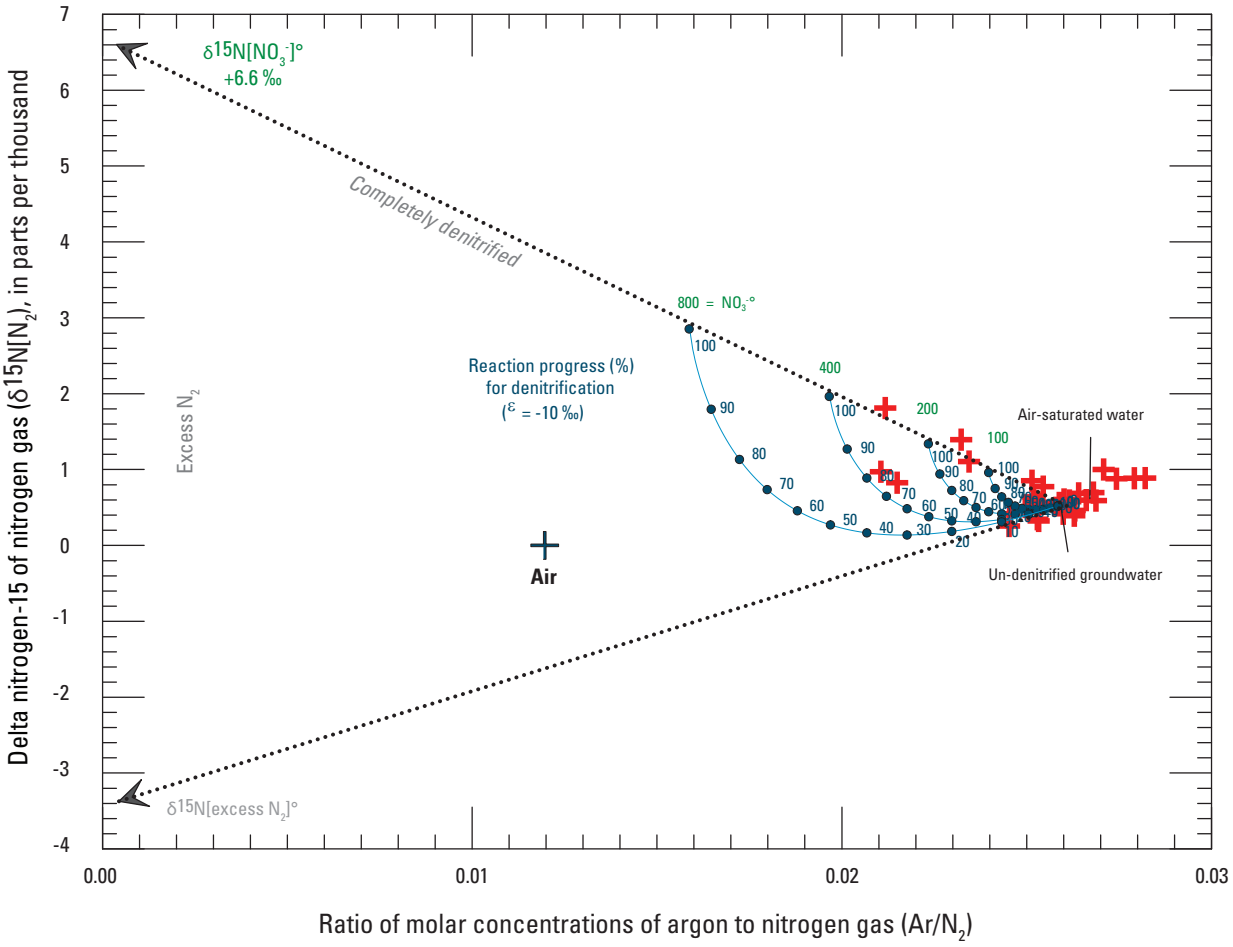

Figure 27. Relation between delta nitrogen-15 of nitrogen gas ($\delta^{15}N[N_2]$) and the argon to nitrogen gas (Ar/N_2) concentration ratio in samples from this study (red plus signs). Samples were collected September 23 to 25, 2013, and are identified on figure 25. The black plus sign is the corresponding value for air. Curves indicate model trajectories followed by hypothetical water samples undergoing progressive denitrification (Böhlke, 2002; Böhlke and others, 2002). Each curve represents a different initial nitrate concentration and is labeled with reaction progress in percent (%). Arrows point to the initial $\delta^{15}N$ value of reacting nitrate (+6.6 parts per thousand [‰], equal to the mean of unreacted nitrate from the main transect) and the initial $\delta^{15}N$ value of reaction-product N_2 (–3.4‰). The assumed hypothetical value of the isotope fractionation factor, epsilon (ε), is –10‰, and the initial values of $\delta^{15}N[N_2]$ and Ar/N_2 are +0.52‰ and +0.0258, respectively. Samples plotting near the lower dotted arrow with $\delta^{15}N[N_2]$ less than the initial value could indicate partial denitrification with low reaction progress values or uncertainty in excess air and solubility effects. Samples plotting near the upper dotted arrow with $\delta^{15}N[N_2]$ greater than the initial value are most likely to have reached advanced stages of denitrification, in some cases near 100 percent. $NO_3°$, initial nitrate concentration; $\delta^{15}N[NO_3]°$, initial delta nitrogen-15 of nitrate; $\delta^{15}N[\text{excess } N_2]°$, initial delta nitrogen-15 of excess nitrogen gas reaction product.

of nitrate attenuation by denitrification or anammox. Between altitudes of −5 and −10.4 m, near the top of the freshwater/saltwater interface, nitrate concentrations ranged from 1,000 to 1,700 µmol/L, 2 to 3 times the estimated mean of 500 µmol/L. Although nitrate concentrations are expected to vary spatially because of varying patterns of home occupancy, local land use, and recharge (for example, from roads, ditches, houses, yards, and drain fields), these factors do not necessarily account for the large volume of high-nitrate groundwater below −4 m altitude. Five possible explanations for the high nitrogen are explored:

1. *The assumptions used to calculate the loading were not correct.*—The 500 µmol/L estimated volume-averaged nitrate concentration for the Eel River site was obtained from known housing density, occupancy, water use, and recharge and assumed 20 percent loss of nitrogen at the leachfield (Colman and others, 2015). Weiskel and Howes (1992) studied a site in Wareham, Mass., with a slightly higher density of septic system sources (10 as opposed to 9 per hectare) but with similar hydrologic and water-use characteristics. Adjusting the 500-µmol/L Eel River estimate for the higher septic-system density yields an estimated mean concentration of groundwater nitrogen for the Wareham site of 555 µmol/L. This value is similar to observed, vertically averaged (300 µmol/L) and maximum (650 µmol/L) nitrate concentrations in a 4-m-thick nitrate-containing zone at the Wareham site that is far enough downgradient from septic-system sources for individual plumes to have dispersed and merged (Weiskel and Howes, 1992, fig. 7). The similarity between estimated and observed concentrations at Wareham supports the conclusion that the anomalously high nitrate concentrations below an altitude of −4 m at the Eel River site are not likely due to an underestimation of the expected mean nitrogen concentration in the groundwater.

2. *The higher concentrations are from undispersed wastewater plumes.*—Weiskel and Howes (1992) reported dissolved inorganic nitrogen as high as 3,400 µmol/L in groundwater from septic system leachate at a near-field location (5 m downgradient from a leach field) at the Wareham site. At the farthest downgradient sampling location in Wareham along one 400-m-long flowpath, the zone of highest nitrate concentrations (>600 µmol/L) was only 1 m thick, indicating that there was substantial dispersion of nitrate plumes from individual septic systems.

   At the Eel River site, the zone with nitrate concentrations greater than 600 µmol/L was about 5–8 m thick at the profiles along the *B*–*B′* section (figs. 20 and 21), and elevated nitrate concentrations extended over a wide area that included the historical wells at the western and eastern sides of the Seacoast Shores peninsula (fig. 3*C*). If the nitrate were present as narrow and undispersed plumes, concentrations might be expected to change over time at individual sampling locations given that flow direction at the site varies temporally (fig. 10). However, the distribution of high concentrations (figs. 20 and 21) did not vary substantially over time. Because the high-concentration zone is thick, extensive in the direction of flow, and temporally persistent, which are characteristics not expected for undispersed plumes from individual sources, a lack of dispersion of individual plumes is an unlikely explanation for the high nitrate concentrations deep at the Eel River site.

3. *The higher concentrations in the deep zone result from more concentrated effluent sinking to greater depths than less concentrated effluent.*—The highest nitrate concentrations near the bottom of the freshwater profiles could be the result of density-driven sinking of wastewater plumes in the aquifer. Increased density could be imparted by total ion concentrations in the wastewater that are elevated compared to concentrations in ambient groundwater. Undiluted leachate from septic systems and cesspools can have specific conductances as high as 4,000 microsiemens per centimeter at 25 °C (µS/cm at 25 °C) (Colman and Friesz, 2001), representing dissolved solutes that increase density by 0.22 percent over that of ambient freshwater (specific conductance of 100 µS/cm at 25 °C) (Chen and Millero, 1986). For reference, analytical and numerical modeling was used to estimate that an initial density difference of 0.1 percent between ambient groundwater and a 7,600-liter injected tracer cloud caused about 1 m of downward displacement of the cloud relative to 99 m of lateral transport in a sand and gravel aquifer during a period of 237 days (LeBlanc, 2001).

   Comparison of nitrate and specific conductance profiles at F724 indicates a slight association of the deep, high nitrate concentrations with higher specific conductance (fig. 28). Specific conductance increased from 171 µS/cm at the water table to 323 µS/cm at −10.37 m altitude, where nitrate concentration also was highest. However, the specific conductance across most of the deep, high-nitrate zone (−5 to −10 m altitude) was not elevated (fig. 28). The proximity of the highest nitrate to the freshwater/saltwater interface is consistent with the conceptual model of a high-concentration wastewater plume that sinks downward until encountering ambient groundwater with a similar density near the interface, but the density gradient implied by the shallow and deep specific conductance data is small and may be more indicative of the mixing zone between freshwater and saltwater than dense groundwater derived from wastewater.

   If plumes from individual septic or cesspool systems were sinking to near the freshwater/saltwater interface at the Seacoast Shores peninsula, then the short distance

to the groundwater divide, low associated horizontal velocities, and small freshwater saturated thickness (12 m) were likely contributing factors. Additional field and modeling investigations could improve understanding of whether density-driven sinking is enhanced by these factors and may help explain the deep high-nitrate zone near the freshwater/saltwater interface.

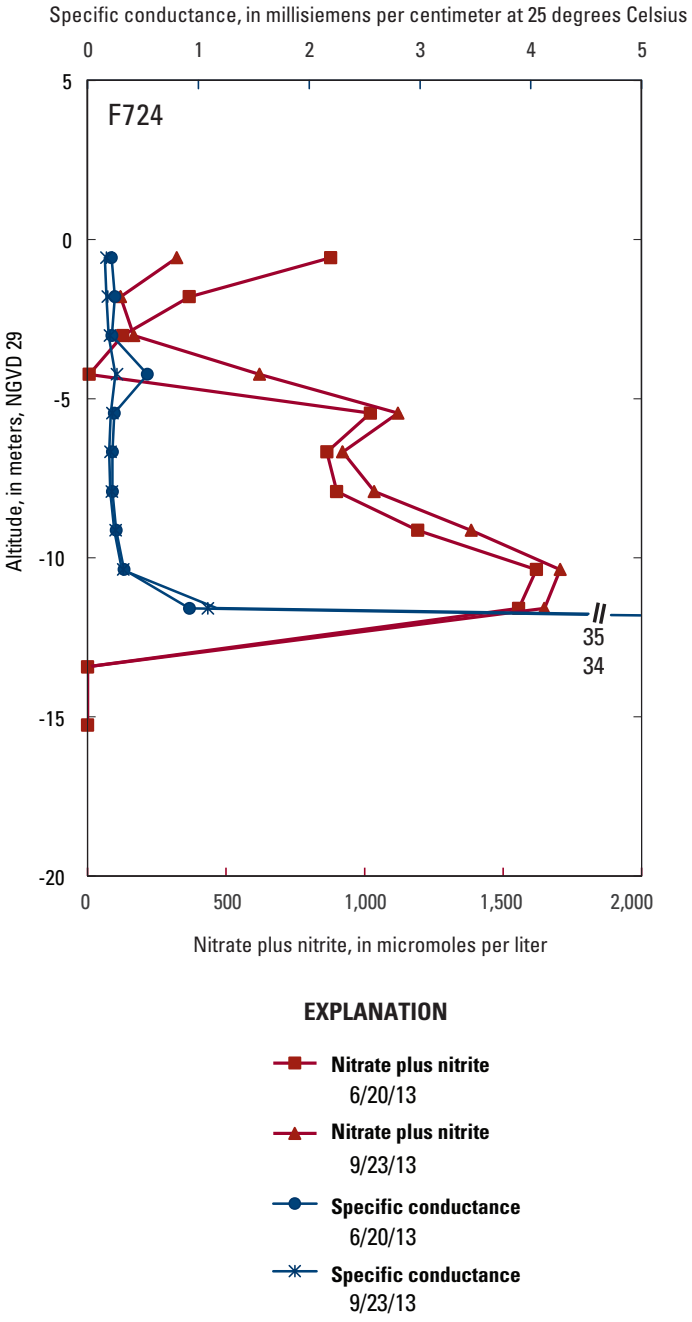

Figure 28. Vertical profiles of nitrate plus nitrite and specific conductance at multilevel sampler F724 near the Eel River, Seacoast Shores peninsula, East Falmouth, Massachusetts, sampled June 20 and September 23, 2013. Location of the site is shown on figure 5.

4. *The higher concentrations reflect changes in historical wastewater loading or hydrologic conditions.*—High nitrate concentrations in deep freshwater zones could be a legacy of historical changes in onsite wastewater disposal practices or patterns. Tritium concentrations in selected groundwater samples were fairly constant (3.8±0.6 tritium units, *n*=6). Measured values such as these, when adjusted for radioactive decay, could represent precipitation recharge in coastal areas of the northeastern U.S. during the late 1970s to present (Böhlke and Krantz, 2003; Böhlke and others, 2009. However, no major historical shifts since the late 1970s in wastewater disposal practices, such as a substantial shift from cesspools to septic systems, were identified in conversations with town and county officials (Raymond Jack, Town of Falmouth, and George Heufelder, Barnstable County, oral commun., February 2018) that might have resulted in high nitrate concentrations in older groundwater near the bottom of the freshwater lens.

5. *The higher concentrations result from a different source with higher nitrogen concentrations than wastewater effluent disposed on the peninsula.*—Measured water-table gradients were consistently toward the Eel River and indicate that any hypothesized source of the deep, high nitrate concentrations other than wastewater would have to have been on the peninsula east of the Eel River study site (see fig. 10 for flow directions). But this area includes only housing on approximately equal-sized lots on gridded streets and has no golf courses, plant nurseries, landfills, or other nitrogen sources. Historically, the area was forested and undeveloped through the 1930s and used by the U.S. Army during World War II to access an adjacent island in Waquoit Bay for amphibious training. The area was subdivided for development in 1947. A historical nitrogen source other than domestic wastewater disposal appears unlikely.

Intertidal Saltwater Cell

In the conventional subterranean estuary model (fig. 4), an intertidal saltwater cell develops in shallow groundwater because of tidal run-up of saltwater during spring tides, when saltwater infiltrates into the beach and fills the pore spaces in sand that had drained during previous periods of lower high tide. The infiltrated water tends to flow through the beach to discharge in the region of low tide during subsequent periods of lower high tide (Abarca and others, 2013). During the 5-day period (September 20 to 25, 2013) of nearshore, shallow subsurface sampling to investigate the effects of spring tides on the shallow groundwater, the maximum daily tide range was 0.71 m (fig. 11*A*). The intertidal zone that was flooded between the tidal extremes was about 6 m wide perpendicular to shore.

In the detailed sampling of the intertidal subsurface, the salinity pattern confirmed features of an intertidal saltwater cell (fig. 22). Sampling on three occasions within 5 days showed the presence of a shoreward zone of elevated salinity that shifted over time, as was also observed at Waquoit Bay (Abarca and others, 2013). In the same shoreward zone, dissolved oxygen concentrations initially were high and decreased over time (fig. 23). The dissolved oxygen decrease over time might be evidence of microbial processes that could have led to denitrification if sufficient organic carbon was infiltrated with the seawater and mixed with shallow fresh groundwater containing dissolved oxygen and nitrate, but samples collected from this zone during this study were not analyzed for nitrate-reduction indicators.

Influence of Local and Regional Groundwater Flow on the Freshwater/Saltwater Interface

Measurements of hydraulic head in the onshore well network were used to infer a local groundwater-flow system beneath the Seacoast Shores peninsula that is driven by recharge on land and discharge at the coast (figs. 9 and 10). This inferred flow regime is typical of nearshore coastal settings and similar to that of Waquoit Bay. Hydraulic gradients are low and, therefore, the groundwater-flow rate likely also is low. The freshwater/saltwater interface at the shore is deeper (about 12 m) than the depth to the interface at Waquoit Bay (6 m). The depth to the interface at the Eel River site does not appear to decrease significantly with distance offshore based on profiles as far as 18 m from shore, and freshwater was detected in the shallow bottom sediments at 31 m offshore, the farthest point from shore sampled during this study (F725–A16, fig. 6). In contrast, the interface at Waquoit Bay rises upward and intersects the sediment/water interface at a distance of approximately 4.5 m offshore. Differences in geologic controls (not investigated during this study) operating at the two sites could explain the differences between the shapes of the freshwater/saltwater interfaces. Fresh groundwater extending much farther from shore has been documented in subterranean estuaries elsewhere—for example, hundreds of meters in Delaware and Maryland coastal bays, possibly related to offshore variations in lithology and partial confinement of the aquifer (Bratton and others, 2004, 2009).

Differences in the locations of the two Cape Cod sites relative to the shoreline and the regional flow system may also contribute to the differences in the shapes of the freshwater/saltwater interfaces at the sites. The Eel River study site is near the confluence of the two arms of the Eel River (fig. 2). The Waquoit Bay site, in contrast, is on a large saltwater bay where the shoreline is approximately perpendicular to the seaward direction of regional groundwater flow. Water-table simulations from a regional groundwater-flow model (Walter and Whealan, 2005) indicated strong hydraulic gradients from the northwest in the area just north of the coastal salt ponds in Falmouth (fig. 1). The extent and manner in which those gradients are changed at the shore by flow and discharge from the Seacoast Shores peninsula are unknown. It is possible that the regional groundwater flow underflows fine-grained sediments at the bottoms of the saltwater ponds and discharges wherever coarser sediment is present, including at the western shore of the Seacoast Shores peninsula, creating a complex three-dimensional groundwater-flow system beneath the Eel River.

Chemical Distributions in Groundwater as Evidence for Flow Patterns and Reactions

The chemical distributions in groundwater at the Eel River study are evidence of complex patterns of groundwater flow and chemical reactions in the subterranean estuary. This evidence is discussed in the next several sections.

Dissolved Oxygen

Dissolved oxygen concentrations generally were low throughout most of the onshore and shoreline profiles (fig. 29). Groundwater at the profile 9 m offshore (F733) was substantially oxygenated, however, which would not be expected if flow were toward the estuary and parallel to the transect. The appearance of oxygenated water at site F733 indicates that the flow direction was not along a simple path from the shore to the offshore profile at 9 m. One possibility is that the dissolved oxygen pattern offshore could be consistent with upward flow toward a nearshore freshwater discharge zone, as identified by low specific conductance between sites F738 and F736 (fig. 13). The deep zone of elevated dissolved oxygen offshore might be connected with the shallow zone of elevated dissolved oxygen near the river bottom (as is shown in fig. 29), in which case the deep oxygenated zone would also appear to be discharging to the Eel River near sites F737 and F736. The overlying saltwater is not likely a source of the shallow dissolved oxygen at these sites because the water in the shallow zone near the sites had a low specific conductance. Where the specific conductance in the shallow zone was high, indicating seawater infiltration, dissolved oxygen was absent (compare figs. 13 and 29 between F735 and F746).

It is also possible that the apparent offshore increase in dissolved oxygen near F733 (fig. 29) indicates that the sampling transect is not parallel to the flow direction. In this case, the three-dimensional boundary between aerobic and anaerobic groundwater beneath the estuary may have a complex shape because different flow paths intersected by the sampling transect have different recharge areas and different biogeochemical reaction paths. Alternatively, the deep dissolved oxygen at F733 may have originated from eastward flowing groundwater, perhaps from the regional flow system. Additional data offshore from F733 (dissolved oxygen was not measured at the F743 profile) could help resolve some of these questions.

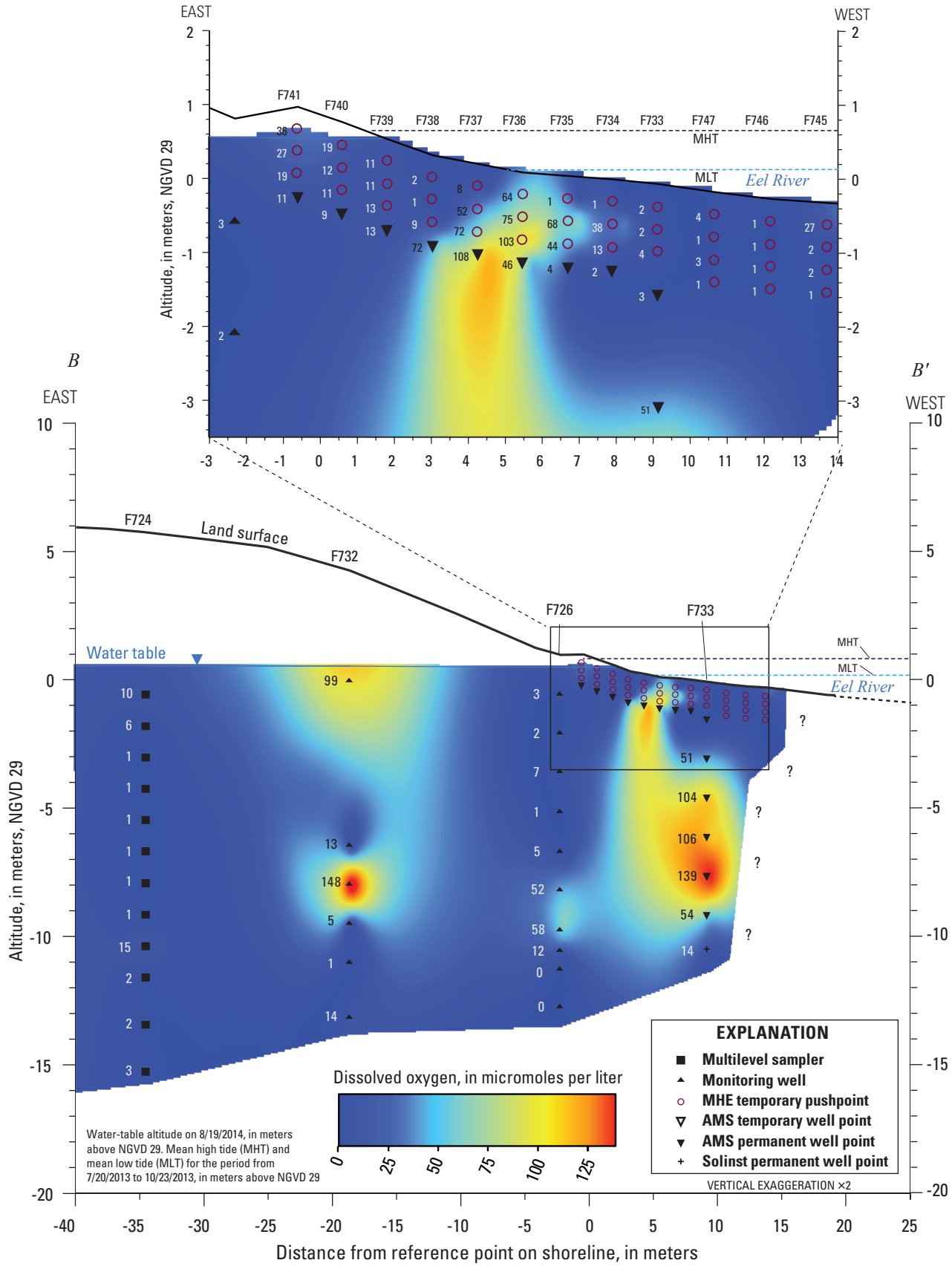

Figure 29. Distribution of dissolved oxygen in groundwater along section *B*–*B′* beneath the Eel River, Seacoast Shores peninsula, East Falmouth, Massachusetts, sampled September 22 to 25, 2013. Dissolved oxygen concentrations were not measured in samples from sites F742 and F743. Dissolved oxygen concentrations are reported in micromoles per liter as O_2. Location of the section is shown on figure 5.

Ammonium

Ammonium concentrations generally were low in fresh groundwater (fig. 30) except in the shallow zone at F724 where excess N_2 also was detected (see fig. 25). Low ammonium concentrations are typical of recharge beneath conventional septic systems. The location of the ammonium-rich freshwater zone might be related to a relatively fine-grained sedimentary unit (fig. 3*A*), which could have supplied reactive organic carbon and ammonium to the groundwater, or it might indicate a nearby area in which recharge water was relatively reducing. Coexistence of ammonium with documented evidence of nitrate reduction in shallow freshwater could indicate conditions favorable for anammox (Smith and others, 2015), but this reaction could not be confirmed with the available data.

Geochemical conditions favorable for anammox also existed at the deep freshwater/saltwater transition zone. Ammonium was present in the saline groundwater likely because of organic matter diagenesis in the estuarine sediment. Mixing of groundwaters containing ammonium and nitrate in the transition zone could have created conditions for anammox. As discussed in the section "Geochemical Indicators of Nitrogen Attenuation," stable isotope and nitrogen gas data from the transition zone indicate that nitrate reduction had occurred but did not provide clear evidence for anammox because the isotopic composition of ammonium was not substantially fractionated.

Nitrate

Nitrate concentrations at the Eel River study site generally were high in the deep freshwater zone and low in the shallow zone (fig. 31). Nitrate concentrations were low in both freshwater and saltwater near the sediment/water interface in offshore groundwater profiles (fig. 31). The estimated volume-averaged nitrogen concentration from septic systems (about 500 µmol/L) was reached or exceeded in the shallow zone only at the nearest inshore (F741, F740) and at the farthest offshore (F743) sampling sites. The shallow zones between these sampling sites are also areas of low dissolved oxygen (fig. 29) and elevated dissolved organic carbon concentrations, which are conditions that favor the nitrogen attenuation reactions.

Whereas the high concentrations of nitrate in shallow wells at the shore (F740, F741) do not appear to be connected to the high concentrations of nitrate near the bottom of the freshwater zone, the high nitrate concentrations at the profile 18 m offshore (F743) are more continuous with depth. At this site, the coarse sediments of the subterranean estuary were capped with soft sediment that increases in thickness in the offshore direction (fig. 8). The capping may have restricted infiltration of seawater into the subsurface in this zone, allowing freshwater containing high nitrate concentrations to persist closer to the river bottom than at sites closer to shore.

Groundwater-Flow Considerations

The vertical sections of specific conductance, dissolved oxygen, and nitrate, when considered together, provide evidence of possible converging flow paths beneath the offshore transect. Hydraulic gradients and specific conductance indicated a flow direction from land to the Eel River estuary (figs. 10, 12, and 13). The distribution of dissolved oxygen beneath the estuary might seem to imply upward flow in the landward direction (fig. 29). However, it is not clear what the source of the deep oxygen-rich water would be, nor why nitrate would be lost while dissolved oxygen remained high along the upward flow path.

As indicated in the section "Dissolved Oxygen," an alternative explanation is that the transect was not parallel to flow, in which case the offshore groundwater with elevated dissolved oxygen concentrations (fig. 29) may have originated from a different recharge area on land and encountered different aquifer materials than the onshore groundwater with lower dissolved oxygen concentrations. The data on groundwater levels and hydrogeologic structure in three dimensions, particularly offshore, were insufficient to resolve these questions.

Nitrogen Attenuation

Nitrogen attenuation was examined by using flow-path analysis and measurement of geochemical indicators of attenuation reactions. Nitrogen loss on flow paths starting where nitrogen concentrations were between the estimated volume-averaged groundwater concentration (about 500 µmol/L) and the observed deep, high concentration (1,706 µmol/L) and ending at a hypothesized nearshore discharge location (F738, F737, F736, mean nitrate concentration 68 µmol/L in fig. 31) would be large; loss factors were calculated by dividing 500 and 1,706 each by 68, yielding loss factors of 7.5 and 25. But these loss factors depend on several assumptions about flow and constancy of source, as discussed in the following paragraphs.

Although the hypothesis of groundwater flow from the peninsula to the estuary is supported by measured hydraulic gradients both at the water table and near the freshwater/saltwater interface (see the section "Water Levels and Hydraulic Gradients"), groundwater deep in the freshwater zone and flowing toward the estuary may be prevented from discharging near the shore by overlying fine-grained confining units such as those present at SCS–2 (F732, fig. 3*A*). The deep flow pattern at the Eel River estuary appears to be different from the flow pattern where the freshwater/saltwater interface rises to intersect the sediment/water interface just offshore and all freshwater discharges within 4.5 m of shore, as observed at Waquoit Bay and simulated in a density-dependent groundwater-flow model based on the coastal peninsulas (Colman and others, 2015). If the high-nitrate groundwater moves farther offshore before discharging, then the large nitrogen-loss factors estimated by comparing shallow and deep nearshore data might not apply.

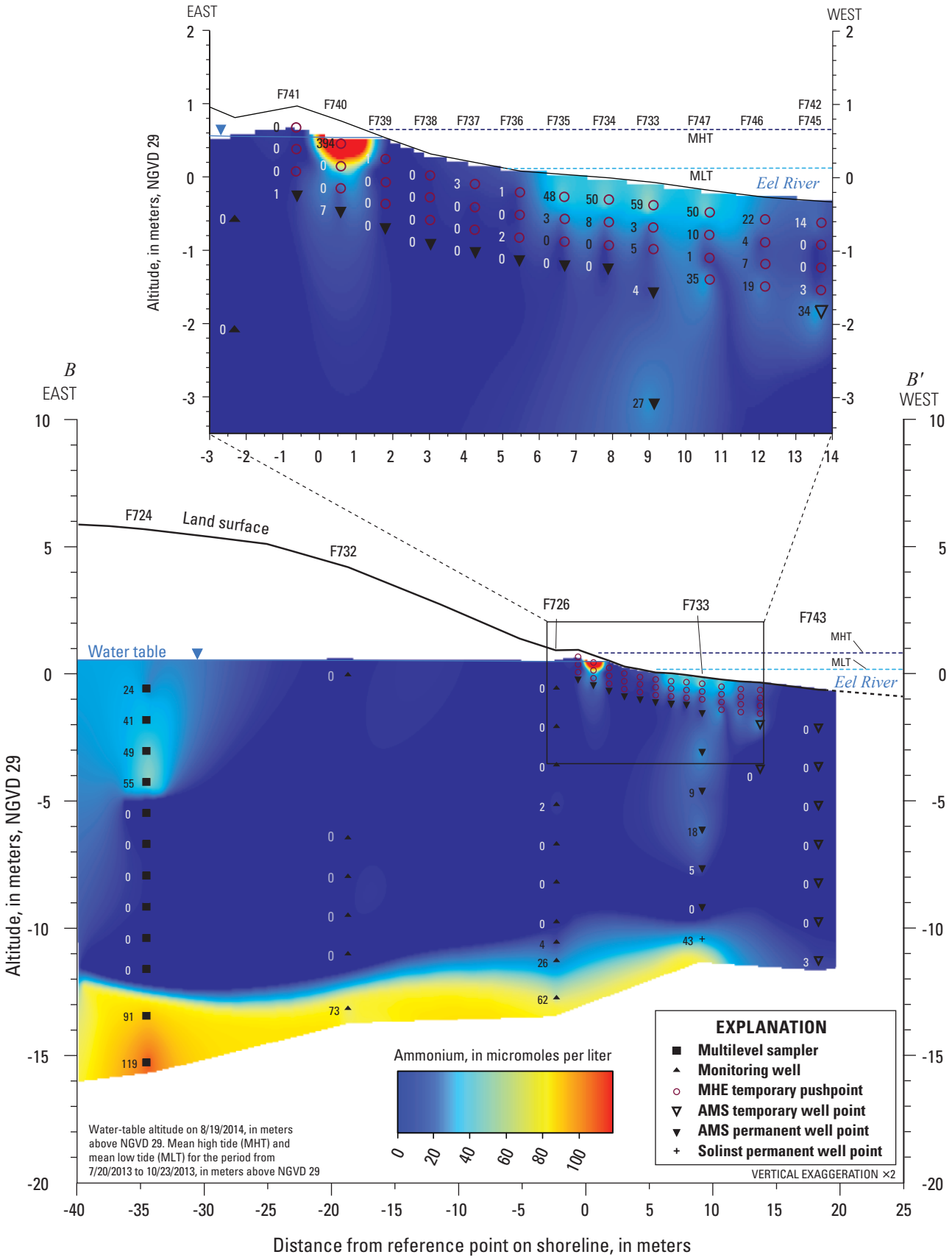

Figure 30. Distribution of ammonium in shallow groundwater along section *B*–*B*′ beneath the Eel River, Seacoast Shores peninsula, East Falmouth, Massachusetts, sampled September 22 to 25, 2013, except F742 and F743 sampled September 5, 2013. Location of the section is shown on figure 5.

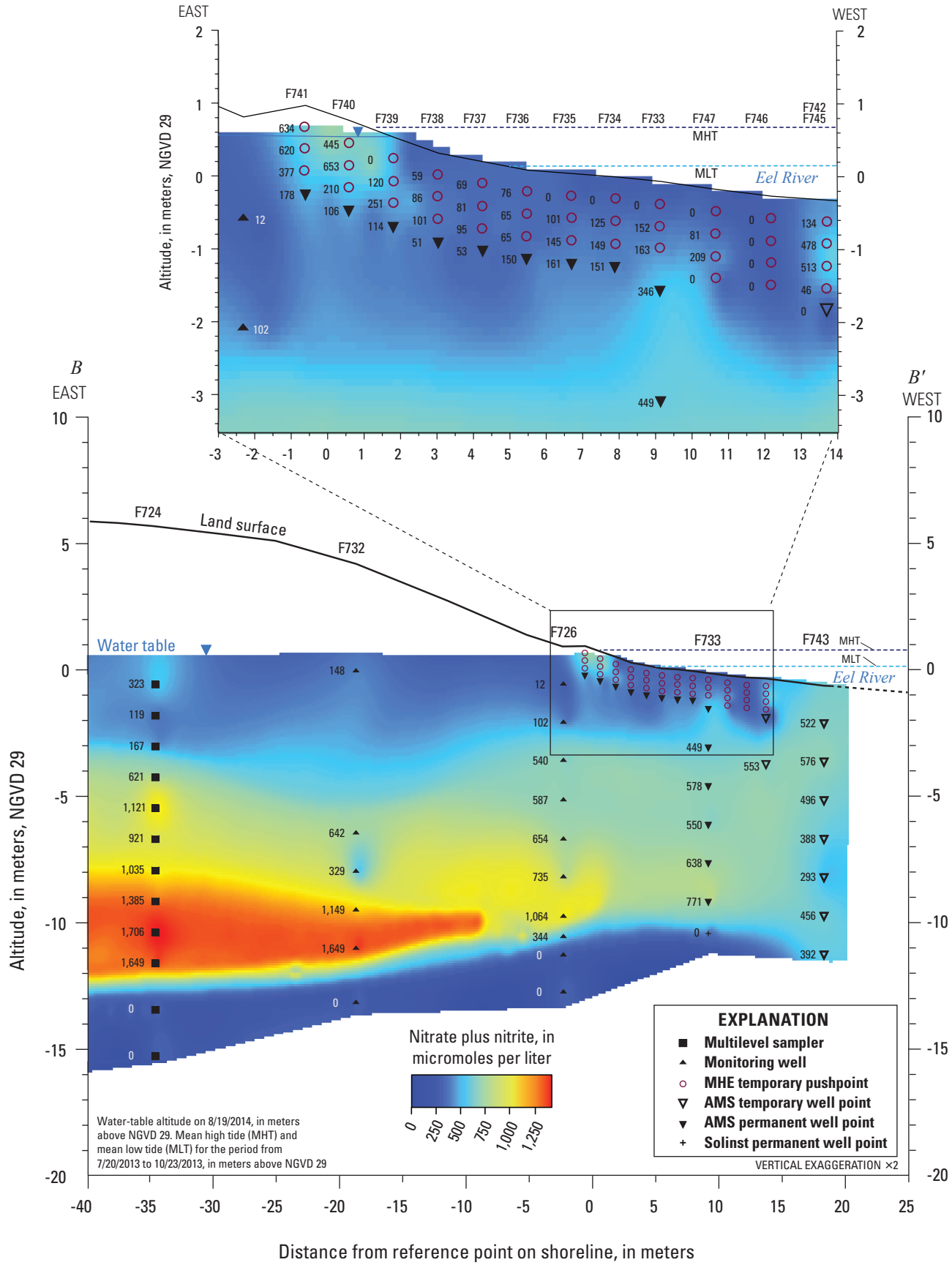

Figure 31. Distribution of nitrate plus nitrite in groundwater along section *B*–*B′* beneath the Eel River, Seacoast Shores peninsula, East Falmouth, Massachusetts, sampled September 22 to 25, 2013, except F742 and F743 sampled September 5, 2013. Location of the section is shown on figure 5.

Shallow flow from the land to discharge locations near the shore could still imply significant nitrate loss if the initial concentration is assumed to be 500 µmol/L. But whereas high nitrate concentrations were present deep in the fresh groundwater on both sides of the peninsula and through a significant section of the water column, the nitrate concentrations in the shallow fresh groundwater were more variable spatially. Three of five water-table wells (F728–0026, F729–0028, and F731–0029 [fig. 5], sampled on August 20, 2013) had both low nitrate concentrations and nearly saturated dissolved oxygen concentrations, unlike the shallow moderate nitrate and low dissolved oxygen concentrations at F724. Thus, the apparent changes in nitrate and dissolved oxygen concentrations along a shallow flow path might be evidence of flow paths from different sources that intersect the sampling transect obliquely rather than evidence of nitrate attenuation reactions along a flow path.

Finally, as indicated in the section "Influence of Local and Regional Groundwater Flow on the Freshwater/Saltwater Interface," flow-path analysis at the Eel River may be confounded by convergent flow in the expected region of discharge resulting from interaction of local flow from the peninsula and regional flow from the west. The uncertainties associated with flow-path analysis given the available data preclude its use for computing nitrogen loss at the Eel River study site.

Whereas flow-path analysis did not provide reliable evidence for aquifer-scale nitrate loss, direct measurements of dissolved gas concentrations, isotopes, and alkalinity provided evidence for nitrate reduction at all three profiles (F724, F726, F733) in shallow fresh groundwater at altitudes above approximately −3 m, and at two of the profiles (F726, F733) in saltwater near the deep freshwater/saltwater transition zone (fig. 24). Calculated nitrate losses by denitrification ranged from <40 to 294 µmol/L in samples with calculated initial nitrate concentrations of <40 to 479 µmol/L. Shallow freshwater samples from the shoreline profile (F726 −0.59, F726 −2.10) exhibited isotopic evidence of nitrate reduction with little or no excess N_2 (figs. 25 and 26), indicating initial nitrate concentrations less than approximately 150 µmol/L. According to these methods, none of the samples with direct evidence of nitrate reduction had more than about 500 µmol/L nitrate when recharged.

Sample locations with evidence of nitrate reduction commonly also had measurable ammonium, whereas ammonium was largely absent from other areas. For example, the zone from −4-m altitude to the freshwater/saltwater interface at the bottom of the onshore profile at F724 had conditions that could permit nitrate reduction (presence of nitrate and low dissolved oxygen concentration), but there was no indication from the geochemical measurements of nitrate attenuation. A likely limitation to nitrate attenuation in otherwise favorable conditions is lack of reactive organic carbon. Mixing of groundwaters containing nitrate and ammonium could produce conditions favorable for anammox, which might not necessarily require organic carbon, but this reaction was not demonstrated.

Although results from direct geochemical measurements are important for understanding nitrogen transport and attenuation in the Cape Cod aquifer, too few measurements were taken offshore to indicate the overall effect of nitrogen attenuation in the subterranean estuary. Concentrations of dissolved oxygen in some of the offshore samples were unfavorable for denitrification or anammox, and a thick freshwater zone with elevated nitrate concentrations was present at the farthest offshore profile sampled (F743, about 18 m from the shoreline). Farther offshore (beyond the limits of this study), it is possible that fresh groundwater containing nitrate might discharge to the estuary or that further mixing and reaction might reduce nitrate concentrations prior to discharge.

According to the direct measurements, nitrate was lost in the shallow part of the aquifer, but there was no indication of nitrate loss in the deeper, high-nitrate zones. If the sources of the shallow and deep groundwater were similar, and if the aquifer geology was uniform, then the deep groundwater might be expected to retain evidence of nitrate loss in the shallow zone through which it must have passed. These observations may indicate that shallow nitrate reduction was a result of local interaction with a chemically reactive or less transmissive lithologic unit that was present near the shoreline but was not widespread inland (fig. 3*A*). Alternatively, nearby recharge conditions for the shallow groundwater in the onshore profile may have been different from the more distant recharge conditions of the deep groundwater in the profile.

Conceptual Model of Nitrogen Attenuation at the Eel River Subterranean Estuary

In summary, the observations and analysis described in this report lead to a conceptual model of nitrogen attenuation at the Eel River subterranean estuary that differs in some respects from the model based on Waquoit Bay (fig. 4) and the modeling study of Colman and others (2015). The fresh groundwater lens at the western shore of the Eel River (fig. 32*A*) is about 11 m thick at the shoreline, but unlike at Waquoit Bay the freshwater/saltwater interface does not curve strongly upward beneath the river, at least within the limits of the area studied. An intertidal saltwater cell forms near the shoreline during spring tides, as was also observed at Waquoit Bay. Although lithologic data are limited, fine-grained sediments were reported near the shore in a shallow interval (−1 m to −6 m altitude) and near the freshwater/saltwater interface (top at −13 m altitude). Water levels measured in wells onshore indicate groundwater flow westward and upward toward the river, although hydraulic head was not measured offshore to confirm flow direction in the subterranean estuary beneath the river.

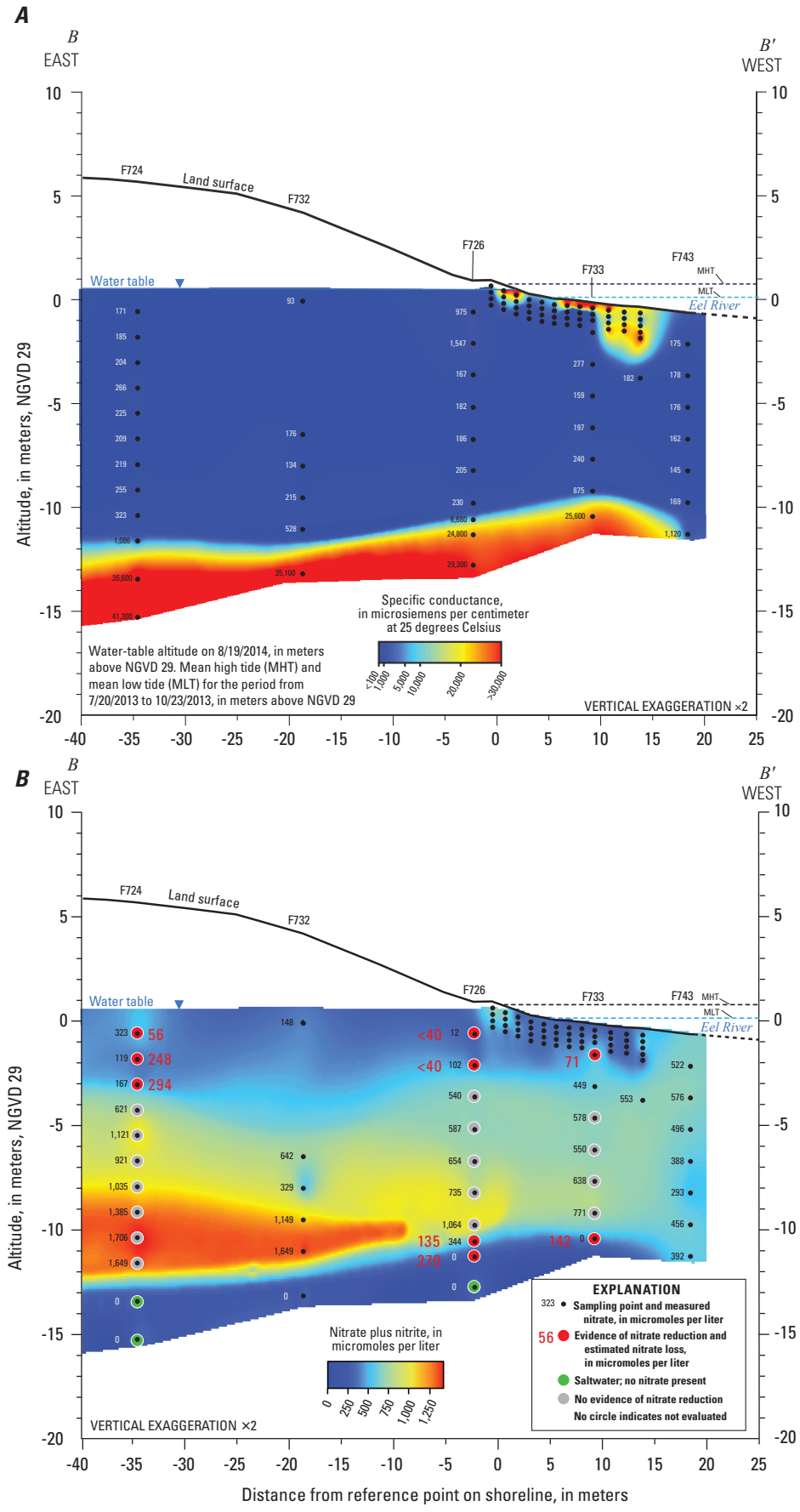

Figure 32. Distributions of *A*, specific conductance and *B*, measured nitrate plus nitrite in groundwater and selected features of the conceptual model of nitrogen transport and attenuation, including estimated nitrate loss at selected points, along section *B*–*B*′ beneath the Eel River, Seacoast Shores peninsula, East Falmouth, Massachusetts, sampled September 5 to 25, 2013. Location of the section is shown on figure 5.

Geochemical indicators of nitrate reduction, including concentrations of the reaction product nitrogen gas, stable isotope ratios of nitrate and nitrogen gas, and changes in alkalinity, provide evidence for nitrate reduction in two zones separated vertically by a zone 7–8 m thick with no evidence of nitrate reduction (fig. 32*B*). The shallow nitrate-reduction zone is near the water table in fresh groundwater onshore, and evidence of nitrate reduction may extend a short distance offshore in shallow fresh groundwater (F733–005, fig. 32). Nitrate reduction in this zone may be related to particular recharge conditions at nearby sources or to the shallow fine-grained sediments at about the same altitude (−1 to −6 m), where flow may be slower and reactive electron donors such as solid organic carbon, iron, or sulfide phases may be present to drive the reduction process. The deep nitrate-reduction zone is near the freshwater/saltwater transition zone, and nitrate reduction in this zone may be related to the mixing of freshwater containing nitrate and saltwater containing dissolved organic carbon or to the fine-grained sediments that are present at about the same altitude as the transition zone (fig. 3*A*). The maximum amount of nitrogen converted to N_2 in the sampled parts of the shallow and deep nitrate-reduction zones was estimated to be approximately 300 micromoles per liter.

Ammonium concentrations were elevated in both nitrate-reduction zones (fig. 30), which would be consistent with, but is not definitely a result of, ammonium release from sediments with high organic carbon content. Similarly, elevated alkalinity in some shallow samples is consistent with organic carbon being the electron donor for nitrate reduction, but identification of electron donors in the deep samples is difficult because saline water has high background concentrations of sulfate and bicarbonate. Although evidence for nitrate reduction is strong in some samples, the data are not sufficient to determine the relative importance of different nitrate-reduction processes, including denitrification and anammox.

The high nitrate concentrations and low dissolved oxygen concentrations in the thick intermediate zone between the shallow and deep nitrate-reduction zones (fig. 32*B*) are conditions that could favor nitrate reduction. The absence of nitrate reduction in this zone may result from the lack of reactive electron donors in this depth interval. The high-nitrate zone dissipates somewhat in the offshore direction, but the current study did not extend far enough to encompass the fresh groundwater discharge area or determine how much of the nitrate was removed prior to discharge.

A shallow intertidal saltwater cell was observed to form at the shore during tidal run-up of saltwater during a spring tide (fig. 32*A*). The decrease over time of dissolved oxygen following the infiltration of saltwater during the spring tide (fig. 23) might be evidence of microbial processes that could have led to denitrification if sufficient organic carbon was infiltrated with the seawater and mixed with shallow fresh groundwater containing oxygen and nitrate, but samples collected from this zone during this study were not analyzed for indicators of nitrate reduction.

The presence of elevated dissolved oxygen concentrations 9 m offshore (fig. 29) may indicate that groundwater flow was partly oblique to the sampling transect, or that groundwater from the regional flow system was converging under the river near the study area. Flow directions may also have been affected by aquifer heterogeneity such as the shallow fine-grained sediments onshore (fig. 3*A*) and at the bottom of the Eel River (fig. 8). Additional data on hydraulic heads and lithology may help determine groundwater-flow directions.

The heterogeneous aquifer materials, fine-grained sediments on the river bottom, and convergence of the local peninsular and regional fresh groundwater-flow systems are likely typical of many settings like that of the Eel River study site. Improved understanding of the fate of nitrate in this type of complex setting might be gained by extending investigations of nitrate reduction to the shallow sediments in the intertidal saltwater cell and adjacent subtidal zone and to locations farther offshore beneath the estuary. Further field studies also could refine understanding of the flow and geochemical system and enable computation of nitrogen attenuation as a fraction of nitrogen recharged in the aquifer as a whole, which was not possible with the data collected in this study. Site-specific hydrologic and geochemical conditions, however, may limit the transferability of such a computed result to other locations, even within the same subterranean estuary.

References Cited

Abarca, E., Karam, H., Hemond, H.F., and Harvey, C.F., 2013, Transient groundwater dynamics in a coastal aquifer—The effects of tides, the lunar cycle, and the beach profile: Water Resources Research, v. 49, no. 5, p. 2473–2488. [Also available at https://doi.org/10.1002/wrcr.20075.]

Abrams, R.H., Loague, K., and Kent, D.B., 1998, Development and testing of a compartmentalized reaction network model for redox zones in contaminated aquifers: Water Resources Research, v. 34, no. 6, p. 1531–1541. [Also available at http://dx.doi.org/10.1029/98WR00485.]

American Water Works Association, 2017, 2520—Salinity, in Standard methods for the examination of water and wastewater: Denver, Colo., American Water Works Association, p. 2–62.

Anwar, N., Robinson, C., and Barry, D.A., 2014, Influence of tides and waves on the fate of nutrients in a nearshore aquifer—Numerical simulations: Advances in Water Resources, v. 73, p. 203–213. [Also available at https://doi.org/10.1016/j.advwatres.2014.08.015.]

Barbaro, J.R., Walter, D.A., and LeBlanc, D.R., 2013, Transport of nitrogen in a treated-wastewater plume to coastal discharge areas, Ashumet Valley, Cape Cod, Massachusetts: U.S. Geological Survey Scientific Investigations Report 2013–5061, 37 p. [Also available at https://pubs.er.usgs.gov/publication/sir20135061/.]

Bau, M., Alexander, B., Chesley, J.T., Dulski, P., and Brantley, S.L., 2004, Mineral dissolution in the Cape Cod aquifer, Massachusetts, USA—I. Reaction stoichiometry and impact of accessory feldspar and glauconite on strontium isotopes, solute concentrations, and REY distribution: Geochimica et Cosmochimica Acta, v. 68, no. 6, p. 1199–1216. [Also available at http://dx.doi.org/10.1016/j.gca.2003.08.015.]

Belaval, M., Lane, J.W., Jr., Lesmes, D.P., and Kineke, G.C., 2003, Continuous-resistivity profiling for coastal groundwater investigations—Three case studies, in Proceedings of the Symposium on the Application of Geophysics to Engineering and Environmental Problems (SAGEEP), San Antonio, Texas, April 6–10, 2003: Denver, Colo., Environmental and Engineering Geophysical Society, CD–ROM, 14 p.

Böhlke, J.K., 2002, Groundwater recharge and agricultural contamination: Hydrogeology Journal, v. 10, no. 1, p. 153–179. [Also available at https://doi.org/10.1007/s10040-001-0183-3.]

Böhlke, J.K., 2003, Sources, transport, and reaction of nitrate in ground water, *in* Lindsey, B.D., and others, eds., Residence times and nitrate transport in ground water discharging to streams in the Chesapeake Bay Watershed: U.S. Geological Survey Water-Resources Investigations Report 03–4035, p. 25–39. [Also available at https://pubs.er.usgs.gov/publication/wri034035.]

Böhlke, J.K., Hatzinger, P.B, Sturchio, N.C., Gu, B., Abbene, I., and Mroczkowski, S.J., 2009, Atacama perchlorate as an agricultural contaminant in groundwater—Isotopic and chronologic evidence from Long Island, New York: Environmental Science & Technology, v. 43, p. 5619–5625. [Also available at https://doi.org/10.1021/es9006433.]

Böhlke, J.K., and Krantz, D.E., 2003, Isotope geochemistry and chronology of offshore ground water beneath Indian River Bay, Delaware: U.S. Geological Survey Water-Resources Investigations Report 03–4192, 37 p. [Also available at https://pubs.water.usgs.gov/wri03-4192/.]

Böhlke, J.K., Wanty, R.B., Tuttle, M.L., Delin, G.N., and Landon, M.K., 2002, Denitrification in the recharge area and discharge area of a transient agricultural nitrate plume in a glacial outwash sand aquifer, Minnesota: Water Resources Research, v. 38, no. 7, p. 10–1 to 10–26. [Also available at https://doi.org/10.1029/2001WR000663.]

Bratton, J.F., Böhlke, J.K., Krantz, D.E., and Tobias, C.R., 2009, Flow and geochemistry of groundwater beneath a back-barrier lagoon—The subterranean estuary at Chincoteague Bay, Maryland, USA: Marine Chemistry, v. 113, no. 1−2, p. 78–92. [Also available at https://doi.org/10.1016/j.marchem.2009.01.004.]

Bratton, J.F., Böhlke, J.K., Manheim, F.T., and Krantz, D.E., 2004, Ground water beneath coastal bays of the Delmarva Peninsula—Ages and nutrients: Ground Water, v. 42, no. 7, p. 1021–1034. [Also available at https://doi.org/10.1111/j.1745-6584.2004.tb02641.x.]

Brunner, B., Contreras, S., Lehmann, M.F., Matantseva, O., Rollog, M., Kalvelage, T., Klockgether, G., Lavik, G., Jetten, M.S., Kartal, B., and Kuypers, M.M., 2013, Nitrogen isotope effects induced by anammox bacteria: Proceedings of the National Academy of Sciences, v. 110, no. 47, p. 18994–18999. [Also available at https://doi.org/10.1073/pnas.1310488110.]

Cape Cod Commission, 2015, WatershedMVP—Multivariant planner: Cape Cod Commission Watershed MVP application, accessed October 15, 2015, at http://www.watershedmvp.org/.

Casciotti, K.L., Böhlke, J.K., McIlvin, M.R., Mroczkowski, S.J., and Hannon, J.E., 2007, Oxygen isotopes in nitrite—Analysis, calibration, and equilibration: Analytical Chemistry, v. 79, no. 6, p. 2427–2436. [Also available at https://doi.org/10.1021/ac061598h.]

Chen, C.T.A., and Millero, F.J., 1986, Thermodynamic properties for natural waters covering only the limnological range: Limnology and Oceanography, v. 31, no. 3, p. 657–662. [Also available at https://doi.org/10.4319/lo.1986.31.3.0657.]

Christensen, T.H., Kjeldsen, P., Albrechtsen, H.-J., Heron, G., Nielsen, P.H., Bjerg, P.L., and Holm, P.E., 1994, Attenuation of landfill leachate pollutants in aquifers: Critical Reviews in Environmental Science and Technology, v. 24, no. 2, p. 119–202. [Also available at https://doi.org/10.1080/10643389409388463.]

Colman, J.A., Carlson, C.S., and Robinson, C., 2015, Simulation of nitrogen attenuation in a subterranean estuary, representative of the southern coast of Cape Cod, Massachusetts: U.S. Geological Survey Open-File Report 2015–1085, 30 p., accessed June 2015 at https://dx.doi.org/10.3133/ofr20151085.

Colman, J.A., and Friesz, P.J., 2001, Geohydrology and limnology of Walden Pond, Concord, Massachusetts: U.S. Geological Survey Water-Resources Investigations Report 01–4137, 61 p. [Also available at https://pubs.er.usgs.gov/publication/wri014137.]

Costa, J.E., Heufelder, G., Foss, S., Millham, N.P., and Howes, B., 2002, Nitrogen removal efficiencies of three alternative septic system technologies and a conventional septic system: Environment Cape Cod, v. 5, no. 1, p. 15–24. [Also available at http://www.buzzardsbay.org/etistuff/results/costaenvccarticle2.pdf.]

Cozzarelli, I.M., Böhlke, J.K., Masoner, J., Breit, G.N., Lorah, M.M., Tuttle, M.L.W., and Jaeschke, J.B., 2011, Biogeochemical evolution of a landfill leachate plume—Long-term process studies: Ground Water, v. 49, no. 5, p. 663–687. [Also available at https://dx.doi.org//10.1111/j.1745-6584.2010.00792.x.]

Cross, V.A., Bratton, J.F., Crusius, J., Colman, J.A., and McCobb, T.D., 2008, Submarine hydrological data from Cape Cod National Seashore: U.S. Geological Survey Open-File Report 2006–1169, DVD–ROM. [Also available at https://woodshole.er.usgs.gov/pubs/of2006-1169.]

Crusius, J., Koopmans, D., Bratton, J.F., Charette, M.A., Kroeger, K., Henderson, P., Ryckman, L., Halloran, K., and Colman, J.A., 2005, Submarine groundwater discharge to a small estuary estimated from radon and salinity measurements and a box model: Biogeosciences, v. 2, no. 2, p. 141–157. [Also available at https://doi.org/10.5194/bg-2-141-2005.]

DeSimone, L.A., Barlow, P.M., and Howes, B.L., 1996, A nitrogen-rich septage-effluent plume in a glacial aquifer, Cape Cod, Massachusetts, February 1990 through December 1992: U.S. Geological Survey Water-Supply Paper 2456, 89 p. [Also available at https://pubs.er.usgs.gov/publication/wsp2456.]

Fairchild, G.M., Lane, J.W., Jr., Voytek, E.B., and LeBlanc, D.R., 2012, Bedrock topography of western Cape Cod, Massachusetts, based on bedrock altitudes from geologic borings and analysis of ambient seismic noise by the horizontal-to-vertical spectral-ratio method: U.S. Geological Survey Scientific Investigations Map 3233, 1 sheet, maps variously scaled, 17-p. pamphlet, on one CD–ROM. [Also available at https://pubs.er.usgs.gov/publication/sim3233.]

Howarth, R.W., Sharpley, A., and Walker, D., 2002, Sources of nutrient pollution to coastal waters in the United States—Implications for achieving coastal water quality goals: Estuaries, v. 25, no. 4, p. 656–676. [Also available at https://doi.org/10.1007/BF02804898.]

Huntington, T.G., Pirolli, G.F., McCobb, T.D., Böhlke, J.K., Colman, J.A., Kroeger, K.D., Brooks, T.W., and LeBlanc, D.R., 2018, Geochemical data supporting analysis of geochemical conditions and nitrogen transport in nearshore groundwater and the subterranean estuary at a Cape Cod embayment, East Falmouth, Massachusetts, 2013: U.S. Geological Survey data release, https://doi.org/10.5066/F7RR1WF0.

Hyer, K.E., Denver, J.M., Langland, M.J., Webber, J.S., Böhlke, J.K., Hively, W.D., and Clune, J.W., 2016, Spatial and temporal variation of stream chemistry associated with contrasting geology and land-use patterns in the Chesapeake Bay watershed—Summary of results from Smith Creek, Virginia; Upper Chester River, Maryland; Conewago Creek, Pennsylvania; and Difficult Run, Virginia, 2010–2013: U.S. Geological Survey Scientific Investigations Report 2016–5093, 211 p. [Also available at https://pubs.er.usgs.gov/publication/sir20165093.]

Jackson, W.A., Böhlke, J.K., Gu, B., Hatzinger, P.B., and Sturchio, N.C., 2010, Isotopic composition and origin of indigenous natural perchlorate and co-occurring nitrate in the southwestern United States: Environmental Science & Technology, v. 44, no. 13, p. 4869–4876. [Also available at https://doi.org/10.1021/es903802j.]

Keay, D.L., 2001, A history of Washburn Island: Bridgewater Review, v. 20, no. 2, p. 22–25. [Also available at https://vc.bridgew.edu/br_rev/vol20/iss2/10/.]

Kroeger, K.D., and Charette, M.A., 2008, Nitrogen biogeochemistry of submarine groundwater discharge: Limnology and Oceanography, v. 53, no. 3, p. 1025–1039. [Also available at https://doi.org/10.4319/lo.2008.53.3.1025.]

LeBlanc, D.R., 1984, Sewage plume in a sand and gravel aquifer, Cape Cod, Massachusetts: U.S. Geological Survey Water-Supply Paper 2218, 28 p. [Also available at https://pubs.usgs.gov/wsp/wsp2218/.]

LeBlanc, D.R., 2001, Density and recharge effects during the Cape Cod natural-gradient tracer test: Cambridge, Mass., Massachusetts Institute of Technology, master's thesis, 246 p.

LeBlanc, D.R., Guswa, J.H., Frimpter, M.H., and Londquist, C.J., 1986, Ground-water resources of Cape Cod, Massachusetts: U.S. Geological Survey Hydrologic Atlas 692, 4 sheets, scale 1:48,000. [Also available at https://pubs.er.usgs.gov/publication/ha692.]

Massachusetts Department of Environmental Protection, 2018, The Massachusetts Estuaries Project: Massachusetts Department of Environmental Protection web page, accessed March 2018 at http://www.mass.gov/eea/agencies/massdep/water/watersheds/the-massachusetts-estuaries-project-and-reports.html.

Masterson, J.P., Stone, B.D., Walter, D.A., and Savoie, J.G., 1997, Hydrogeologic framework of western Cape Cod, Massachusetts: U.S. Geological Survey Hydrologic Investigations Atlas HA–741, 1 sheet, scale 1:50,000. [Also available at https://pubs.er.usgs.gov/publication/ha741.]

McCobb, T.D., and LeBlanc, D.R., 2002, Detection of fresh ground water and a contaminant plume beneath Red Brook Harbor, Cape Cod, Massachusetts, 2000: U.S. Geological Survey Water-Resources Investigations Report 02–4166, 36 p. [Also available at https://pubs.er.usgs.gov/publication/wri024166.]

McCobb, T.D., LeBlanc, D.R., and Hess, K.M., 1999, Determination of temporal and spatial variability of hydraulic gradients in an unconfined aquifer using three-point triangulation, Cape Cod, Massachusetts, *in* Morganwalp, D.W., and Buxton, H.T., eds., U.S. Geological Survey Toxic Substances Hydrology Program—Proceedings of the technical meeting, Charleston, South Carolina, March 8–12, 1999—Volume 3 of 3—Subsurface Contamination from Point Sources: U.S. Geological Survey Water-Resources Investigations Report 99–4018C, p. 349–360. [Also available at https://toxics.usgs.gov/pubs/wri99-4018/Volume3/SectionC/3411_McCobb/index.html.]

Michael, H.A., Charette, M.A., and Harvey, C.F., 2011, Patterns and variability of groundwater flow and radium activity at the coast—A case study from Waquoit Bay, Massachusetts: Marine Chemistry, v. 127, nos. 1–4, p. 100–114. [Also available at https://doi.org/10.1016/j.marchem.2011.08.001.]

Michael, H.A., Lubetsky, J.S., and Harvey, C.F., 2003, Characterizing submarine groundwater discharge—A seepage meter study in Waquoit Bay, Massachusetts: Geophysical Research Letters, v. 30, no. 6, 4 p. [Also available at https://doi.org/10.1029/2002GL016000.]

Michael, H.A., Mulligan, A.E., and Harvey, C.F., 2005, Seasonal oscillations in water exchange between aquifers and the coastal ocean: Nature, v. 436, no. 7054, p. 1145–1148. [Also available at https://doi.org/10.1038/nature03935.]

Nixon, S.W., 1995, Coastal marine eutrophication—A definition, social causes, and future concerns: Ophelia, v. 41, no. 1, p. 199–219. [Also available at https://doi.org/10.1080/00785236.1995.10422044.]

Oldale, R.N., 1992, Cape Cod and the Islands—The geologic story: East Orleans, Mass., Parnassus Imprints, 205 p.

Repert, D.A., Barber, L.B., Hess, K.M., Keefe, S.H., Kent, D.B., LeBlanc, D.R., and Smith, R.L., 2006, Long-term natural attenuation of carbon and nitrogen within a groundwater plume after removal of the treated wastewater source: Environmental Science & Technology, v. 40, no. 4, p. 1154–1162. [Also available at https://doi.org/10.1021/es051442j.]

Short, F.T., and Burdick, D.M., 1996, Quantifying eelgrass habitat loss in relation to housing development and nitrogen loading in Waquoit Bay, Massachusetts: Estuaries, v. 19, no. 3, p. 730–739. [Also available at https://doi.org/10.2307/1352532.]

Smith, R.L., Böhlke, J.K., Garabedian, S.P., Revesz, K.M., and Yoshinari, T., 2004, Assessing denitrification in groundwater using natural gradient tracer tests with 15N—In situ measurement of a sequential multistep reaction: Water Resources Research, v. 40, no. 7, 16 p. [Also available at https://doi.org/10.1029/2003WR002919.]

Smith, R.L., Böhlke, J.K., Song, B., and Tobias, C.R., 2015, Role of anaerobic ammonium oxidation (anammox) in nitrogen removal from a freshwater aquifer: Environmental Science & Technology, v. 49, no. 20, p. 12169–12177. [Also available at https://doi.org/10.1021/acs.est.5b02488.]

Smith, R.L., Repert, D.A., Barber, L.B., and LeBlanc, D.R., 2013, Long-term groundwater contamination after source removal—The role of sorbed carbon and nitrogen on the rate of reoxygenation of a treated-wastewater plume on Cape Cod, Massachusetts, USA: Chemical Geology, v. 337–338, p. 38–47. [Also available at https://doi.org/10.1016/j.chemgeo.2012.11.007.]

Spiteri, C., Slomp, C.P., Charette, M.A., Tuncay, K., and Meile, C., 2008, Flow and nutrient dynamics in a subterranean estuary (Waquoit Bay, MA, USA)—Field data and reactive transport modeling: Geochimica et Cosmochimica Acta, v. 72, no. 14, p. 3398–3412. [Also available at https://doi.org/10.1016/j.gca.2008.04.027.]

U.S. Geological Survey, 2018, USGS water data for the Nation: U.S. Geological Survey National Water Information System database, accessed March 24, 2018, at https://doi.org/10.5066/F7P55KJN.

Valiela, I., Foreman, K., LaMontagne, M., Hersh, D., Costa, J., Peckol, P., DeMeo-Andreson, B., D'Avanzo, C., Babione, M., Sham, C.-H., Brawley, J., and Lajtha, K., 1992, Coupling of watersheds and coastal waters—Sources and consequences of nutrient enrichment in Waquoit Bay, Massachusetts: Estuaries, v. 15, no. 4, p. 443–457. [Also available at https://doi.org/10.2307/1352389.]

Valiela, I., Geist, M., McClelland, J., and Tomasky, G., 2000, Nitrogen loading from watersheds to estuaries—Verification of Waquoit Bay nitrogen loading model: Biogeochemistry, v. 49, no. 3, p. 277–293. [Also available at https://doi.org/10.1023/A:1006345024374.]

Walter, D.A., Masterson, J.P., and Hess, K.M., 2004, Ground-water recharge areas and traveltimes to pumped wells, ponds, streams, and coastal water bodies, Cape Cod, Massachusetts: U.S. Geological Survey Scientific Investigations Map I–2857, 1 sheet. [Also available at https://pubs.usgs.gov/sim/2004/2857/.]

Walter, D.A., McCobb, T.D., Masterson, J.P., and Fienen, M.N., 2016, Potential effects of sea-level rise on the depth to saturated sediments of the Sagamore and Monomoy flow lenses on Cape Cod, Massachusetts (ver. 1.1, October 18, 2016): U.S. Geological Survey Scientific Investigations Report 2016–5058, 55 p., accessed October 2016 at http://dx.doi.org/10.3133/sir20165058.

Walter, D.A., and Whealan, A.T., 2005, Simulated water sources and effects of pumping on surface and ground water, Sagamore and Monomoy flow lenses, Cape Cod, Massachusetts: U.S. Geological Survey Scientific Investigations Report 2004–5181, 85 p. [Also available at https://pubs.er.usgs.gov/publication/sir20045181.]

Weiskel, P.K., and Howes, B.L., 1992, Differential transport of sewage-derived nitrogen and phosphorus through a coastal watershed: Environmental Science & Technology, v. 26, no. 2, p. 352–360. [Also available at https://doi.org/10.1021/es00026a017.]

Appendix 1. Methods for Field Sampling, Laboratory Analysis, and Determination of Denitrification

Contents

Figures

Tables

Appendix 1. Methods for Field Sampling, Laboratory Analysis, and Determination of Denitrification

Site Selection and Field Instrumentation

Site Selection

Instruments were deployed on land and in the estuaries at several prospective sites in southern Falmouth, Massachusetts. Several rounds of field measurements and preliminary interpretations were done at these sites to assess whether conditions at the sites were appropriate, in terms of hydraulic gradients and nitrogen concentrations, for a more comprehensive field investigation. Field screening methods were used initially to determine relative concentrations of analytes. The data generated by using these methods were used to guide the selection of locations for the collection of additional samples to be analyzed by using standard laboratory techniques.

Field results indicated that the more northern of the two potential study sites at the Eel River contained water-quality depth profiles more nearly approximating the initial conceptual model for the study, and further site development (with water-table wells, a shoreline well cluster, and offshore instrumentation) was confined to this site. Throughout the 2013 summer, additional wells were installed and sampled. The placement of wells onshore was intended to assess water-table gradients near the shore, to define the depth of the freshwater/saltwater boundary, and to characterize the onshore geochemical environment. The purpose of the offshore wells was to define the chemistry and location of the intertidal saltwater cell and deep saltwater wedge shown in the conceptual model (fig. 4). Sampling of the well network took place on June 20, July 19, August 20 to 24, and September 3 to 5, 2013. The final sampling, resulting in the largest dataset and areal extent, was done on September 20 to 25, 2013.

Sampling Points and Tidal Gage

Several types of temporary and permanent sampling points were used for the measurement of groundwater and tide levels and the collection of water samples. A hollow-stem auger drilling rig was used to install the two permanent multilevel samplers (MLSs) near the Eel River in May 2013. The MLSs are constructed of 15 color-coded polyethylene tubes 0.64 centimeter (cm) in diameter that extend to various depths through a 3.2-cm-diameter polyvinyl chloride (PVC) pipe. The tubes are screened with nylon mesh secured to the outside of the PVC pipe.

Permanent monitoring wells were installed at the study site by using a direct-push drilling rig (GeoProbe Model 54DT, Salinas, Kansas) (fig. 1.1). The wells are constructed of 2.5-cm-diameter PVC pipe and slotted screens. Five

Figure 1.1. Direct-push drilling rig on the shore of the Eel River, Seacoast Shores peninsula, East Falmouth, Massachusetts, July 16, 2013. Photograph by Denis LeBlanc, U.S. Geological Survey.

water-table wells were installed in June 2013 in the general area of MLS F724 for determination of the water-table shape and estimation of hydraulic gradients (fig. 5). The water-table wells have 3.1-meter-long screens that are set just below the water table (to a maximum depth of 9.4 meters [m] below land surface). A cluster of 10 monitoring wells was installed in July 2013 at one site (F726) (figs. 5 and 6) to obtain profiles of hydraulic head and water quality at the shoreline of the Eel River. The wells have screens 0.25 m long set at depths below land surface ranging from 1.5 to 13.7 m.

Shallow offshore surveys were done in June 2013 by using temporary pushpoint samplers to collect shallow groundwater samples at depths up to 1.7 m below the offshore bottom sediments (sites F725–A01 to F725–A21 [fig. 6]). The pushpoint sampler (MHE Products, East Tawas, Michigan) is a stainless-steel tube 6.4 millimeters (mm) in diameter with a machined point and 4-cm-long slotted screen at the tip (Henry, 2001). Groundwater was sampled by using a syringe or peristaltic pump. In September 2013, temporary pushpoint samplers (sites F734 to F741, F745 to F747) were set at depths of up to 1.2 m into the offshore bottom sediments to obtain a vertical section of water quality in the intertidal zone. The positions of offshore locations are reported relative to the shoreline, defined for the purposes of the field investigation as the point approximately halfway between shoreline positions at the maximum and mean high tides during the study period.

Two methods were used from a floating platform (fig. 1.2) to obtain deeper groundwater-quality profiles beneath the Eel River bottom sediments. In August 2013, at locations 9 to 27 m from shore (sites F733–A01, F778–A01,

Figure 1.2. Well-point installation on a floating platform on the Eel River, Seacoast Shores peninsula, East Falmouth, Massachusetts, August 21, 2013. Photograph by Denis LeBlanc, U.S. Geological Survey.

F779–A01), a 15-cm-long well point (Solinst Canada Ltd., Georgetown, Ontario, Canada) connected to a 1.9-cm-diameter black steel pipe was advanced by using a vibratory hammer. Dedicated polyethylene sample-collection tubing was connected to the well point by a barbed fitting and extended to the surface through the steel pipe. Samples were collected every 1.5 m to a depth of 10.4 m. The well point was left permanently at 10.4 m (F733–0034) for future sampling. In September 2013, a modified porewater profiler (AMS, Inc., Retract-A-Tip system, American Falls, Idaho) was used to collect vertical profiles of water quality at locations 13 m (F742) and 18.3 m (F743) from shore. The well point on the AMS system is protected with a stainless steel mesh and is connected to polyethylene sampling tubing (0.6-cm-diameter). The tubing runs through hollow, 1.6-cm-diameter steel threaded rods to the surface. The well point was modified by inserting a titanium insert in the screened interval to keep the screen in the open position. The modification resulted in a 3.4-cm-long screened interval. At 14 m from shore, samples were collected at depths of 1.5 and 3.7 m below the estuary bottom. At 18 m from shore, samples were collected every 1.5 m to a depth of 10.7 m below the estuary bottom. No permanent monitoring points were left at these locations.

Permanent sampling points were installed from the floating platform into the estuary bottom in September 2013. At the site 9 m from shore (F733) originally profiled by using the Solinst points, permanent sampling points were installed by using a modified soil-gas sampling system (AMS, Inc., gas-vapor probe, American Falls, Idaho). The AMS system utilizes a dedicated gas-vapor tip connected to polyethylene sample-collection tubing (0.6-cm-diameter). The tubing runs to the surface through hollow, 1.6-cm-diameter steel-threaded rods that are driven to the target depth. Once the device has been driven to the desired depth, the rods are removed, leaving the sampling tip and tubing in place. The dedicated tip is 0.6 cm long and contains sampling ports that are covered by a stainless steel screen. AMS points of this design were also installed at a depth of 1.2 m below the estuary bottom at the same locations in the intertidal zone (F734 to F741) where shallow, temporary pushpoint samplers were installed in September 2013.

Location coordinates, land-surface and screen altitudes, well diameters, drilling methods, and casing and screen materials for the monitoring wells, well points, pushpoints, and multilevel samplers are included in table 1.1 (in back of report). Selected values in the table (for example, screen length versus difference between the top and bottom screen depths) may not be internally consistent owing to rounding and unit conversions. The locations of all temporary and permanent monitoring sites were determined by using a high-accuracy Global Positioning System (GPS) device. The altitudes of the measuring points at the permanent monitoring sites and at selected temporary monitoring sites were determined by differential leveling from benchmarks, accurate to ±3 mm.

A pressure-transducer tide gage that consisted of an open-bottom PVC standpipe was secured to a permanent dock piling at a nearby private residence. The standpipe was set about 11 m from shore, where the bottom of the pipe remained submerged throughout the tidal cycle. A self-contained pressure transducer (Onset Computer Corp., HOBO logger U20–001–01–Ti, Bourne, Mass.) was secured inside the bottom of the standpipe. Barometric pressure was also recorded in a second, nearby transducer so that absolute pressure could be converted to gage pressure, and the tide stage was also measured manually so that the pressure record could be converted to tidal stage relative to the National Geodetic Vertical Datum of 1929.

Sampling and Analytical Methods

Field screening samples were collected for measurement of specific conductance, temperature, and pH and for concentrations of dissolved oxygen, nitrate, and ammonium. Specific conductance, temperature, and pH were measured onsite; concentrations of dissolved oxygen were measured by using a colorimetric spectrophotometer (CHEMetrics V–2000 photometer and Vacu-vial test kits [CHEMetrics, 2018). For field samples with dissolved oxygen concentrations greater than 31 micromoles per liter (as O_2), samples were also collected in biochemical oxygen demand (BOD) bottles for analysis within 8 hours by using a dissolved oxygen probe and digital meter.

Multiple laboratories were used in this collaborative project. Laboratories, analytical methods, and reporting limits are given in table 1.2 and in the data release associated with this publication (Huntington and others, 2018), available at https://doi.org/10.5066/F7RR1WF0. Quality assurance included analysis of blind standard reference, field blank, and field duplicate samples. Results of the blind standard reference

Table 1.2. Laboratories, preservation, and detection limits for field and laboratory analysis of water samples.

[Chilled and frozen samples were shipped overnight on ice and dry ice, respectively. USGS, U.S. Geological Survey; WSC, Water Science Center; EPA, U.S. Environmental Protection Agency; GWERD, Ground Water and Ecosystems Restoration Division research laboratory; RSIL, Reston Stable Isotope Laboratory; RGWDL, Reston Groundwater Dating Laboratory; WHCMSC, Woods Hole Coastal and Marine Science Center; MPTL, Menlo Park Tritium Laboratory; AED, Atlantic Ecology Division; MPSAPSPL, Menlo Park Solid-Aqueous-Phase Solute Partitioning Laboratory; BBCNAEL, Boulder Biogeochemistry of Carbon and Nitrogen in Aquatic Environments Laboratory; <, less than; °C, degree Celsius; H_3PO_4, phosphoric acid; H_2SO_4, sulfuric acid; mL, milliliter; mg, milligram; KOH, potassium hydroxide; >, greater than; HNO_3, nitric acid; n/a, not applicable; µmol/L; micromole per liter; TU, tritium unit]

Constituent	Laboratory	Preservation	Detection limit	Filtered (0.45 micrometer)
Alkalinity	USGS New England WSC	Chill to <4 °C	n/a	Yes
Dissolved organic carbon (DOC)	EPA GWERD	H_3PO_4 to pH <2; chill to <4 °C	4.1 µmol/L	Yes
Nitrate (NO_3) plus nitrite (NO_2)	EPA GWERD	H_2SO_4 to pH <2; chill to <4° C	0.64 µmol/L	Yes
Ammonium (NH_4)	EPA GWERD	H_2SO_4 to pH <2; chill to <4 °C	1.4 µmol/L	Yes
Total Kjeldahl nitrogen (TKN)	EPA GWERD	H_2SO_4 to pH <2; chill to <4 °C	2.2 µmol/L	Yes
Total dissolved phosphorus (P)	EPA GWERD	H_2SO_4 to pH <2; chill to <4 °C	0.16 µmol/L	Yes
Ammonium (NH_4) stable isotopes	USGS RSIL	H_2SO_4 to pH 1.8–2.2	n/a	Yes
Nitrate (NO_3) stable isotopes	USGS RSIL	Preserve 125-mL sample with 1 pellet (100 mg) KOH to pH >11	n/a	Yes
Nitrogen gas (N_2) stable isotopes	USGS RSIL	Preserve sample in 160-mL serum bottle with 2 pellets (200 mg) KOH to pH >11	n/a	No
Nitrogen, argon, and methane gas (N_2, Ar, and CH_4)	USGS RGWDL	Preserve sample in 160-mL serum bottle with 2 pellets (200 mg) KOH to pH >11	n/a	No
Nitrogen and argon gas (N^2 and Ar)	USGS WHCMSC	Chill to <4 °C	n/a	No
Nitrite (NO_2)	USGS RSIL	Preserve 125-mL sample with 1 pellet (100 mg) KOH to pH >11	0.1 µmol/L	Yes
Tritium	USGS MPTL	None	0.41 TU	No
Iron (Fe)	EPA AED	HNO_3 to pH <2; chill to <4 °C	0.090–0.23 µmol/L	Yes
Manganese (Mn)	EPA AED	HNO_3 to pH <2; chill to <4 °C	0.27–0.33 µmol/L	Yes
Cations and minor elements	USGS MPSAPSPL	HNO_3 to pH <2; chill to <4 °C	Varies by species	Yes
Major anions	USGS BBCNAEL	Freeze to <0 °C	Varies by species	Yes
Specific conductance	Field	Onsite determination	n/a	No
pH	Field	Onsite determination	n/a	No
Temperature	Field	Onsite determination	n/a	No
Dissolved oxygen	Field	Onsite determination	n/a	No

materials were within the acceptable range of accuracy. Results of field blank samples indicated that field methods were not contaminating samples. Results of field duplicate samples indicated that precision met the quality objective for all constituents. Average relative percent difference was less than 10 percent for most constituents, but it rose to 34 and 36 percent for iron and manganese, respectively, which were analyzed by the U.S. Environmental Protection Agency Atlantic Ecology Division. These averages were dominated by relative percent difference values of a few samples that were close to the detection limits of the methods.

Interlaboratory Comparison of Nitrogen-Argon Results

Two methods of sampling and analysis were compared for nitrogen gas (N_2) and argon (Ar) determination. Samples for the U.S. Geological Survey (USGS) Woods Hole Coastal and Marine Science Center laboratory were collected in glass tubes, and the samples were stored under ice water in the field and refrigerated after shipment to the laboratory. Analysis was by membrane-inlet mass spectrometry (Young and others, 2013). Samples for the USGS Reston Groundwater Dating

Laboratory were collected in 150-milliliter glass serum bottles with rubber stoppers and preserved with hydroxide (pH>11). A needle in the stopper was used to allow air to escape as the stopper was inserted into the bottle. Analysis was by gas chromatography with a thermal conductivity detector after headspace extraction (USGS, 2018). Results indicated that the N_2/Ar ratio did not differ substantially between the two methods (relative mean square error=0.6 percent) (fig. 1.3). Discrepancies could be due to some combination of sample collection artifacts or analytical differences.

Determination of Denitrification

Dissolved Gases

As a first approximation, denitrification was quantified directly by monitoring the production of N_2 gas, because every 4 moles of NO_3^- denitrified result in 2 moles of N_2 (eq. 1.1):

$$4NO_3^- + 5CH_2O = 2N_2 + 3H_2O + 4HCO_3^- + CO_2 \qquad (1.1)$$

Dissolved N_2 in groundwater was assumed to be a combination of atmospheric N_2 incorporated during recharge and N_2 from denitrification (Böhlke and others, 2002; Böhlke and Krantz, 2003). The concentration of N_2 from recharge depends on temperature at recharge. Also, gas bubbles entrained during recharge can cause greater amounts of air to be dissolved that do not degas further along the flow path because of increased pressure at depth. The total amount of atmospheric N_2 in water from air-water equilibrium and entrained air bubbles can be estimated by comparison with Ar, a component of the atmosphere without a subsurface source from microbial activity, and with other indicators of denitrifying conditions, such as O_2 concentrations and nitrate isotopic composition. N_2 produced by microbial reaction is assumed to be equal to the measured value minus the N_2 from air-water equilibrium and entrained air bubbles. The resulting value is called the excess N_2. To compute excess N_2 from Ar and N_2 data alone, it is usually necessary to assume all samples had either similar recharge temperatures or similar amounts of excess air. In some cases, these assumptions can be evaluated by considering first the samples that lack other evidence of denitrification (for example, high O_2 and isotopically unfractionated nitrate; see the following section). Anammox (anaerobic ammonium oxidation) is another potential source of excess N_2 in which the N_2-N comes from both ammonium and nitrite (commonly derived from nitrate).

Isotopic Composition of Nitrate

Biogeochemical transformations change the stable isotope ratios of nitrogen species in solution because molecules containing the rare heavier isotope of nitrogen react at lower rates than do molecules containing the lighter isotope. For example, during nitrate reduction to N_2 (for example, denitrification), nitrate containing the heavier nitrogen isotope is left preferentially unreacted, and nitrate containing the lighter nitrogen isotope is preferentially converted to N_2. Vertical profiles of $\delta^{15}N$, which is a measure of the difference between the $^{15}N/^{14}N$ ratio in the sample and the $^{15}N/^{14}N$ ratio in atmospheric N_2, show increases for nitrate in zones of nitrate reduction. Similarly, $\delta^{18}O$ values increase in nitrate during denitrification, such that $\delta^{15}N$ and $\delta^{18}O$ are positively correlated. Values of $\delta^{15}N$ in dissolved N_2 are also affected by denitrification; those variations are relatively small and can be either positive or negative, depending on the initial nitrate $\delta^{15}N$ and the progress of the reaction.

Alkalinity

The chemical reaction for denitrification (eq. 1.1) indicates that 4 moles of HCO_3^- (or 5 moles of total dissolved inorganic carbon [DIC]) are generated for every 4 moles of NO_3^- denitrified. The alkalinity approach to assessing denitrification assumes that denitrification is the principal redox source of alkalinity variation in a chemical depth profile in the aquifer, and that other reactions that might buffer pH (for example, mineral-water interactions) are not significant. Other reactions produce CO_2, such as aerobic bacterial respiration ($CH_2O + O_2 = CO_2 + H_2O$). However, reactions with CO_2 entering or leaving solution do not change alkalinity (Stumm and Morgan, 1996). Although CO_2 combines with water to form carbonic acid ($CO_2 + H_2O \rightarrow H_2CO_3$), and although H_2CO_3 can disassociate to form $H^+ + HCO_3^-$, the alkalinity stays the same. In the absence of other buffers in the system, the acid formed decreases alkalinity to the same degree that the bicarbonate formed increases alkalinity, and the net effect on alkalinity is zero.

Nitrification is another process that changes alkalinity (eq. 1.2):

$$NH_4^+ + 2O_2 + 2HCO_3^- = NO_3^- + 2CO_2 + 3H_2O \qquad (1.2)$$

Nitrification is particularly active in the unsaturated zone, where ammonium can be converted completely to nitrate (Costa and others, 2002). Under a septic-system leachfield, the zone of nitrification is close (within 30 cm) to the trenches. A reaction in such a zone would decrease alkalinity in the recharging water by acidification of HCO_3^-. To the extent that leachate from the septic system is evenly distributed in the aquifer, the effect could be relatively uniform if the reaction goes to completion before leachate reaches the water table.

Other processes contribute to background alkalinity, including a high loading from seawater salt spray near the coast. Dissolution of carbonate minerals in an aquifer can also contribute to alkalinity, but carbonates are not abundant in the Cape Cod aquifer, which consists primarily of quartz and feldspar. Manganese and iron reduction also change alkalinity, but reduction of nitrate is energetically more favorable. If

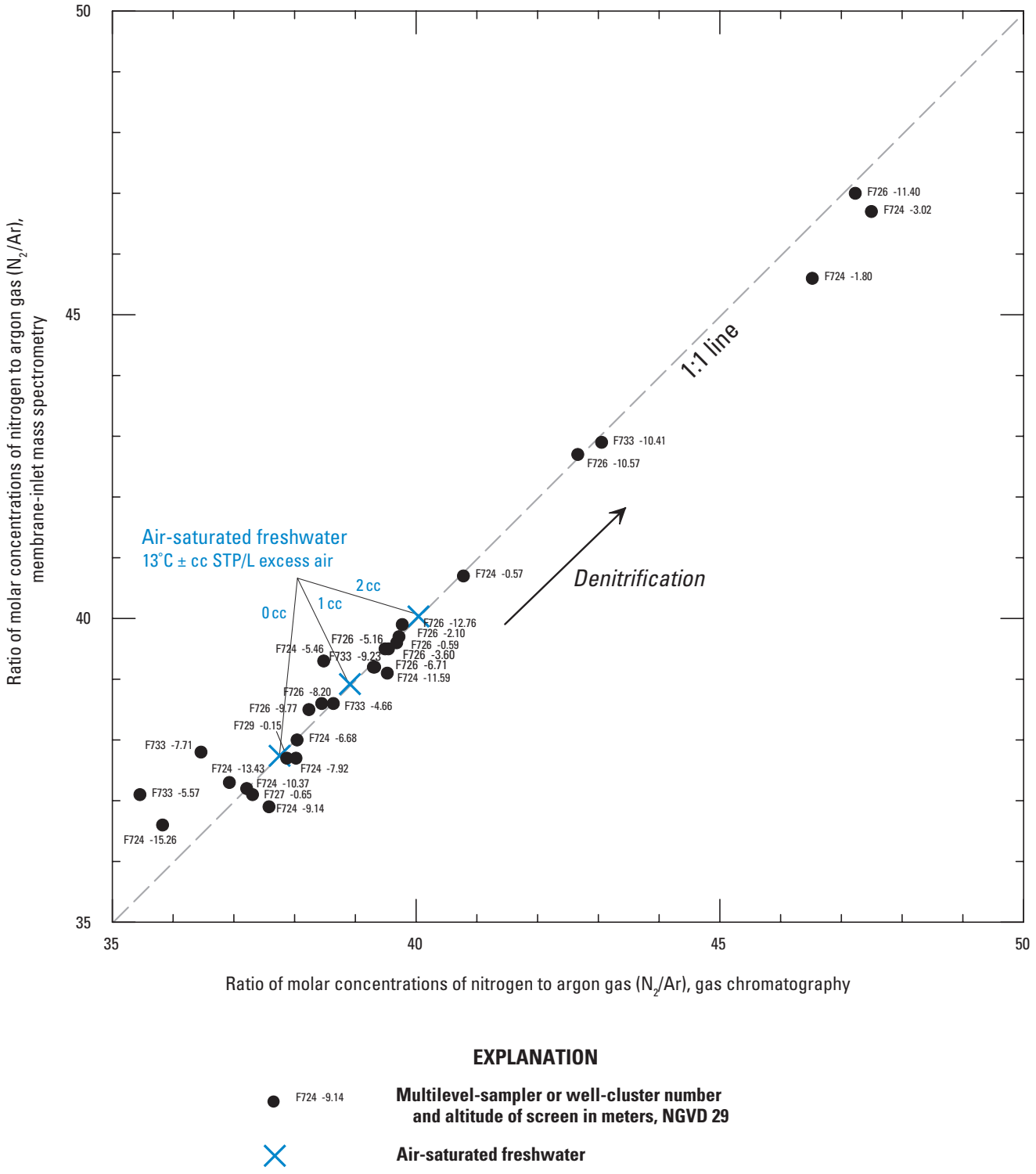

Figure 1.3. Comparison of nitrogen and argon ratios, measured by the membrane-inlet mass spectrometry and gas chromatography methods, for samples collected in groundwater near the Eel River, Seacoast Shores peninsula, East Falmouth, Massachusetts, August 7, 2013, to October 23, 2013. ccSTP/L, cubic centimeter of excess air at standard temperature and pressure per liter of water. Locations of sites are shown on figure 5.

nitrate is not exhausted and if measurements of manganese and iron indicate that their reduced (soluble) forms are not elevated in solution, then these reduction reactions are less likely to have proceeded.

In contrast to other redox reactions in groundwater, denitrification is more likely to produce a depth-profile of alkalinity that reflects the amount of denitrification that has taken place. Interpretation of such profiles, however, depends on uniform distribution of septic systems in the recharge areas contributing to the profiles and minimal effects of other pH buffering reactions. Carbon mass balance calculations commonly are performed by using concentrations of DIC, which can be derived from alkalinity and pH data (Böhlke and others, 2002). Alkalinity and DIC methods of evaluating denitrification reactions should be used along with other methods, such as analysis of nitrogen gases, to increase confidence in the result.

References Cited

Böhlke, J.K., and Krantz, D.E., 2003, Isotope geochemistry and chronology of offshore ground water beneath Indian River Bay, Delaware: U.S. Geological Survey Water-Resources Investigations Report 03–4192, 37 p. [Also available at https://pubs.water.usgs.gov/wri03-4192/.]

Böhlke, J.K., Wanty, R.B., Tuttle, M.L., Delin, G.N., and Landon, M.K., 2002, Denitrification in the recharge area and discharge area of a transient agricultural nitrate plume in a glacial outwash sand aquifer, Minnesota: Water Resources Research, v. 38, no. 7, p. 10–1 to 10–26. [Also available at https://doi.org/10.1029/2001WR000663.]

CHEMetrics, 2018, Water analysis kits: CHEMetrics web page, accessed March 24, 2018, at https://www.chemetrics.com/.

Costa, J.E., Heufelder, G., Foss, S., Millham, N.P., and Howes, B., 2002, Nitrogen removal efficiencies of three alternative septic system technologies and a conventional septic system: Environment Cape Cod, v. 5, no. 1, p. 15–24. [Also available at http://www.buzzardsbay.org/etistuff/results/costaenvccarticle2.pdf.]

Henry, M.E., 2001, PushPoint Sampler operators manual and applications guide, version 2.00: MHE Products user guide, accessed December 8, 2004, at http://www-personal.engin.umich.edu/~markhen/ MHE-instructions-ver-2.00.doc.

Huntington, T.G., Pirolli, G.F., McCobb, T.D., Böhlke, J.K., Colman, J.A., Kroeger, K.D., Brooks, T.W., and LeBlanc, D.R., 2018, Geochemical data supporting analysis of geochemical conditions and nitrogen transport in nearshore groundwater and the subterranean estuary at a Cape Cod embayment, East Falmouth, Massachusetts, 2013: U.S. Geological Survey data release, https://doi.org/10.5066/F7RR1WF0.

Stumm, W., and Morgan, J.J., 1996, Aquatic chemistry—Chemical equilibria and rates in natural waters: New York, Wiley, 1,022 p.

U.S. Geological Survey [USGS], 2018, Analytical procedures for dissolved gasses N_2/Ar: U.S. Geological Survey web page, accessed March 24, 2018, at https://water.usgs.gov/lab/dissolved-gas/lab/analytical_procedures/.

Young, C., Kroeger, K.D., and Hanson, G., 2013, Limited denitrification in glacial deposit aquifers having thick unsaturated zones (Long Island, USA): Hydrogeology Journal, v. 21, no. 8, p. 1773–1786. [Also available at https://doi.org/10.1007/s10040-013-1038-4.]

Table 1.1.A. Location coordinates, land-surface and screen altitudes, well diameters, drilling methods, and casing and screen materials for monitoring wells, well points, pushpoints, and multilevel samplers near the Eel River, Seacoast Shores peninsula, East Falmouth, Massachusetts.

[Abbreviated site names, in which "F" is short for "MA-FSW," are used throughout this report. Values shown may not be internally consistent owing to rounding and unit conversions. Locations of sites are shown on figures 5 and 6. Locations were determined by using a global positioning system and are relative to the North American Datum of 1983 (NAD 83). Altitude is relative to the National Geodetic Vertical Datum of 1929 (NGVD 29). USGS, U.S. Geological Survey; MHE, M.H.E. Products Inc., East Tawas, Michigan; AMS, AMS Inc., American Falls, Idaho; cm, centimeter; m, meter; LS, land surface; RB, river bottom; MP, measuring point; PVC, polyvinyl chloride; n/a, not applicable; ---, no data]

USGS site name	USGS 15-digit site identifier	Site type	Drilling method	Temporary or permanent	Casing material	Screen material	Well diameter (cm)	Easting (NAD 83 m)	Northing (NAD 83 m)
Eel River tide	n/a	Tide gage	n/a	Temporary	PVC	Open end pipe	2.50	279878.56	813556.62
MA-FSW 724-M01-02GNT	413404070323302	Multilevel sampler	Auger rig	Permanent	Polyethylene tube	Nylon mesh	0.64	279914.98	813529.65
MA-FSW 724-M01-03RT	413404070323303	Multilevel sampler	Auger rig	Permanent	Polyethylene tube	Nylon mesh	0.64	279914.98	813529.65
MA-FSW 724-M01-04BUT	413404070323304	Multilevel sampler	Auger rig	Permanent	Polyethylene tube	Nylon mesh	0.64	279914.98	813529.65
MA-FSW 724-M01-05BKT	413404070323305	Multilevel sampler	Auger rig	Permanent	Polyethylene tube	Nylon mesh	0.64	279914.98	813529.65
MA-FSW 724-M01-06WT	413404070323306	Multilevel sampler	Auger rig	Permanent	Polyethylene tube	Nylon mesh	0.64	279914.98	813529.65
MA-FSW 724-M01-07O	413404070323307	Multilevel sampler	Auger rig	Permanent	Polyethylene tube	Nylon mesh	0.64	279914.98	813529.65
MA-FSW 724-M01-08GY	413404070323308	Multilevel sampler	Auger rig	Permanent	Polyethylene tube	Nylon mesh	0.64	279914.98	813529.65
MA-FSW 724-M01-09Y	413404070323309	Multilevel sampler	Auger rig	Permanent	Polyethylene tube	Nylon mesh	0.64	279914.98	813529.65
MA-FSW 724-M01-10P	413404070323310	Multilevel sampler	Auger rig	Permanent	Polyethylene tube	Nylon mesh	0.64	279914.98	813529.65
MA-FSW 724-M01-11GN	413404070323311	Multilevel sampler	Auger rig	Permanent	Polyethylene tube	Nylon mesh	0.64	279914.98	813529.65
MA-FSW 724-M01-12R	413404070323312	Multilevel sampler	Auger rig	Permanent	Polyethylene tube	Nylon mesh	0.64	279914.98	813529.65
MA-FSW 724-M01-13BU	413404070323313	Multilevel sampler	Auger rig	Permanent	Polyethylene tube	Nylon mesh	0.64	279914.98	813529.65
MA-FSW 725-A01-0001.5	n/a	MHE pushpoint	Hand installed	Temporary	Stainless steel	Stainless steel	0.64	279882.83	813542.03
MA-FSW 725-A02-0001.5	n/a	MHE pushpoint	Hand installed	Temporary	Stainless steel	Stainless steel	0.64	279881.22	813542.78
MA-FSW 725-A03-0001.5	n/a	MHE pushpoint	Hand installed	Temporary	Stainless steel	Stainless steel	0.64	279879.85	813543.64
MA-FSW 725-A04-0001.5	n/a	MHE pushpoint	Hand installed	Temporary	Stainless steel	Stainless steel	0.64	279878.14	813540.54
MA-FSW 725-A05-0001.5	n/a	MHE pushpoint	Hand installed	Temporary	Stainless steel	Stainless steel	0.64	279880.44	813545.92
MA-FSW 725-A06-0001.5	n/a	MHE pushpoint	Hand installed	Temporary	Stainless steel	Stainless steel	0.64	279881.77	813548.59
MA-FSW 725-A07-0001.5	n/a	MHE pushpoint	Hand installed	Temporary	Stainless steel	Stainless steel	0.64	279875.70	813545.39
MA-FSW 725-A08-0001.5	n/a	MHE pushpoint	Hand installed	Temporary	Stainless steel	Stainless steel	0.64	279876.85	813537.56
MA-FSW 725-A09-0001.5	n/a	MHE pushpoint	Hand installed	Temporary	Stainless steel	Stainless steel	0.64	279871.04	813546.58
MA-FSW 725-A10-0001.5	n/a	MHE pushpoint	Hand installed	Temporary	Stainless steel	Stainless steel	0.64	279869.89	813543.22
MA-FSW 725-A11-0001.5	n/a	MHE pushpoint	Hand installed	Temporary	Stainless steel	Stainless steel	0.64	279872.28	813548.71
MA-FSW 725-A12-0001.5	n/a	MHE pushpoint	Hand installed	Temporary	Stainless steel	Stainless steel	0.64	279868.70	813540.56
MA-FSW 725-A13-0001.5	n/a	MHE pushpoint	Hand installed	Temporary	Stainless steel	Stainless steel	0.64	279873.32	813551.37
MA-FSW 725-A14-0004.1	n/a	MHE pushpoint	Hand installed	Temporary	Stainless steel	Stainless steel	0.64	279867.00	813548.00
MA-FSW 725-A15-0003.6	n/a	MHE pushpoint	Hand installed	Temporary	Stainless steel	Stainless steel	0.64	279864.00	813549.00
MA-FSW 725-A16-0002.5	n/a	MHE pushpoint	Hand installed	Temporary	Stainless steel	Stainless steel	0.64	279853.31	813553.26

Table 1.1.A. Location coordinates, land-surface and screen altitudes, well diameters, drilling methods, and casing and screen materials for monitoring wells, well points, pushpoints, and multilevel samplers near the Eel River, Seacoast Shores peninsula, East Falmouth, Massachusetts.—Continued

[Abbreviated site names, in which "F" is short for "MA-FSW," are used throughout this report. Values shown may not be internally consistent owing to rounding and unit conversions. Locations of sites are shown on figures 5 and 6. Locations were determined by using a global positioning system and are relative to the North American Datum of 1983 (NAD 83). Altitude is relative to the National Geodetic Vertical Datum of 1929 (NGVD 29). USGS, U.S. Geological Survey; MHE, M.H.E. Products Inc., East Tawas, Michigan; AMS, AMS Inc., American Falls, Idaho; cm, centimeter; m, meter; LS, land surface; RB, river bottom; MP, measuring point; PVC, polyvinyl chloride; n/a, not applicable; ---, no data]

USGS site name	USGS 15-digit site identifier	Site type	Drilling method	Temporary or permanent	Casing material	Screen material	Well diameter (cm)	Easting (NAD 83 m)	Northing (NAD 83 m)
MA-FSW 725-A18-0001.5	n/a	MHE pushpoint	Hand installed	Temporary	Stainless steel	Stainless steel	0.64	279871.04	813546.58
MA-FSW 725-A19-0003.0	n/a	MHE pushpoint	Hand installed	Temporary	Stainless steel	Stainless steel	0.64	279871.04	813546.58
MA-FSW 725-A20-0004.5	n/a	MHE pushpoint	Hand installed	Temporary	Stainless steel	Stainless steel	0.64	279871.04	813546.58
MA-FSW 725-A21-0005.7	n/a	MHE pushpoint	Hand installed	Temporary	Stainless steel	Stainless steel	0.64	279871.04	813546.58
MA-FSW 726-0005	413404070323401	Monitoring well	Direct push rig	Permanent	PVC	PVC	2.5	279881.62	813535.81
MA-FSW 726-0010	413404070323402	Monitoring well	Direct push rig	Permanent	PVC	PVC	2.5	279881.62	813535.81
MA-FSW 726-0015	413404070323403	Monitoring well	Direct push rig	Permanent	PVC	PVC	2.5	279881.62	813535.81
MA-FSW 726-0020	413404070323404	Monitoring well	Direct push rig	Permanent	PVC	PVC	2.5	279881.62	813535.81
MA-FSW 726-0025	413404070323405	Monitoring well	Direct push rig	Permanent	PVC	PVC	2.5	279881.62	813535.81
MA-FSW 726-0030	413404070323406	Monitoring well	Direct push rig	Permanent	PVC	PVC	2.5	279881.62	813535.81
MA-FSW 726-0035	413404070323407	Monitoring well	Direct push rig	Permanent	PVC	PVC	2.5	279881.62	813535.81
MA-FSW 726-0037.5	413404070323408	Monitoring well	Direct push rig	Permanent	PVC	PVC	2.5	279881.62	813535.81
MA-FSW 726-0040	413404070323409	Monitoring well	Direct push rig	Permanent	PVC	PVC	2.5	279881.62	813535.81
MA-FSW 726-0045	413404070323410	Monitoring well	Direct push rig	Permanent	PVC	PVC	2.5	279881.62	813535.81
MA-FSW 727-0031	413413070322101	Monitoring well	Direct push rig	Permanent	PVC	PVC	2.5	280194.22	813795.32
MA-FSW 728-0026	413411070322701	Monitoring well	Direct push rig	Permanent	PVC	PVC	2.5	280037.40	813730.83
MA-FSW 729-0028	413406070322501	Monitoring well	Direct push rig	Permanent	PVC	PVC	2.5	280083.37	813575.25
MA-FSW 730-0022	413360070323501	Monitoring well	Direct push rig	Permanent	PVC	PVC	2.5	279862.47	813392.38
MA-FSW 731-0029	413358070322801	Monitoring well	Direct push rig	Permanent	PVC	PVC	2.5	280032.77	813343.73
MA-FSW 732-0015	413404070323316	Monitoring well	Auger rig	Permanent	PVC	PVC	1.9	279901.37	813536.89
MA-FSW 732-0036	413404070323317	Monitoring well	Auger rig	Permanent	PVC	PVC	1.9	279901.37	813536.89
MA-FSW 732-0041	413404070323318	Monitoring well	Auger rig	Permanent	PVC	PVC	1.9	279901.37	813536.89
MA-FSW 732-0046	413404070323319	Monitoring well	Auger rig	Permanent	PVC	PVC	1.9	279901.37	813536.89
MA-FSW 732-0051	413404070323320	Monitoring well	Auger rig	Permanent	PVC	PVC	1.9	279901.37	813536.89
MA-FSW 732-0058	413404070323321	Monitoring well	Auger rig	Permanent	PVC	PVC	1.9	279901.37	813536.89

Table 1.1.A. Location coordinates, land-surface and screen altitudes, well diameters, drilling methods, and casing and screen materials for monitoring wells, well points, pushpoints, and multilevel samplers near the Eel River, Seacoast Shores peninsula, East Falmouth, Massachusetts.—Continued

[Abbreviated site names, in which "F" is short for "MA-FSW," are used throughout this report. Values shown may not be internally consistent owing to rounding and unit conversions. Locations of sites are shown on figures 5 and 6. Locations were determined by using a global positioning system and are relative to the North American Datum of 1983 (NAD 83). Altitude is relative to the National Geodetic Vertical Datum of 1929 (NGVD 29). USGS, U.S. Geological Survey; MHE, M.H.E. Products Inc., East Tawas, Michigan; AMS, AMS Inc., American Falls, Idaho; cm, centimeter; m, meter; LS, land surface; RB, river bottom; MP, measuring point; PVC, polyvinyl chloride; n/a, not applicable; ---, no data]

USGS site name	USGS 15-digit site identifier	Site type	Drilling method	Temporary or permanent	Casing material	Screen material	Well diameter (cm)	Easting (NAD 83 m)	Northing (NAD 83 m)
MA-FSW 733-A01-0001	n/a	MHE pushpoint	Hand installed	Temporary	Stainless steel	Stainless steel	0.64	279874.55	813543.90
MA-FSW 733-A02-0001	n/a	MHE pushpoint	Hand installed	Temporary	Stainless steel	Stainless steel	0.64	279874.55	813543.90
MA-FSW 733-A03-0001	n/a	MHE pushpoint	Hand installed	Temporary	Stainless steel	Stainless steel	0.64	279874.55	813543.90
MA-FSW 733-A01-0002	n/a	MHE pushpoint	Hand installed	Temporary	Stainless steel	Stainless steel	0.64	279874.55	813543.90
MA-FSW 733-A02-0002	n/a	MHE pushpoint	Hand installed	Temporary	Stainless steel	Stainless steel	0.64	279874.55	813543.90
MA-FSW 733-A03-0002	n/a	MHE pushpoint	Hand installed	Temporary	Stainless steel	Stainless steel	0.64	279874.55	813543.90
MA-FSW 733-A01-0003	n/a	MHE pushpoint	Hand installed	Temporary	Stainless steel	Stainless steel	0.64	279874.55	813543.90
MA-FSW 733-A02-0003	n/a	MHE pushpoint	Hand installed	Temporary	Stainless steel	Stainless steel	0.64	279874.55	813543.90
MA-FSW 733-A03-0003	n/a	MHE pushpoint	Hand installed	Temporary	Stainless steel	Stainless steel	0.64	279874.55	813543.90
MA-FSW 733-A01-0015	n/a	Solinst well point	Vibratory hammer	Temporary	Polyethylene tube	Stainless steel	1.27	279874.55	813543.90
MA-FSW 733-A01-0020	n/a	Solinst well point	Vibratory hammer	Temporary	Polyethylene tube	Stainless steel	1.27	279874.55	813543.90
MA-FSW 733-A01-0025	n/a	Solinst well point	Vibratory hammer	Temporary	Polyethylene tube	Stainless steel	1.27	279874.55	813543.90
MA-FSW 733-A01-0030	n/a	Solinst well point	Vibratory hammer	Temporary	Polyethylene tube	Stainless steel	1.27	279874.55	813543.90
MA-FSW 733-0005	413405070323401	AMS well point	Vibratory hammer	Permanent	Polyethylene tube	Stainless steel	0.48	279874.55	813543.90
MA-FSW 733-0010	413405070323402	AMS well point	Vibratory hammer	Permanent	Polyethylene tube	Stainless steel	0.48	279874.55	813543.90
MA-FSW 733-0015	413405070323403	AMS well point	Vibratory hammer	Permanent	Polyethylene tube	Stainless steel	0.48	279874.55	813543.90
MA-FSW 733-0018	413405070323404	AMS well point	Vibratory hammer	Permanent	Polyethylene tube	Stainless steel	0.48	279874.55	813543.90
MA-FSW 733-0025	413405070323405	AMS well point	Vibratory hammer	Permanent	Polyethylene tube	Stainless steel	0.48	279874.55	813543.90
MA-FSW 733-0030	413405070323406	AMS well point	Vibratory hammer	Permanent	Polyethylene tube	Stainless steel	0.48	279874.55	813543.90
MA-FSW 733-0034	413405070323407	Solinst well point	Vibratory hammer	Permanent	Polyethylene tube	Stainless steel	1.27	279874.55	813543.90
MA-FSW 734-A01-0001	n/a	MHE pushpoint	Hand installed	Temporary	Stainless steel	Stainless steel	0.64	279875.81	813543.51
MA-FSW 734-A02-0001	n/a	MHE pushpoint	Hand installed	Temporary	Stainless steel	Stainless steel	0.64	279875.81	813543.51
MA-FSW 734-A03-0001	n/a	MHE pushpoint	Hand installed	Temporary	Stainless steel	Stainless steel	0.64	279875.81	813543.51
MA-FSW 734-A01-0002	n/a	MHE pushpoint	Hand installed	Temporary	Stainless steel	Stainless steel	0.64	279875.81	813543.51
MA-FSW 734-A02-0002	n/a	MHE pushpoint	Hand installed	Temporary	Stainless steel	Stainless steel	0.64	279875.81	813543.51
MA-FSW 734-A03-0002	n/a	MHE pushpoint	Hand installed	Temporary	Stainless steel	Stainless steel	0.64	279875.81	813543.51
MA-FSW 734-A01-0003	n/a	MHE pushpoint	Hand installed	Temporary	Stainless steel	Stainless steel	0.64	279875.81	813543.51

Table 1.1.A. Location coordinates, land-surface and screen altitudes, well diameters, drilling methods, and casing and screen materials for monitoring wells, well points, pushpoints, and multilevel samplers near the Eel River, Seacoast Shores peninsula, East Falmouth, Massachusetts.—Continued

[Abbreviated site names, in which "F" is short for "MA-FSW," are used throughout this report. Values shown may not be internally consistent owing to rounding and unit conversions. Locations of sites are shown on figures 5 and 6. Locations were determined by using a global positioning system and are relative to the North American Datum of 1983 (NAD 83). Altitude is relative to the National Geodetic Vertical Datum of 1929 (NGVD 29). USGS, U.S. Geological Survey; MHE, M.H.E. Products Inc., East Tawas, Michigan; AMS, AMS Inc., American Falls, Idaho; cm, centimeter; m, meter; LS, land surface; RB, river bottom; MP, measuring point; PVC, polyvinyl chloride; n/a, not applicable; ---, no data]

USGS site name	USGS 15-digit site identifier	Site type	Drilling method	Temporary or permanent	Casing material	Screen material	Well diameter (cm)	Easting (NAD 83 m)	Northing (NAD 83 m)
MA-FSW 734-A02-0003	n/a	MHE pushpoint	Hand installed	Temporary	Stainless steel	Stainless steel	0.64	279875.81	813543.51
MA-FSW 734-A03-0003	n/a	MHE pushpoint	Hand installed	Temporary	Stainless steel	Stainless steel	0.64	279875.81	813543.51
MA-FSW 734-0004	n/a	AMS well point	Slide hammer	Permanent	Polyethylene tube	Stainless steel	0.5	279875.81	813543.51
MA-FSW 735-A01-0001	n/a	MHE pushpoint	Hand installed	Temporary	Stainless steel	Stainless steel	0.64	279876.71	813543.01
MA-FSW 735-A02-0001	n/a	MHE pushpoint	Hand installed	Temporary	Stainless steel	Stainless steel	0.64	279876.71	813543.01
MA-FSW 735-A03-0001	n/a	MHE pushpoint	Hand installed	Temporary	Stainless steel	Stainless steel	0.64	279876.71	813543.01
MA-FSW 735-A01-0002	n/a	MHE pushpoint	Hand installed	Temporary	Stainless steel	Stainless steel	0.64	279876.71	813543.01
MA-FSW 735-A02-0002	n/a	MHE pushpoint	Hand installed	Temporary	Stainless steel	Stainless steel	0.64	279876.71	813543.01
MA-FSW 735-A03-0002	n/a	MHE pushpoint	Hand installed	Temporary	Stainless steel	Stainless steel	0.64	279876.71	813543.01
MA-FSW 735-A01-0003	n/a	MHE pushpoint	Hand installed	Temporary	Stainless steel	Stainless steel	0.64	279876.71	813543.01
MA-FSW 735-A02-0003	n/a	MHE pushpoint	Hand installed	Temporary	Stainless steel	Stainless steel	0.64	279876.71	813543.01
MA-FSW 735-A03-0003	n/a	MHE pushpoint	Hand installed	Temporary	Stainless steel	Stainless steel	0.64	279876.71	813543.01
MA-FSW 735-0004	n/a	AMS well point	Slide hammer	Permanent	Polyethylene tube	Stainless steel	0.48	279876.71	813543.01
MA-FSW 736-A01-0001	n/a	MHE pushpoint	Hand installed	Temporary	Stainless steel	Stainless steel	0.64	279877.52	813542.56
MA-FSW 736-A02-0001	n/a	MHE pushpoint	Hand installed	Temporary	Stainless steel	Stainless steel	0.64	279877.52	813542.56
MA-FSW 736-A03-0001	n/a	MHE pushpoint	Hand installed	Temporary	Stainless steel	Stainless steel	0.64	279877.52	813542.56
MA-FSW 736-A01-0002	n/a	MHE pushpoint	Hand installed	Temporary	Stainless steel	Stainless steel	0.64	279877.52	813542.56
MA-FSW 736-A02-0002	n/a	MHE pushpoint	Hand installed	Temporary	Stainless steel	Stainless steel	0.64	279877.52	813542.56
MA-FSW 736-A03-0002	n/a	MHE pushpoint	Hand installed	Temporary	Stainless steel	Stainless steel	0.64	279877.52	813542.56
MA-FSW 736-A01-0003	n/a	MHE pushpoint	Hand installed	Temporary	Stainless steel	Stainless steel	0.64	279877.52	813542.56
MA-FSW 736-A02-0003	n/a	MHE pushpoint	Hand installed	Temporary	Stainless steel	Stainless steel	0.64	279877.52	813542.56
MA-FSW 736-A03-0003	n/a	MHE pushpoint	Hand installed	Temporary	Stainless steel	Stainless steel	0.64	279877.52	813542.56
MA-FSW 736-0004	n/a	AMS well point	Slide hammer	Permanent	Polyethylene tube	Stainless steel	0.48	279877.52	813542.56
MA-FSW 737-A01-0001	n/a	MHE pushpoint	Hand installed	Temporary	Stainless steel	Stainless steel	0.64	279878.32	813542.10
MA-FSW 737-A02-0001	n/a	MHE pushpoint	Hand installed	Temporary	Stainless steel	Stainless steel	0.64	279878.32	813542.10
MA-FSW 737-A03-0001	n/a	MHE pushpoint	Hand installed	Temporary	Stainless steel	Stainless steel	0.64	279878.32	813542.10

Table 1.1.A. Location coordinates, land-surface and screen altitudes, well diameters, drilling methods, and casing and screen materials for monitoring wells, well points, pushpoints, and multilevel samplers near the Eel River, Seacoast Shores peninsula, East Falmouth, Massachusetts.—Continued

[Abbreviated site names, in which "F" is short for "MA-FSW," are used throughout this report. Values shown may not be internally consistent owing to rounding and unit conversions. Locations of sites are shown on figures 5 and 6. Locations were determined by using a global positioning system and are relative to the North American Datum of 1983 (NAD 83). Altitude is relative to the National Geodetic Vertical Datum of 1929 (NGVD 29). USGS, U.S. Geological Survey; MHE, M.H.E. Products Inc., East Tawas, Michigan; AMS, AMS Inc., American Falls, Idaho; cm, centimeter; m, meter; LS, land surface; RB, river bottom; MP, measuring point; PVC, polyvinyl chloride; n/a, not applicable; ---, no data]

USGS site name	USGS 15-digit site identifier	Site type	Drilling method	Temporary or permanent	Casing material	Screen material	Well diameter (cm)	Easting (NAD 83 m)	Northing (NAD 83 m)
MA-FSW 737-A01-0002	n/a	MHE pushpoint	Hand installed	Temporary	Stainless steel	Stainless steel	0.64	279878.32	813542.10
MA-FSW 737-A02-0002	n/a	MHE pushpoint	Hand installed	Temporary	Stainless steel	Stainless steel	0.64	279878.32	813542.10
MA-FSW 737-A03-0002	n/a	MHE pushpoint	Hand installed	Temporary	Stainless steel	Stainless steel	0.64	279878.32	813542.10
MA-FSW 737-A01-0003	n/a	MHE pushpoint	Hand installed	Temporary	Stainless steel	Stainless steel	0.64	279878.32	813542.10
MA-FSW 737-A02-0003	n/a	MHE pushpoint	Hand installed	Temporary	Stainless steel	Stainless steel	0.64	279878.32	813542.10
MA-FSW 737-A03-0003	n/a	MHE pushpoint	Hand installed	Temporary	Stainless steel	Stainless steel	0.64	279878.32	813542.10
MA-FSW 737-0004	n/a	AMS well point	Slide hammer	Permanent	Polyethylene tube	Stainless steel	0.48	279878.32	813542.10
MA-FSW 738-A01-0001	n/a	MHE pushpoint	Hand installed	Temporary	Stainless steel	Stainless steel	0.64	279879.36	813541.51
MA-FSW 738-A02-0001	n/a	MHE pushpoint	Hand installed	Temporary	Stainless steel	Stainless steel	0.64	279879.36	813541.51
MA-FSW 738-A03-0001	n/a	MHE pushpoint	Hand installed	Temporary	Stainless steel	Stainless steel	0.64	279879.36	813541.51
MA-FSW 738-A01-0002	n/a	MHE pushpoint	Hand installed	Temporary	Stainless steel	Stainless steel	0.64	279879.36	813541.51
MA-FSW 738-A02-0002	n/a	MHE pushpoint	Hand installed	Temporary	Stainless steel	Stainless steel	0.64	279879.36	813541.51
MA-FSW 738-A03-0002	n/a	MHE pushpoint	Hand installed	Temporary	Stainless steel	Stainless steel	0.64	279879.36	813541.51
MA-FSW 738-A01-0003	n/a	MHE pushpoint	Hand installed	Temporary	Stainless steel	Stainless steel	0.64	279879.36	813541.51
MA-FSW 738-A02-0003	n/a	MHE pushpoint	Hand installed	Temporary	Stainless steel	Stainless steel	0.64	279879.36	813541.51
MA-FSW 738-A03-0003	n/a	MHE pushpoint	Hand installed	Temporary	Stainless steel	Stainless steel	0.64	279879.36	813541.51
MA-FSW 738-0004	n/a	AMS well point	Slide hammer	Permanent	Polyethylene tube	Stainless steel	0.48	279879.36	813541.51
MA-FSW 739-A01-0001	n/a	MHE pushpoint	Hand installed	Temporary	Stainless steel	Stainless steel	0.64	279880.38	813540.75
MA-FSW 739-A02-0001	n/a	MHE pushpoint	Hand installed	Temporary	Stainless steel	Stainless steel	0.64	279880.38	813540.75
MA-FSW 739-A03-0001	n/a	MHE pushpoint	Hand installed	Temporary	Stainless steel	Stainless steel	0.64	279880.38	813540.75
MA-FSW 739-A01-0002	n/a	MHE pushpoint	Hand installed	Temporary	Stainless steel	Stainless steel	0.64	279880.38	813540.75
MA-FSW 739-A02-0002	n/a	MHE pushpoint	Hand installed	Temporary	Stainless steel	Stainless steel	0.64	279880.38	813540.75
MA-FSW 739-A03-0002	n/a	MHE pushpoint	Hand installed	Temporary	Stainless steel	Stainless steel	0.64	279880.38	813540.75
MA-FSW 739-A01-0003	n/a	MHE pushpoint	Hand installed	Temporary	Stainless steel	Stainless steel	0.64	279880.38	813540.75
MA-FSW 739-A02-0003	n/a	MHE pushpoint	Hand installed	Temporary	Stainless steel	Stainless steel	0.64	279880.38	813540.75
MA-FSW 739-A03-0003	n/a	MHE pushpoint	Hand installed	Temporary	Stainless steel	Stainless steel	0.64	279880.38	813540.75
MA-FSW 739-0004	n/a	AMS well point	Slide hammer	Permanent	Polyethylene tube	Stainless steel	0.48	279880.38	813540.75

Table 1.1.A. Location coordinates, land-surface and screen altitudes, well diameters, drilling methods, and casing and screen materials for monitoring wells, well points, pushpoints, and multilevel samplers near the Eel River, Seacoast Shores peninsula, East Falmouth, Massachusetts.—Continued

[Abbreviated site names, in which "F" is short for "MA-FSW," are used throughout this report. Values shown may not be internally consistent owing to rounding and unit conversions. Locations of sites are shown on figures 5 and 6. Locations were determined by using a global positioning system and are relative to the North American Datum of 1983 (NAD 83). Altitude is relative to the National Geodetic Vertical Datum of 1929 (NGVD 29). USGS, U.S. Geological Survey; MHE, M.H.E. Products Inc., East Tawas, Michigan; AMS, AMS Inc., American Falls, Idaho; cm, centimeter; m, meter; LS, land surface; RB, river bottom; MP, measuring point; PVC, polyvinyl chloride; n/a, not applicable; ---, no data]

USGS site name	USGS 15-digit site identifier	Site type	Drilling method	Temporary or permanent	Casing material	Screen material	Well diameter (cm)	Easting (NAD 83 m)	Northing (NAD 83 m)
MA-FSW 740-A01-0001	n/a	MHE pushpoint	Hand installed	Temporary	Stainless steel	Stainless steel	0.64	279881.42	813540.04
MA-FSW 740-A02-0001	n/a	MHE pushpoint	Hand installed	Temporary	Stainless steel	Stainless steel	0.64	279881.42	813540.04
MA-FSW 740-A03-0001	n/a	MHE pushpoint	Hand installed	Temporary	Stainless steel	Stainless steel	0.64	279881.42	813540.04
MA-FSW 740-A01-0002	n/a	MHE pushpoint	Hand installed	Temporary	Stainless steel	Stainless steel	0.64	279881.42	813540.04
MA-FSW 740-A02-0002	n/a	MHE pushpoint	Hand installed	Temporary	Stainless steel	Stainless steel	0.64	279881.42	813540.04
MA-FSW 740-A03-0002	n/a	MHE pushpoint	Hand installed	Temporary	Stainless steel	Stainless steel	0.64	279881.42	813540.04
MA-FSW 740-A01-0003	n/a	MHE pushpoint	Hand installed	Temporary	Stainless steel	Stainless steel	0.64	279881.42	813540.04
MA-FSW 740-A02-0003	n/a	MHE pushpoint	Hand installed	Temporary	Stainless steel	Stainless steel	0.64	279881.42	813540.04
MA-FSW 740-A03-0003	n/a	MHE pushpoint	Hand installed	Temporary	Stainless steel	Stainless steel	0.64	279881.42	813540.04
MA-FSW 740-0004	n/a	AMS well point	Slide hammer	Permanent	Polyethylene tube	Stainless steel	0.48	279881.42	813540.04
MA-FSW 741-A01-0001.2	n/a	MHE pushpoint	Hand installed	Temporary	Stainless steel	Stainless steel	0.64	279882.32	813539.51
MA-FSW 741-A02-0001.5	n/a	MHE pushpoint	Hand installed	Temporary	Stainless steel	Stainless steel	0.64	279882.32	813539.51
MA-FSW 741-A03-0001.5	n/a	MHE pushpoint	Hand installed	Temporary	Stainless steel	Stainless steel	0.64	279882.32	813539.51
MA-FSW 741-A01-0002	n/a	MHE pushpoint	Hand installed	Temporary	Stainless steel	Stainless steel	0.64	279882.32	813539.51
MA-FSW 741-A02-0002	n/a	MHE pushpoint	Hand installed	Temporary	Stainless steel	Stainless steel	0.64	279882.32	813539.51
MA-FSW 741-A03-0002	n/a	MHE pushpoint	Hand installed	Temporary	Stainless steel	Stainless steel	0.64	279882.32	813539.51
MA-FSW 741-A01-0003	n/a	MHE pushpoint	Hand installed	Temporary	Stainless steel	Stainless steel	0.64	279882.32	813539.51
MA-FSW 741-A02-0003	n/a	MHE pushpoint	Hand installed	Temporary	Stainless steel	Stainless steel	0.64	279882.32	813539.51
MA-FSW 741-A03-0003	n/a	MHE pushpoint	Hand installed	Temporary	Stainless steel	Stainless steel	0.64	279882.32	813539.51
MA-FSW 741-0004	n/a	AMS well point	Slide hammer	Permanent	Polyethylene tube	Stainless steel	0.48	279882.32	813539.51
MA-FSW 742-A01-0005	n/a	AMS well point	Vibratory hammer	Temporary	Polyethylene tube	Stainless steel	0.48	279870.77	813545.46
MA-FSW 742-A01-0012	n/a	AMS well point	Vibratory hammer	Temporary	Polyethylene tube	Stainless steel	0.48	279870.77	813545.46
MA-FSW 743-A01-0005	n/a	AMS well point	Vibratory hammer	Temporary	Polyethylene tube	Stainless steel	0.48	279867.29	813545.33
MA-FSW 743-A01-0010	n/a	AMS well point	Vibratory hammer	Temporary	Polyethylene tube	Stainless steel	0.48	279867.29	813545.33
MA-FSW 743-A01-0015	n/a	AMS well point	Vibratory hammer	Temporary	Polyethylene tube	Stainless steel	0.48	279867.29	813545.33
MA-FSW 743-A01-0020	n/a	AMS well point	Vibratory hammer	Temporary	Polyethylene tube	Stainless steel	0.48	279867.29	813545.33

Table 1.1.A. Location coordinates, land-surface and screen altitudes, well diameters, drilling methods, and casing and screen materials for monitoring wells, well points, pushpoints, and multilevel samplers near the Eel River, Seacoast Shores peninsula, East Falmouth, Massachusetts.—Continued

[Abbreviated site names, in which "F" is short for "MA-FSW," are used throughout this report. Values shown may not be internally consistent owing to rounding and unit conversions. Locations of sites are shown on figures 5 and 6. Locations were determined by using a global positioning system and are relative to the North American Datum of 1983 (NAD 83). Altitude is relative to the National Geodetic Vertical Datum of 1929 (NGVD 29). USGS, U.S. Geological Survey; MHE, M.H.E. Products Inc., East Tawas, Michigan; AMS, AMS Inc., American Falls, Idaho; cm, centimeter; m, meter; LS, land surface; RB, river bottom; MP, measuring point; PVC, polyvinyl chloride; n/a, not applicable; ---, no data]

USGS site name	USGS 15-digit site identifier	Site type	Drilling method	Temporary or permanent	Casing material	Screen material	Well diameter (cm)	Easting (NAD 83 m)	Northing (NAD 83 m)
MA-FSW 743-A01-0025	n/a	AMS well point	Vibratory hammer	Temporary	Polyethylene tube	Stainless steel	0.48	279867.29	813545.33
MA-FSW 743-A01-0030	n/a	AMS well point	Vibratory hammer	Temporary	Polyethylene tube	Stainless steel	0.48	279867.29	813545.33
MA-FSW 743-A01-0035	n/a	AMS well point	Vibratory hammer	Temporary	Polyethylene tube	Stainless steel	0.48	279867.29	813545.33
MA-FSW 745-A01-0001	n/a	MHE pushpoint	Hand installed	Temporary	Stainless steel	Stainless steel	0.64	279870.35	813545.71
MA-FSW 745-A01-0002	n/a	MHE pushpoint	Hand installed	Temporary	Stainless steel	Stainless steel	0.64	279870.35	813545.71
MA-FSW 745-A01-0003	n/a	MHE pushpoint	Hand installed	Temporary	Stainless steel	Stainless steel	0.64	279870.35	813545.71
MA-FSW 745-A01-0004	n/a	MHE pushpoint	Hand installed	Temporary	Stainless steel	Stainless steel	0.64	279870.35	813545.71
MA-FSW 746-A01-0001	n/a	MHE pushpoint	Hand installed	Temporary	Stainless steel	Stainless steel	0.64	279871.76	813545.20
MA-FSW 746-A01-0002	n/a	MHE pushpoint	Hand installed	Temporary	Stainless steel	Stainless steel	0.64	279871.76	813545.20
MA-FSW 746-A01-0003	n/a	MHE pushpoint	Hand installed	Temporary	Stainless steel	Stainless steel	0.64	279871.76	813545.20
MA-FSW 746-A01-0004	n/a	MHE pushpoint	Hand installed	Temporary	Stainless steel	Stainless steel	0.64	279871.76	813545.20
MA-FSW 747-A01-0001	n/a	MHE pushpoint	Hand installed	Temporary	Stainless steel	Stainless steel	0.64	279873.17	813544.56
MA-FSW 747-A01-0002	n/a	MHE pushpoint	Hand installed	Temporary	Stainless steel	Stainless steel	0.64	279873.17	813544.56
MA-FSW 747-A01-0003	n/a	MHE pushpoint	Hand installed	Temporary	Stainless steel	Stainless steel	0.64	279873.17	813544.56
MA-FSW 747-A01-0004	n/a	MHE pushpoint	Hand installed	Temporary	Stainless steel	Stainless steel	0.64	279873.17	813544.56
MA-FSW 778-A01-0003	n/a	Solinst well point	Slide hammer	Temporary	Polyethylene tube	Stainless steel	0.48	279864.34	813547.69
MA-FSW 778-A01-0007	n/a	Solinst well point	Slide hammer	Temporary	Polyethylene tube	Stainless steel	0.48	279864.34	813547.69
MA-FSW 779-A01-0004	n/a	Solinst well point	Slide hammer	Temporary	Polyethylene tube	Stainless steel	0.48	279857.21	813549.83
MA-FSW 779-A01-0006	n/a	Solinst well point	Slide hammer	Temporary	Polyethylene tube	Stainless steel	0.48	279857.21	813549.83

Table 1.1.B. Location coordinates, land-surface and screen altitudes, well diameters, drilling methods, and casing and screen materials for monitoring wells, well points, pushpoints, and multilevel samplers near the Eel River, Seacoast Shores peninsula, East Falmouth, Massachusetts.

[Abbreviated site names, in which "F" is short for "MA-FSW," are used throughout this report. Values shown may not be internally consistent owing to rounding and unit conversions. Locations of sites are shown on figures 5 and 6. Locations were determined by using a global positioning system and are relative to the North American Datum of 1983 (NAD 83). Altitude is relative to the National Geodetic Vertical Datum of 1929 (NGVD 29). USGS, U.S. Geological Survey; MHE, M.H.E. Products Inc., East Tawas, Michigan; AMS, AMS Inc., American Falls, Idaho; cm, centimeter; m, meter; LS, land surface; RB, river bottom; MP, measuring point; PVC, polyvinyl chloride; n/a, not applicable; --, no data]

USGS site name	USGS 15-digit site identifier	LS or RB altitude (m above NGVD 29)	MP height (m)	MP altitude (m)	Depth, top of screen below LS (m)	Depth, bottom of screen below LS (m)	Screen length (cm)	Altitude, top of screen (m above NGVD 29)	Altitude, bottom of screen (m above NGVD 29)
Eel River tide	n/a	n/a	n/a	2.15	n/a	n/a	n/a	n/a	n/a
MA-FSW 724-M01-02GNT	413404070323302	5.75	-0.17	5.58	6.30	6.33	3.0	-0.55	-0.59
MA-FSW 724-M01-03RT	413404070323303	5.75	-0.17	5.58	7.53	7.56	3.0	-1.78	-1.81
MA-FSW 724-M01-04BUT	413404070323304	5.75	-0.17	5.58	8.75	8.78	3.0	-3.00	-3.03
MA-FSW 724-M01-05BKT	413404070323305	5.75	-0.17	5.58	9.97	10.00	3.0	-4.22	-4.25
MA-FSW 724-M01-06WT	413404070323306	5.75	-0.17	5.58	11.19	11.22	3.0	-5.44	-5.47
MA-FSW 724-M01-07O	413404070323307	5.75	-0.17	5.58	12.41	12.44	3.0	-6.66	-6.69
MA-FSW 724-M01-08GY	413404070323308	5.75	-0.17	5.58	13.65	13.68	3.0	-7.90	-7.93
MA-FSW 724-M01-09Y	413404070323309	5.75	-0.17	5.58	14.87	14.90	3.0	-9.12	-9.15
MA-FSW 724-M01-10P	413404070323310	5.75	-0.17	5.58	16.11	16.14	3.0	-10.36	-10.39
MA-FSW 724-M01-11GN	413404070323311	5.75	-0.17	5.58	17.32	17.36	3.0	-11.58	-11.61
MA-FSW 724-M01-12R	413404070323312	5.75	-0.17	5.58	19.16	19.19	3.0	-13.41	-13.44
MA-FSW 724-M01-13BU	413404070323313	5.75	-0.17	5.58	20.99	21.02	3.0	-15.24	-15.27
MA-FSW 725-A01-0001.5	n/a	---	---	---	1.46	1.50	4.0	---	---
MA-FSW 725-A02-0001.5	n/a	---	---	---	1.46	1.50	4.0	---	---
MA-FSW 725-A03-0001.5	n/a	---	---	---	1.46	1.50	4.0	---	---
MA-FSW 725-A04-0001.5	n/a	---	---	---	1.46	1.50	4.0	---	---
MA-FSW 725-A05-0001.5	n/a	---	---	---	1.46	1.50	4.0	---	---
MA-FSW 725-A06-0001.5	n/a	---	---	---	1.46	1.50	4.0	---	---
MA-FSW 725-A07-0001.5	n/a	---	---	---	1.46	1.50	4.0	---	---
MA-FSW 725-A08-0001.5	n/a	---	---	---	1.46	1.50	4.0	---	---
MA-FSW 725-A09-0001.5	n/a	---	---	---	1.46	1.50	4.0	---	---
MA-FSW 725-A10-0001.5	n/a	---	---	---	1.46	1.50	4.0	---	---
MA-FSW 725-A11-0001.5	n/a	---	---	---	1.46	1.50	4.0	---	---
MA-FSW 725-A12-0001.5	n/a	---	---	---	1.46	1.50	4.0	---	---
MA-FSW 725-A13-0001.5	n/a	---	---	---	1.46	1.50	4.0	---	---
MA-FSW 725-A14-0004.1	n/a	---	---	---	4.06	4.10	4.0	---	---
MA-FSW 725-A15-0003.6	n/a	---	---	---	3.56	3.60	4.0	---	---
MA-FSW 725-A16-0002.5	n/a	---	---	---	2.46	2.50	4.0	---	---

Table 1.1.B. Location coordinates, land-surface and screen altitudes, well diameters, drilling methods, and casing and screen materials for monitoring wells, well points, pushpoints, and multilevel samplers near the Eel River, Seacoast Shores peninsula, East Falmouth, Massachusetts.—Continued

[Abbreviated site names, in which "F" is short for "MA-FSW," are used throughout this report. Values shown may not be internally consistent owing to rounding and unit conversions. Locations of sites are shown on figures 5 and 6. Locations were determined by using a global positioning system and are relative to the North American Datum of 1983 (NAD 83). Altitude is relative to the National Geodetic Vertical Datum of 1929 (NGVD 29). USGS, U.S. Geological Survey; MHE, M.H.E. Products Inc., East Tawas, Michigan; AMS, AMS Inc., American Falls, Idaho; cm, centimeter; m, meter; LS, land surface; RB, river bottom; MP, measuring point; PVC, polyvinyl chloride; n/a, not applicable; --, no data]

USGS site name	USGS 15-digit site identifier	LS or RB altitude (m above NGVD 29)	MP height (m)	MP altitude (m)	Depth, top of screen below LS (m)	Depth, bottom of screen below LS (m)	Screen length (cm)	Altitude, top of screen (m above NGVD 29)	Altitude, bottom of screen (m above NGVD 29)
MA-FSW 725-A18-0001.5	n/a	---	---	---	1.46	1.50	4.0	---	---
MA-FSW 725-A19-0003.0	n/a	---	---	---	2.96	3.00	4.0	---	---
MA-FSW 725-A20-0004.5	n/a	---	---	---	4.46	4.50	4.0	---	---
MA-FSW 725-A21-0005.7	n/a	---	---	---	5.66	5.70	4.0	---	---
MA-FSW 726-0005	413404070323401	0.81	-0.09	0.72	1.26	1.52	25.9	-0.46	-0.72
MA-FSW 726-0010	413404070323402	0.82	-0.09	0.73	2.79	3.05	25.9	-1.97	-2.23
MA-FSW 726-0015	413404070323403	0.84	-0.09	0.75	4.31	4.57	25.9	-3.47	-3.73
MA-FSW 726-0020	413404070323404	0.81	-0.09	0.72	5.84	6.10	25.9	-5.03	-5.29
MA-FSW 726-0025	413404070323405	0.78	-0.09	0.69	7.36	7.62	25.9	-6.58	-6.84
MA-FSW 726-0030	413404070323406	0.81	-0.09	0.72	8.88	9.14	25.9	-8.07	-8.33
MA-FSW 726-0035	413404070323407	0.78	-0.09	0.69	10.41	10.67	25.9	-9.63	-9.89
MA-FSW 726-0037.5	413404070323408	0.73	-0.09	0.64	11.17	11.43	25.9	-10.44	-10.70
MA-FSW 726-0040	413404070323409	0.76	-0.09	0.67	11.93	12.19	25.9	-11.17	-11.43
MA-FSW 726-0045	413404070323410	0.83	-0.09	0.74	13.46	13.72	25.9	-12.63	-12.89
MA-FSW 727-0031	413413070322101	7.28	-0.09	7.18	6.40	9.45	304.8	0.87	-2.17
MA-FSW 728-0026	413411070322701	5.70	-0.09	5.61	4.88	7.92	304.8	0.82	-2.23
MA-FSW 729-0028	413406070322501	6.86	-0.09	6.77	5.49	8.53	304.8	1.37	-1.67
MA-FSW 730-0022	413360070323501	4.68	-0.09	4.58	3.66	6.71	304.8	1.02	-2.03
MA-FSW 731-0029	413358070322801	6.62	-0.09	6.53	5.79	8.84	304.8	0.83	-2.22
MA-FSW 732-0015	413404070323316	4.20	-0.09	4.11	3.96	4.57	61.0	0.24	-0.37
MA-FSW 732-0036	413404070323317	4.21	-0.09	4.11	10.36	10.97	61.0	-6.16	-6.77
MA-FSW 732-0041	413404070323318	4.21	-0.09	4.12	11.89	12.50	61.0	-7.67	-8.28
MA-FSW 732-0046	413404070323319	4.20	-0.09	4.11	13.41	14.02	61.0	-9.21	-9.82
MA-FSW 732-0051	413404070323320	4.21	-0.09	4.12	14.94	15.54	61.0	-10.73	-11.34
MA-FSW 732-0058	413404070323321	4.20	-0.09	4.11	17.07	17.68	61.0	-12.87	-13.48

Table 1.1.B. Location coordinates, land-surface and screen altitudes, well diameters, drilling methods, and casing and screen materials for monitoring wells, well points, pushpoints, and multilevel samplers near the Eel River, Seacoast Shores peninsula, East Falmouth, Massachusetts.—Continued

[Abbreviated site names, in which "F" is short for "MA-FSW," are used throughout this report. Values shown may not be internally consistent owing to rounding and unit conversions. Locations of sites are shown on figures 5 and 6. Locations were determined by using a global positioning system and are relative to the North American Datum of 1983 (NAD 83). Altitude is relative to the National Geodetic Vertical Datum of 1929 (NGVD 29). USGS, U.S. Geological Survey; MHE, M.H.E. Products Inc., East Tawas, Michigan; AMS, AMS Inc., American Falls, Idaho; cm, centimeter; m, meter; LS, land surface; RB, river bottom; MP, measuring point; PVC, polyvinyl chloride; n/a, not applicable; --, no data]

USGS site name	USGS 15-digit site identifier	LS or RB altitude (m above NGVD 29)	MP height (m)	MP altitude (m)	Depth, top of screen below LS (m)	Depth, bottom of screen below LS (m)	Screen length (cm)	Altitude, top of screen (m above NGVD 29)	Altitude, bottom of screen (m above NGVD 29)
MA-FSW 733-A01-0001	n/a	-0.09	0.00	-0.09	0.27	0.30	4.0	-0.35	-0.39
MA-FSW 733-A02-0001	n/a	-0.09	0.00	-0.09	0.27	0.30	4.0	-0.35	-0.39
MA-FSW 733-A03-0001	n/a	-0.09	0.00	-0.09	0.27	0.30	4.0	-0.35	-0.39
MA-FSW 733-A01-0002	n/a	-0.09	0.00	-0.09	0.57	0.61	4.0	-0.66	-0.70
MA-FSW 733-A02-0002	n/a	-0.09	0.00	-0.09	0.57	0.61	4.0	-0.66	-0.70
MA-FSW 733-A03-0002	n/a	-0.09	0.00	-0.09	0.57	0.61	4.0	-0.66	-0.70
MA-FSW 733-A01-0003	n/a	-0.09	0.00	-0.09	0.87	0.91	4.0	-0.96	-1.00
MA-FSW 733-A02-0003	n/a	-0.09	0.00	-0.09	0.87	0.91	4.0	-0.96	-1.00
MA-FSW 733-A03-0003	n/a	-0.09	0.00	-0.09	0.87	0.91	4.0	-0.96	-1.00
MA-FSW 733-A01-0015	n/a	-0.09	0.00	-0.09	4.49	4.57	8.2	-4.58	-4.66
MA-FSW 733-A01-0020	n/a	-0.09	0.00	-0.09	6.01	6.10	8.2	-6.10	-6.18
MA-FSW 733-A01-0025	n/a	-0.09	0.00	-0.09	7.54	7.62	8.2	-7.63	-7.71
MA-FSW 733-A01-0030	n/a	-0.09	0.00	-0.09	9.06	9.14	8.2	-9.15	-9.23
MA-FSW 733-0005	413405070323401	-0.09	0.00	-0.09	1.52	1.52	0.6	-1.61	-1.61
MA-FSW 733-0010	413405070323402	-0.09	0.00	-0.09	3.04	3.05	0.6	-3.13	-3.14
MA-FSW 733-0015	413405070323403	-0.09	0.00	-0.09	4.57	4.57	0.6	-4.65	-4.66
MA-FSW 733-0018	413405070323404	-0.09	0.00	-0.09	5.48	5.49	0.6	-5.57	-5.57
MA-FSW 733-0025	413405070323405	-0.09	0.00	-0.09	7.61	7.62	0.6	-7.70	-7.71
MA-FSW 733-0030	413405070323406	-0.09	0.00	-0.09	9.14	9.14	0.6	-9.23	-9.23
MA-FSW 733-0034	413405070323407	-0.09	0.00	-0.09	10.28	10.36	8.2	-10.37	-10.45
MA-FSW 734-A01-0001	n/a	-0.02	0.00	-0.02	0.27	0.30	4.0	-0.29	-0.33
MA-FSW 734-A02-0001	n/a	-0.02	0.00	-0.02	0.27	0.30	4.0	-0.29	-0.33
MA-FSW 734-A03-0001	n/a	-0.02	0.00	-0.02	0.27	0.30	4.0	-0.29	-0.33
MA-FSW 734-A01-0002	n/a	-0.02	0.00	-0.02	0.57	0.61	4.0	-0.59	-0.63
MA-FSW 734-A02-0002	n/a	-0.02	0.00	-0.02	0.57	0.61	4.0	-0.59	-0.63
MA-FSW 734-A03-0002	n/a	-0.02	0.00	-0.02	0.57	0.61	4.0	-0.59	-0.63

Table 1.1.B. Location coordinates, land-surface and screen altitudes, well diameters, drilling methods, and casing and screen materials for monitoring wells, well points, pushpoints, and multilevel samplers near the Eel River, Seacoast Shores peninsula, East Falmouth, Massachusetts.—Continued

[Abbreviated site names, in which "F" is short for "MA-FSW," are used throughout this report. Values shown may not be internally consistent owing to rounding and unit conversions. Locations of sites are shown on figures 5 and 6. Locations were determined by using a global positioning system and are relative to the North American Datum of 1983 (NAD 83). Altitude is relative to the National Geodetic Vertical Datum of 1929 (NGVD 29). USGS, U.S. Geological Survey; MHE, M.H.E. Products Inc., East Tawas, Michigan; AMS, AMS Inc., American Falls, Idaho; cm, centimeter; m, meter; LS, land surface; RB, river bottom; MP, measuring point; PVC, polyvinyl chloride; n/a, not applicable; --, no data]

USGS site name	USGS 15-digit site identifier	LS or RB altitude (m above NGVD 29)	MP height (m)	MP altitude (m)	Depth, top of screen below LS (m)	Depth, bottom of screen below LS (m)	Screen length (cm)	Altitude, top of screen (m above NGVD 29)	Altitude, bottom of screen (m above NGVD 29)
MA-FSW 734-A01-0003	n/a	-0.02	0.00	-0.02	0.87	0.91	4.0	-0.90	-0.94
MA-FSW 734-A02-0003	n/a	-0.02	0.00	-0.02	0.87	0.91	4.0	-0.90	-0.94
MA-FSW 734-A03-0003	n/a	-0.02	0.00	-0.02	0.87	0.91	4.0	-0.90	-0.94
MA-FSW 734-0004	n/a	-0.0	0.0	-0.0	1.2	1.2	0.6	-1.2	-1.2
MA-FSW 735-A01-0001	n/a	0.02	0.00	0.02	0.27	0.30	4.0	-0.24	-0.28
MA-FSW 735-A02-0001	n/a	0.02	0.00	0.02	0.27	0.30	4.0	-0.24	-0.28
MA-FSW 735-A03-0001	n/a	0.02	0.00	0.02	0.27	0.30	4.0	-0.24	-0.28
MA-FSW 735-A01-0002	n/a	0.02	0.00	0.02	0.57	0.61	4.0	-0.55	-0.59
MA-FSW 735-A02-0002	n/a	0.02	0.00	0.02	0.57	0.61	4.0	-0.55	-0.59
MA-FSW 735-A03-0002	n/a	0.02	0.00	0.02	0.57	0.61	4.0	-0.55	-0.59
MA-FSW 735-A01-0003	n/a	0.02	0.00	0.02	0.87	0.91	4.0	-0.85	-0.89
MA-FSW 735-A02-0003	n/a	0.02	0.00	0.02	0.87	0.91	4.0	-0.85	-0.89
MA-FSW 735-A03-0003	n/a	0.02	0.00	0.02	0.87	0.91	4.0	-0.85	-0.89
MA-FSW 735-0004	n/a	0.02	0.00	0.02	1.21	1.22	0.6	-1.19	-1.19
MA-FSW 736-A01-0001	n/a	0.08	0.00	0.08	0.27	0.30	4.0	-0.19	-0.23
MA-FSW 736-A02-0001	n/a	0.08	0.00	0.08	0.27	0.30	4.0	-0.19	-0.23
MA-FSW 736-A03-0001	n/a	0.08	0.00	0.08	0.27	0.30	4.0	-0.19	-0.23
MA-FSW 736-A01-0002	n/a	0.08	0.00	0.08	0.57	0.61	4.0	-0.49	-0.53
MA-FSW 736-A02-0002	n/a	0.08	0.00	0.08	0.57	0.61	4.0	-0.49	-0.53
MA-FSW 736-A03-0002	n/a	0.08	0.00	0.08	0.57	0.61	4.0	-0.49	-0.53
MA-FSW 736-A01-0003	n/a	0.08	0.00	0.08	0.87	0.91	4.0	-0.80	-0.84
MA-FSW 736-A02-0003	n/a	0.08	0.00	0.08	0.87	0.91	4.0	-0.80	-0.84
MA-FSW 736-A03-0003	n/a	0.08	0.00	0.08	0.87	0.91	4.0	-0.80	-0.84
MA-FSW 736-0004	n/a	0.08	0.00	0.08	1.21	1.22	0.6	-1.13	-1.14

Table 1.1.B. Location coordinates, land-surface and screen altitudes, well diameters, drilling methods, and casing and screen materials for monitoring wells, well points, pushpoints, and multilevel samplers near the Eel River, Seacoast Shores peninsula, East Falmouth, Massachusetts.—Continued

[Abbreviated site names, in which "F" is short for "MA-FSW," are used throughout this report. Values shown may not be internally consistent owing to rounding and unit conversions. Locations of sites are shown on figures 5 and 6. Locations were determined by using a global positioning system and are relative to the North American Datum of 1983 (NAD 83). Altitude is relative to the National Geodetic Vertical Datum of 1929 (NGVD 29). USGS, U.S. Geological Survey; MHE, M.H.E. Products Inc., East Tawas, Michigan; AMS, AMS Inc., American Falls, Idaho; cm, centimeter; m, meter; LS, land surface; RB, river bottom; MP, measuring point; PVC, polyvinyl chloride; n/a, not applicable; --, no data]

USGS site name	USGS 15-digit site identifier	LS or RB altitude (m above NGVD 29)	MP height (m)	MP altitude (m)	Depth, top of screen below LS (m)	Depth, bottom of screen below LS (m)	Screen length (cm)	Altitude, top of screen (m above NGVD 29)	Altitude, bottom of screen (m above NGVD 29)
MA-FSW 737-A01-0001	n/a	0.19	0.00	0.19	0.27	0.30	4.0	-0.08	-0.12
MA-FSW 737-A02-0001	n/a	0.19	0.00	0.19	0.27	0.30	4.0	-0.08	-0.12
MA-FSW 737-A03-0001	n/a	0.19	0.00	0.19	0.27	0.30	4.0	-0.08	-0.12
MA-FSW 737-A01-0002	n/a	0.19	0.00	0.19	0.57	0.61	4.0	-0.38	-0.42
MA-FSW 737-A02-0002	n/a	0.19	0.00	0.19	0.57	0.61	4.0	-0.38	-0.42
MA-FSW 737-A03-0002	n/a	0.19	0.00	0.19	0.57	0.61	4.0	-0.38	-0.42
MA-FSW 737-A01-0003	n/a	0.19	0.00	0.19	0.87	0.91	4.0	-0.69	-0.73
MA-FSW 737-A02-0003	n/a	0.19	0.00	0.19	0.87	0.91	4.0	-0.69	-0.73
MA-FSW 737-A03-0003	n/a	0.19	0.00	0.19	0.87	0.91	4.0	-0.69	-0.73
MA-FSW 737-0004	n/a	0.19	0.00	0.19	1.21	1.22	0.6	-1.02	-1.03
MA-FSW 738-A01-0001	n/a	0.31	0.00	0.31	0.27	0.30	4.0	0.05	0.01
MA-FSW 738-A02-0001	n/a	0.31	0.00	0.31	0.27	0.30	4.0	0.05	0.01
MA-FSW 738-A03-0001	n/a	0.31	0.00	0.31	0.27	0.30	4.0	0.05	0.01
MA-FSW 738-A01-0002	n/a	0.31	0.00	0.31	0.57	0.61	4.0	-0.26	-0.30
MA-FSW 738-A02-0002	n/a	0.31	0.00	0.31	0.57	0.61	4.0	-0.26	-0.30
MA-FSW 738-A03-0002	n/a	0.31	0.00	0.31	0.57	0.61	4.0	-0.26	-0.30
MA-FSW 738-A01-0003	n/a	0.31	0.00	0.31	0.87	0.91	4.0	-0.56	-0.60
MA-FSW 738-A02-0003	n/a	0.31	0.00	0.31	0.87	0.91	4.0	-0.56	-0.60
MA-FSW 738-A03-0003	n/a	0.31	0.00	0.31	0.87	0.91	4.0	-0.56	-0.60
MA-FSW 738-0004	n/a	0.31	0.00	0.31	1.21	1.22	0.6	-0.90	-0.91
MA-FSW 739-A01-0001	n/a	0.53	0.00	0.53	0.27	0.30	4.0	0.27	0.23
MA-FSW 739-A02-0001	n/a	0.53	0.00	0.53	0.27	0.30	4.0	0.27	0.23
MA-FSW 739-A03-0001	n/a	0.53	0.00	0.53	0.27	0.30	4.0	0.27	0.23
MA-FSW 739-A01-0002	n/a	0.53	0.00	0.53	0.57	0.61	4.0	-0.04	-0.08
MA-FSW 739-A02-0002	n/a	0.53	0.00	0.53	0.57	0.61	4.0	-0.04	-0.08
MA-FSW 739-A03-0002	n/a	0.53	0.00	0.53	0.57	0.61	4.0	-0.04	-0.08
MA-FSW 739-A01-0003	n/a	0.53	0.00	0.53	0.87	0.91	4.0	-0.34	-0.38
MA-FSW 739-A02-0003	n/a	0.53	0.00	0.53	0.87	0.91	4.0	-0.34	-0.38

Table 1.1.B. Location coordinates, land-surface and screen altitudes, well diameters, drilling methods, and casing and screen materials for monitoring wells, well points, pushpoints, and multilevel samplers near the Eel River, Seacoast Shores peninsula, East Falmouth, Massachusetts.—Continued

[Abbreviated site names, in which "F" is short for "MA-FSW," are used throughout this report. Values shown may not be internally consistent owing to rounding and unit conversions. Locations of sites are shown on figures 5 and 6. Locations were determined by using a global positioning system and are relative to the North American Datum of 1983 (NAD 83). Altitude is relative to the National Geodetic Vertical Datum of 1929 (NGVD 29). USGS, U.S. Geological Survey; MHE, M.H.E. Products Inc., East Tawas, Michigan; AMS, AMS Inc., American Falls, Idaho; cm, centimeter; m, meter; LS, land surface; RB, river bottom; MP, measuring point; PVC, polyvinyl chloride; n/a, not applicable; --, no data]

USGS site name	USGS 15-digit site identifier	LS or RB altitude (m above NGVD 29)	MP height (m)	MP altitude (m)	Depth, top of screen below LS (m)	Depth, bottom of screen below LS (m)	Screen length (cm)	Altitude, top of screen (m above NGVD 29)	Altitude, bottom of screen (m above NGVD 29)
MA-FSW 739-A03-0003	n/a	0.53	0.00	0.53	0.87	0.91	4.0	-0.34	-0.38
MA-FSW 739-0004	n/a	0.53	0.00	0.53	1.21	1.22	0.6	-0.68	-0.69
	n/a								
MA-FSW 740-A01-0001	n/a	0.74	0.00	0.74	0.27	0.30	4.0	0.48	0.44
MA-FSW 740-A02-0001	n/a	0.74	0.00	0.74	0.27	0.30	4.0	0.48	0.44
MA-FSW 740-A03-0001	n/a	0.74	0.00	0.74	0.27	0.30	4.0	0.48	0.44
MA-FSW 740-A01-0002	n/a	0.74	0.00	0.74	0.57	0.61	4.0	0.17	0.13
MA-FSW 740-A02-0002	n/a	0.74	0.00	0.74	0.57	0.61	4.0	0.17	0.13
MA-FSW 740-A03-0002	n/a	0.74	0.00	0.74	0.57	0.61	4.0	0.17	0.13
MA-FSW 740-A01-0003	n/a	0.74	0.00	0.74	0.87	0.91	4.0	-0.13	-0.17
MA-FSW 740-A02-0003	n/a	0.74	0.00	0.74	0.87	0.91	4.0	-0.13	-0.17
MA-FSW 740-A03-0003	n/a	0.74	0.00	0.74	0.87	0.91	4.0	-0.13	-0.17
MA-FSW 740-0004	n/a	0.74	0.00	0.74	1.21	1.22	0.6	-0.47	-0.48
MA-FSW 741-A01-0001.2	n/a	0.97	0.00	0.97	0.33	0.37	4.0	0.65	0.61
MA-FSW 741-A02-0001.5	n/a	0.97	0.00	0.97	0.42	0.46	4.0	0.55	0.52
MA-FSW 741-A03-0001.5	n/a	0.97	0.00	0.97	0.42	0.46	4.0	0.55	0.52
MA-FSW 741-A01-0002	n/a	0.97	0.00	0.97	0.57	0.61	4.0	0.40	0.36
MA-FSW 741-A02-0002	n/a	0.97	0.00	0.97	0.57	0.61	4.0	0.40	0.36
MA-FSW 741-A03-0002	n/a	0.97	0.00	0.97	0.57	0.61	4.0	0.40	0.36
MA-FSW 741-A01-0003	n/a	0.97	0.00	0.97	0.87	0.91	4.0	0.10	0.06
MA-FSW 741-A02-0003	n/a	0.97	0.00	0.97	0.87	0.91	4.0	0.10	0.06
MA-FSW 741-A03-0003	n/a	0.97	0.00	0.97	0.87	0.91	4.0	0.10	0.06
MA-FSW 741-0004	n/a	0.97	0.00	0.97	1.21	1.22	0.6	-0.24	-0.25
MA-FSW 742-A01-0005	n/a	-0.33	0.00	-0.33	1.49	1.52	3.4	-1.82	-1.86
MA-FSW 742-A01-0012	n/a	-0.33	0.00	-0.33	3.62	3.66	3.4	-3.96	-3.99

Table 1.1.B. Location coordinates, land-surface and screen altitudes, well diameters, drilling methods, and casing and screen materials for monitoring wells, well points, pushpoints, and multilevel samplers near the Eel River, Seacoast Shores peninsula, East Falmouth, Massachusetts.—Continued

[Abbreviated site names, in which "F" is short for "MA-FSW," are used throughout this report. Values shown may not be internally consistent owing to rounding and unit conversions. Locations of sites are shown on figures 5 and 6. Locations were determined by using a global positioning system and are relative to the North American Datum of 1983 (NAD 83). Altitude is relative to the National Geodetic Vertical Datum of 1929 (NGVD 29). USGS, U.S. Geological Survey; MHE, M.H.E. Products Inc., East Tawas, Michigan; AMS, AMS Inc., American Falls, Idaho; cm, centimeter; m, meter; LS, land surface; RB, river bottom; MP, measuring point; PVC, polyvinyl chloride; n/a, not applicable; --, no data]

USGS site name	USGS 15-digit site identifier	LS or RB altitude (m above NGVD 29)	MP height (m)	MP altitude (m)	Depth, top of screen below LS (m)	Depth, bottom of screen below LS (m)	Screen length (cm)	Altitude, top of screen (m above NGVD 29)	Altitude, bottom of screen (m above NGVD 29)
MA-FSW 743-A01-0005	n/a	-0.62	0.00	-0.62	1.49	1.52	3.4	-2.11	-2.14
MA-FSW 743-A01-0010	n/a	-0.62	0.00	-0.62	3.01	3.05	3.4	-3.63	-3.66
MA-FSW 743-A01-0015	n/a	-0.62	0.00	-0.62	4.54	4.57	3.4	-5.15	-5.19
MA-FSW 743-A01-0020	n/a	-0.62	0.00	-0.62	6.06	6.10	3.4	-6.68	-6.71
MA-FSW 743-A01-0025	n/a	-0.62	0.00	-0.62	7.59	7.62	3.4	-8.20	-8.24
MA-FSW 743-A01-0030	n/a	-0.62	0.00	-0.62	9.11	9.14	3.4	-9.73	-9.76
MA-FSW 743-A01-0035	n/a	-0.62	0.00	-0.62	10.63	10.67	3.4	-11.25	-11.28
MA-FSW 745-A01-0001	n/a	-0.34	0.00	-0.34	0.27	0.30	4.0	-0.61	-0.64
MA-FSW 745-A01-0002	n/a	-0.34	0.00	-0.34	0.57	0.61	4.0	-0.91	-0.95
MA-FSW 745-A01-0003	n/a	-0.34	0.00	-0.34	0.87	0.91	4.0	-1.21	-1.25
MA-FSW 745-A01-0004	n/a	-0.34	0.00	-0.34	1.18	1.22	4.0	-1.52	-1.56
MA-FSW 746-A01-0001	n/a	-0.29	0.00	-0.29	0.27	0.30	4.0	-0.56	-0.59
MA-FSW 746-A01-0002	n/a	-0.29	0.00	-0.29	0.57	0.61	4.0	-0.86	-0.90
MA-FSW 746-A01-0003	n/a	-0.29	0.00	-0.29	0.87	0.91	4.0	-1.16	-1.20
MA-FSW 746-A01-0004	n/a	-0.29	0.00	-0.29	1.18	1.22	4.0	-1.47	-1.51
MA-FSW 747-A01-0001	n/a	-0.19	0.00	-0.19	0.27	0.30	4.0	-0.46	-0.49
MA-FSW 747-A01-0002	n/a	-0.19	0.00	-0.19	0.57	0.61	4.0	-0.76	-0.80
MA-FSW 747-A01-0003	n/a	-0.19	0.00	-0.19	0.87	0.91	4.0	-1.06	-1.10
MA-FSW 747-A01-0004	n/a	-0.19	0.00	-0.19	1.18	1.22	4.0	-1.37	-1.41
MA-FSW 778-A01-0003	n/a	-0.69	0.00	-0.69	0.68	0.91	23.5	-1.37	-1.60
MA-FSW 778-A01-0007	n/a	-0.69	0.00	-0.69	1.90	2.13	23.5	-2.59	-2.82
MA-FSW 779-A01-0004	n/a	-0.95	0.00	-0.95	0.99	1.22	23.5	-1.94	-2.17
MA-FSW 779-A01-0006	n/a	-0.95	0.00	-0.95	1.60	1.83	23.5	-2.55	-2.78

For more information about this report, contact:
Director, New England Water Science Center
U.S. Geological Survey
10 Bearfoot Road
Northborough, MA 01532
dc_nweng@usgs.gov
or visit our website at
https://newengland.water.usgs.gov

Publishing support provided by the
Pembroke Publishing Service Center

ISSN 2328-0328 (online)
http://dx.doi.org/10.3133/sir20185095